**Forschungsbereich MaschinenbauInformatik und Virtuelle Produktentwicklung**

**Univ.-Prof. Dr.-Ing. Detlef Gerhard**

# Methodology of modeling Composite components with FEM software and investigation of the influence of modeling method in the quality of results

Dissertation

## Hosein Tafaghodi Helali

**TECHNISCHE UNIVERSITÄT WIEN**
Vienna University of Technology

FAKULTÄT FÜR MASCHINENWESEN UND BETRIEBSWISSENSCHAFTEN DER TECHNISCHEN UNIVERSITÄT WIEN

# Dissertation

Methodology of modeling Composite components with FEM software and investigation of the influence of modeling method in the quality of results

ausgeführt zum Zwecke der Erlangung des akademischen Grades eines Doktors der technischen Wissenschaften unter der Leitung von

Ao.Univ.-Prof. Dipl.-Ing. Dr.-techn. Manfred Grafinger

E307

Institut für Konstruktionswissenschaften und Technische Logistik Forschungsbereich Maschinenbauinformatik und Virtuelle Produktentwicklung

eingereicht an der Technischen Universität Wien

Fakultät für Maschinenwesen und Betriebswissenschaften

Von

Hosein Tafaghodi Helali

e1128997

Josefbaumann gasse 8A/254

Wien, am

# Statutory Declaration

Hiermit erkläre ich, dass ich die vorliegende Arbeit selbstständig und nur mit den angegebenen Hilfsmitteln verfasst habe. Aus fremden Quellen wörtlich oder sinngemäß übernommene Zitate sind als solche kenntlich gemacht. Die Arbeit hat noch nicht anderweitig in gleicher oder ähnlicher Form zu Prüfungszwecken vorgelegen und ist auch noch nicht veröffentlicht.

Die Dissertation darf über die Hochschulbibliothek zugänglich gemacht werden.

Ort, Datum:        _____
                           Unterschrift Doktorand

# Acknowledgment

Special thanks to my professor Manfred Grafinger, without his trust and compassion this thesis would not have existed.

Many thanks to my family for all their support!

Dear Mom, thank you for instilling in me the belief that I could do anything I put my mind to. I dedicate this work to you as my first teacher.

# Table of Contents

# 1  Introduction

The development and applications of composite materials and structural elements composed of composite materials have been very rapid in the last decades [1]. Even 20 years ago, engineers recognized composite as a deluxe material which had limited usage in special cases. Nowadays all industrial companies are trying to develop their products by using composite materials. The motivations behind these developments are the significant progress that has been made in material science and technology of the composite and is required for high performance materials not only in aircrafts and aerospace structures, but also in the development of very powerful experimental equipment and numerical methods and the availability of efficient computers [1].

The most significant factor in composite research and application is weight saving in comparison to structures of conventional materials such as steel, alloys, etc. However, to only have the density, stiffness and strength of the material in mind when thinking of composites means to have a very narrow view of the possibilities of materials such as fiber-reinforced plastics because they may often score higher than conventional materials such as metals not only due to their mechanical properties. Fiber reinforced plastics are extremely corrosion-resistant and have interesting electromagnetic properties. In consequence they are used for chemical plants and for structures which require non-magnetic materials. Further carbon fiber reinforced epoxy is used in medical applications because they are transparent to X-rays [1].

In applications outside of the aerospace or aircraft industry, cost competitiveness with conventional materials becomes important. More recently requirements such as quality assurance, predictability of the structure behavior over its life time, recycling, etc. have also become significant [1].

Applications of polymer matrix composites range from the aerospace industry to the industry of sports goods. The military aircraft industry has mainly led the field in the use of polymer composites when compared to commercial airlines which have used composites, because of safety concerns more restrictively and frequently limited to secondary structural elements. Automotive applications, sporting goods, medical devices and many other commercial applications are examples of the application of polymer matrix composites. Also applications in civil engineering are now on the way but it will take some time to achieve their wide use since there are a lot of prescribed conditions to guarantee the reliability of structures. But it is clear that over the last decades considerable advances have been made in the use of composite material in construction and building industries and this trend will continue [1].

With the development of composite materials a new material design becomes possible that will allow an optimal material composition in connection with the

structural design. A useful and correct application of composite materials requires a close interaction of different engineering disciplines such as structural design and analysis, material science, mechanics of materials, process engineering, etc. In summary, the main topics of composite material research and technology are [1]:

- Investigation of all characteristics of the constituent and composite materials
- Material design and optimization for the given working condition
- Development of analytical modelling and solution methods for determining material and structure behavior
- Development of experimental methods for material characteristics, stress and deformation states, failure criteria
- Modeling and analysis of creep, damage and life prediction
- Development of new and efficient fabrication and recycling procedures among others [1]

The $3^{rd}$ topic is studied by mechanical engineers whose specialty is finite element analysis. As theoretical calculations is normally a complicated and time consuming process, the finite element method has been used in the vast area of mechanical engineering for simulating, analyzing and optimizing the structures. By considering that composite materials have more complicated structures than normal materials such as steel, the necessarily of applying the Finite Element Method (FEM) is felt even more than before. Because of this reason many famous FEM software producers add the composite module to their new released products.

A critical requirement for simulating a structure composed of a composite material is applying the useful techniques. In this project some methods for simulating the composite material are presented to achieve this goal. In the first step all these methods including theoretical and FEM methods are introduced. For the theoretical part, the calculation procedure has been described, and for the FEM part, the procedure of modeling has been described. In the second step these methods are used for analyzing simple examples and all obtained results are compared to each other to distinguish the precision and quality of each method. In fact with this comparison the field of usage of each method will be clear. Considering the vast application of composite material in industry, two practical examples have been presented in the last section of this project to show the usage of these methods at the industrial level. It would be useful to know that these examples which are simulated and analyzed by using FEM methods have been produced and tested in industrial companies.

# 2 Theoretical and FEM Methods

## 2.1 Composite Material

Before getting started with composite calculation, it would be useful to first talk about materials and how are they classified.

A composite material is a structural material which consists of two or more combined components mixed at the macroscopic scale but not dissolved in each other. One component is called fiber or reinforcing phase. It is positioned in another component that is called matrix. The reinforcing phase material could also be particles or flakes instead of fibers and the matrix phase material is normally continuous. An example of the composite system is the epoxy matrix reinforced with carbon fibers which is used in the current project.

Structural materials are categorized in three main groups based on their material properties:

- Metals
- Ceramics
- Polymers

The unique structural properties of composite materials separate them from other structural materials; therefore they should be classified in a separate group.

The first property of a material is homogeneity. A material is called homogeneous when its properties are the same in every point and independent to the location. With this definition, inhomogeneous or quasi homogeneous materials are those with different properties in different locations. In other words an inhomogeneous body has material properties that are a function of position on the body. Note that inhomogeneity appears at the macroscopic scale, therefore all material is considered homogenous at the microscopic level. For example consider a steel beam. In a normal situation the steel beam is a homogeneous material but if the beam is heated up from one side the temperature of each point of the beam will change. Since the elasticity modulus depends on temperature, it will be different in each point of the beam and this means the steel beam is no longer homogeneous. For composite material inhomogeneity appears more or less at the micromechanics scale, because in one lamina, the properties of one point in the matrix is quite different from one point in the fiber. But at the macro mechanics scale, the average mechanical properties of one lamina are considered, and the lamina is homogeneous in macro mechanics analysis. [1,2]

The second property of a material is isotropicity. If the properties of the material in one point are the same in all directions, it is called an isotropic material and if not, it is called anisotropic. As an example steel is an isotropic material because its elasticity modulus is the same in all directions. But most composites are anisotropic because stiffness in fiber direction is quite different from stiffness perpendicular to fiber direction. Anisotropic groups of materials consist of monoclinic, orthotropic and transversely isotropic materials and their difference is based on their planes of symmetry and independence parameters of stiffness matrix which will be described in Hooke's law section [1, 2].

It is important to mention that homogeneity and isotropicity are two complete different material properties and should not be mixed up. For instance material can be isotropic but not homogeneous. This can be described with the steel beam example. The heated beam is inhomogeneous because the steel young modulus is different in each position of the beam, but the beam is still isotropic since the material properties of each point are the same in all directions.

There are two definitions for components of composite structure. These two components are lamina and laminate which are used at the macro mechanics scale formulations and also for FEM simulation. A lamina (also called a ply or layer) is a single flat layer of unidirectional fibers arranged in a matrix (depends on composite model fibers could also be woven). A laminate is a stack of plies of composites. Each layer can be laid at various orientations and can be made up of different material systems [2].

## 2.2 Hooke's Law

Hooke's law is a general equation for relating the stress vector to the strain vector with the stiffness matrix (k); parameters of the stiffness matrix come from material properties. Composite structures could be assumed elastic with linear behavior, but considering them isotropic is not a correct assumption. Hooke's law should be extended into the matrix form for composite material; in fact this format is also used in the Finite Element Method. In FEM numerical formulation the matrix format of Hooke's law is used for calculating stress and strain of meshed elements. The formulation shown below is the general state seen, and by having the properties of the lamina, unknown parameters in the stiffness matrix could be reduced [1,2].

$$\begin{bmatrix} \sigma_1 \\ \sigma_2 \\ \sigma_3 \\ \tau_{23} \\ \tau_{31} \\ \tau_{12} \end{bmatrix} = \begin{bmatrix} C_{11} & C_{12} & C_{13} & C_{14} & C_{15} & C_{16} \\ C_{21} & C_{22} & C_{23} & C_{24} & C_{25} & C_{26} \\ C_{31} & C_{32} & C_{33} & C_{34} & C_{35} & C_{36} \\ C_{41} & C_{42} & C_{43} & C_{44} & C_{45} & C_{46} \\ C_{51} & C_{52} & C_{53} & C_{54} & C_{55} & C_{56} \\ C_{61} & C_{62} & C_{63} & C_{64} & C_{65} & C_{66} \end{bmatrix} \begin{bmatrix} \varepsilon_1 \\ \varepsilon_2 \\ \varepsilon_3 \\ \gamma_{23} \\ \gamma_{31} \\ \gamma_{12} \end{bmatrix} \qquad 2\text{-}1$$

This $6\times6$ matrix with 36 parameters is called the stiffness matrix $[C]$, and by reversing the equation the new matrix which is the reverse of the stiffness matrix will appear and is called the flexibility matrix $[S]$ as illustrated below:

$$\begin{bmatrix} \varepsilon_1 \\ \varepsilon_2 \\ \varepsilon_3 \\ \gamma_{23} \\ \gamma_{31} \\ \gamma_{12} \end{bmatrix} = \begin{bmatrix} S_{11} & S_{12} & S_{13} & S_{14} & S_{15} & S_{16} \\ S_{21} & S_{22} & S_{23} & S_{24} & S_{25} & S_{26} \\ S_{31} & S_{32} & S_{33} & S_{34} & S_{35} & S_{36} \\ S_{41} & S_{42} & S_{43} & S_{44} & S_{45} & S_{46} \\ S_{51} & S_{52} & S_{53} & S_{54} & S_{55} & S_{56} \\ S_{61} & S_{62} & S_{63} & S_{64} & S_{65} & S_{66} \end{bmatrix} \begin{bmatrix} \sigma_1 \\ \sigma_2 \\ \sigma_3 \\ \tau_{23} \\ \tau_{31} \\ \tau_{12} \end{bmatrix}$$

2-2

As the matrix $[C]$ is symmetric ($C_{ij} = C_{ji}$), the independent constants are reduced from 36 to 21. The Flexibility matrix $[S]$ also follows this rule and has 21 independent constants. This type of material with 21 elastic constants is called anisotropic material and calculating the result is possible when all these 21 elastic constants are available. In addition some materials have a symmetric behavior; hence elastic properties are equal in the direction of symmetry. This symmetrical behavior decreases the number of independent constants by relating them to each other or making some of them zero [2].

In case of one material symmetry plane, the material is called Monoclinic and the independence constants in stiffness matrix are reduced to 13 like below [2]:

$$\begin{bmatrix} C_{11} & C_{12} & C_{13} & 0 & 0 & C_{16} \\ C_{21} & C_{22} & C_{23} & 0 & 0 & C_{26} \\ C_{31} & C_{32} & C_{33} & 0 & 0 & C_{36} \\ 0 & 0 & 0 & C_{44} & C_{45} & 0 \\ 0 & 0 & 0 & C_{54} & C_{55} & 0 \\ C_{61} & C_{62} & C_{63} & 0 & 0 & C_{66} \end{bmatrix}$$

2-3

In case of three mutually perpendicular planes of material symmetry, we have the orthotropic material and 9 independent constants will be the result [2]:

$$\begin{bmatrix} C_{11} & C_{12} & C_{13} & 0 & 0 & 0 \\ C_{21} & C_{22} & C_{23} & 0 & 0 & 0 \\ C_{31} & C_{32} & C_{33} & 0 & 0 & 0 \\ 0 & 0 & 0 & C_{44} & 0 & 0 \\ 0 & 0 & 0 & 0 & C_{55} & 0 \\ 0 & 0 & 0 & 0 & 0 & C_{66} \end{bmatrix}$$

2-4

As defined in section 2.1, when all surfaces which are passing from one point in material are symmetry elastic surfaces, the material is isotropic. The independent constants are reduced to only 2 as shown in 2-5 equation [2].

$$\begin{bmatrix} C_{11} & C_{12} & C_{12} & 0 & 0 & 0 \\ C_{12} & C_{11} & C_{12} & 0 & 0 & 0 \\ C_{12} & C_{12} & C_{11} & 0 & 0 & 0 \\ 0 & 0 & 0 & \dfrac{C_{11}-C_{12}}{2} & 0 & 0 \\ 0 & 0 & 0 & 0 & \dfrac{C_{11}-C_{12}}{2} & 0 \\ 0 & 0 & 0 & 0 & 0 & \dfrac{C_{11}-C_{12}}{2} \end{bmatrix} \qquad \text{2-5}$$

The stiffness matrix $[C]$ is defined for a lamina that is made by the fiber and the matrix and has mostly one symmetry surface or more. The matrix $[C]$ parameters (material properties) are calculated by mechanical constants of the lamina; therefore each stiffness matrix exhibits the properties of one lamina. Usually a composite structure is made of a stack of layup known as laminate and each lamina may have different orientations or mechanical constants. Consequently the laminate formulations should also be established.

## 2.3 Laminate Calculation

In this chapter two theoretical laminate calculations and one FEM method are introduced. The output of the first method (Classical laminate theory) is used as the input for the FEM software simulation and they create the average method. The second method results (Strain and stress with ABD matrix) could be compared with the third method (FEM simulation results) and of course the average method. These methods are used for analyzing the composite structure.

### 2.3.1 Classical Laminate Theory

The classical laminate theory (CLT) is a basic method for obtaining the stress and strain of multi-ply inhomogeneous laminate lay-ups for all of the orthotropic composite laminates. The procedure used in this method considers all ply mechanical constants and their orientation angles. First all local coordinate systems should be reoriented into the global coordinate system. Then plies are added together by considering each ply thickness and each ply mechanical constants (if the material properties of the lamina are different). The result of this process is an average mechanical constant for the whole laminate.

It should be noted that this method provides a good estimation of stress and strain according to tension stress. However the CLT method also considers twists, and bends that arise when coplanar forces are applied to non-orthotropic laminate lay-ups

and treats the laminate as a plane and considers coplanar stresses and deformations only. This simplification affects the precision of the result in the CLT method.

These two assumptions are also taken into account for the CTL method calculation:
- In this method the smallest element is a ply (known as lamina), as mentioned in section 2-1 a ply consists of the fiber and the matrix which have different mechanical constants, and here the average mechanical constant of the ply is used as an input. With this action the ply is "homogenized".
- For the calculation on the laminate, it is considered that all plies are completely stacked and fixed to each other. [All of the formulations of this section are based on reference 3]

What is necessary as an input for calculation is mechanical constants of plies; these constants can be found in composite standards or factory product details (based on rules of a mixture of the fiber and the matrix):

- $E_1$ :   Elasticity modulus of ply in fibers direction

- $E_2$ :   Elasticity modulus of ply transverse to fibers direction

- $G_{12}$ : Shear modulus of ply

- $\nu$ :    Poison ratio of ply

The first step is to calculate the plies rigidity matrix $[Q]_k$ (k is the number of plies), for orthotropic plies in the ply coordinate system $[Q]_k$ defined as follow:

$$
[Q]_k = \begin{bmatrix} Q_{21} & Q_{12} & 0 \\ Q_{21} & Q_{22} & 0 \\ 0 & 0 & Q_{33} \end{bmatrix} = \begin{bmatrix} \dfrac{E_1}{1-\nu_{12}^2 \cdot \dfrac{E_2}{E_1}} & \dfrac{\nu_{12} \cdot E_2}{1-\nu_{12}^2 \cdot \dfrac{E_2}{E_1}} & 0 \\ \dfrac{\nu_{12} \cdot E_2}{1-\nu_{12}^2 \cdot \dfrac{E_2}{E_1}} & \dfrac{E_2}{1-\nu_{12}^2 \cdot \dfrac{E_2}{E_1}} & 0 \\ 0 & 0 & G_{12} \end{bmatrix}
\qquad 2\text{-}6
$$

The second step is to transform the rigidity matrix of each ply from the local coordinate system of ply (PlyCS) to the global coordinate system of the laminate (LamCS).

$$
[Q]_{LamCS,k} = [T]_k \cdot [Q]_{PlyCS,k} \cdot [T]_k^T
\qquad 2\text{-}7
$$

The transformer matrix $[T]_k$ in equation 2-7 is defined as follow:

$$[\mathrm{T}]_k = \begin{bmatrix} \cos^2 & \sin^2 & 2\sin\cos \\ \sin^2 & \cos^2 & -2\sin\cos \\ -\sin\cos & \sin\cos & \cos^2-\sin^2 \end{bmatrix}$$ 

2-8

And the transverse of the transformer matrix $[T]_k^T$ is:

$$[\mathrm{T}]^T{}_k = \begin{bmatrix} \cos^2 & \sin^2 & -\sin\cos \\ \sin^2 & \cos^2 & \sin\cos \\ 2\sin\cos & -2\sin\cos & \cos^2-\sin^2 \end{bmatrix}$$

2-9

The angle is positive when the one axis of the ply coordinate system is rotated positively (counterclockwise, CCW) toward the one axis of laminate coordinate system.

The third step is to calculate the stiffness matrix of the laminate $[A]$, which is the sum of all transformed plies rigidity and the influence of the ply thickness:

$$[A] = \sum_k \frac{t_k}{t_{lam}} \cdot [Q]_{LamCS,k}$$

2-10

The forth step is to invert the stiffness matrix of the laminate $[A]$ for getting to the flexibility matrix of the laminate $[a]$:

$$[a] = [A]^{-1}$$

2-11

The mechanical constants of the laminate are obtained from elements of the flexibility matrix: [3]

$$[a] = \begin{bmatrix} a_{11} & a_{12} & a_{13} \\ a_{21} & a_{22} & a_{23} \\ a_{31} & a_{32} & a_{33} \end{bmatrix}$$

2-12

- $E_{x,Lam} = \dfrac{1}{a_{11}}$

- $E_{y,Lam} = \dfrac{1}{a_{22}}$

2-13

- $G_{xy,Lam} = \dfrac{1}{a_{33}}$

- $V_{xy,Lam} = V_{yx,Lam} = \dfrac{-a_{21}}{a_{11}}$

The process for calculating the stress and strain can be found in the "handbook of composite.2003 chapter 1 by Herbert Funke" [3], in this project the mechanical constants are not used for calculating the stress and strain, but are used as an input for FEM software which will be described as the "average method" in chapter 3 and 4.

## 2.3.2 Stress_Strain relation with ABD matrix for a laminate

This method known as the ABD method calculates the strain and curvature of the laminate at the middle surface in macro mechanic analysis. The forces and moments are inputs for the ABD equation and the ABD matrix should be obtained from the laminate properties. The result of the equation will give the strain and curvature of the laminate. In this section the theory behind the ABD matrix and its equation will be described. Following the calculation procedure we will gain some knowledge about the ABD matrix and final equation parameters, and also how they can be used. This method is considered as the basic theoretical method in this project. [All of the formulations of this section are based on reference 2]

### 2.3.2.1 Strain equation

In this section the equations will be developed for a plate under in-plane loads such as shear and axial forces, and bending and twisting moments (figure 2-1). The basic equations are borrowed from the classical laminate theory (CLT), but they will be developed to have a precise result for the behavior of a laminate under shear force and bending or twisting moments. Here are some assumptions for this method:

- Each lamina is elastic, orthotropic and homogeneous.
- A line straight and perpendicular to the middle surface remains straight and perpendicular to the middle surface during deformation.
- The laminate is thin and is loaded just in its plane.
- Displacements are small throughout the laminate and continuous.
- It is assumed that no slip occurs between the lamina surfaces [2].

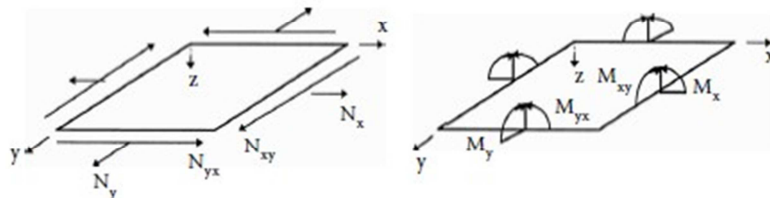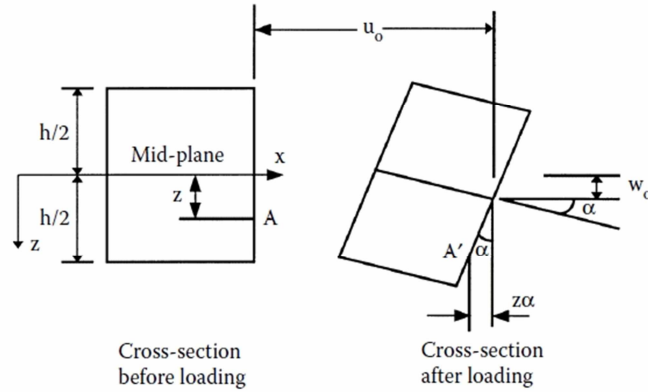*Figure 2-1: Forces and moments on a laminate*

*Figure 2-2: displacement of middle surface and curvature*



In figure 2-2 the section of a plate is shown. The coordinate system center is placed on mid plane (Z=0). Consider $u_0, v_0, w_0$ as the mid-plane displacements in x, y, z directions, respectively displacements at any point in x, y, z directions are $u, v, w$. At any point except at the mid-plane, displacements in the x–y plane are dependent on the axial location of the point and the slope of the laminate mid-plane with the x and y directions. So it can be written:

$$u = u_0 - z\alpha \quad \text{(For small angles} \sin\alpha \sim \alpha\text{)}$$

2-14

$$\alpha = \frac{\partial w_0}{\partial x}$$

2-15

So the u displacement in x direction will be:

$$u = u_0 - z\frac{\partial w_0}{\partial x}$$

2-16

In the same way a cross section in the y–z plane is considered and it will lead to the displacement in the y direction:

$$v = v_0 - z\frac{\partial w_0}{\partial y}$$

2-17

Using the definition of strain in x-y and 2-16 and 2-17 we have:

$$\varepsilon_x = \frac{\partial u}{\partial x} = \frac{\partial u_0}{\partial x} - z\frac{\partial^2 w_0}{\partial x^2}$$

2-18-1

$$\varepsilon_y = \frac{\partial v}{\partial y} = \frac{\partial v_0}{\partial y} - z\frac{\partial^2 w_0}{\partial y^2}$$

2-18-2

$$\gamma_{xy} = \frac{\partial u}{\partial y} + \frac{\partial v}{\partial x} = \frac{\partial u_0}{\partial y} + \frac{\partial v_0}{\partial x} - 2z\frac{\partial^2 w_0}{\partial x \partial y}$$

<div align="right">2-18-3</div>

The strain-displacement equations can be written in the matrix form (2-18-1 to 3) like:

$$\left\{\begin{array}{c} \varepsilon_x \\ \varepsilon_y \\ \gamma_{xy} \end{array}\right\} = \left\{\begin{array}{c} \dfrac{\partial u_0}{\partial x} \\ \dfrac{\partial v_0}{\partial y} \\ \dfrac{\partial u_0}{\partial y} + \dfrac{\partial v_0}{\partial x} \end{array}\right\} + z\left\{\begin{array}{c} -\dfrac{\partial^2 w_0}{\partial x^2} \\ -\dfrac{\partial^2 w_0}{\partial y^2} \\ -2\dfrac{\partial^2 w_0}{\partial x \partial y} \end{array}\right\}$$

<div align="right">2-19</div>

The strain of the mid-surface in equation 2-19 is:

$$\left\{\begin{array}{c} \varepsilon_x^0 \\ \varepsilon_y^0 \\ \gamma_{xy}^0 \end{array}\right\} = \left\{\begin{array}{c} \dfrac{\partial u_0}{\partial x} \\ \dfrac{\partial v_0}{\partial y} \\ \dfrac{\partial u_0}{\partial y} + \dfrac{\partial v_0}{\partial x} \end{array}\right\}$$

<div align="right">2-20</div>

And curvature of mid-surface is:

$$\left\{\begin{array}{c} \kappa_x \\ \kappa_y \\ \kappa_{xy} \end{array}\right\} = \left\{\begin{array}{c} -\dfrac{\partial^2 w_0}{\partial x^2} \\ -\dfrac{\partial^2 w_0}{\partial y^2} \\ -2\dfrac{\partial^2 w_0}{\partial x \partial y} \end{array}\right\}$$

<div align="right">2-21</div>

Hence the strain of the laminate can be written like equation 2-22:

$$\left\{\begin{array}{c} \varepsilon_x \\ \varepsilon_y \\ \gamma_{xy} \end{array}\right\} = \left\{\begin{array}{c} \varepsilon_x^0 \\ \varepsilon_y^0 \\ \gamma_{xy}^0 \end{array}\right\} + z\left\{\begin{array}{c} \kappa_x \\ \kappa_y \\ \kappa_{xy} \end{array}\right\}$$

<div align="right">2-22</div>

The equation 2-22 makes a linear relation between the strains and the curvatures of the laminate. This equation also proves that strains are independent of the x and y coordinates.

### 2.3.2.2 The forces and moments vectors related to strains and curvatures

If the strains at any point along the laminate thickness are known, equation 2-23 can be written as follows:

$$\begin{bmatrix} \sigma_x \\ \sigma_y \\ \tau_{xy} \end{bmatrix} = \begin{bmatrix} \bar{Q}_{11} & \bar{Q}_{12} & \bar{Q}_{16} \\ \bar{Q}_{12} & \bar{Q}_{22} & \bar{Q}_{26} \\ \bar{Q}_{16} & \bar{Q}_{26} & \bar{Q}_{66} \end{bmatrix} \begin{bmatrix} \varepsilon_x \\ \varepsilon_y \\ \gamma_{xy} \end{bmatrix} \qquad\qquad 2\text{-}23$$

The reduced transformed stiffness matrix $\begin{bmatrix} \bar{Q} \end{bmatrix}$ is related to the ply of the laminate which the point is positioned on. Substituting equation 2-23 in equation 2-22 will give:

$$\begin{bmatrix} \sigma_x \\ \sigma_y \\ \tau_{xy} \end{bmatrix} = \begin{bmatrix} \bar{Q}_{11} & \bar{Q}_{12} & \bar{Q}_{16} \\ \bar{Q}_{12} & \bar{Q}_{22} & \bar{Q}_{26} \\ \bar{Q}_{16} & \bar{Q}_{26} & \bar{Q}_{66} \end{bmatrix} \begin{bmatrix} \varepsilon_x^0 \\ \varepsilon_y^0 \\ \gamma_{xy}^0 \end{bmatrix} + z \begin{bmatrix} \bar{Q}_{11} & \bar{Q}_{12} & \bar{Q}_{16} \\ \bar{Q}_{12} & \bar{Q}_{22} & \bar{Q}_{26} \\ \bar{Q}_{16} & \bar{Q}_{26} & \bar{Q}_{66} \end{bmatrix} \begin{bmatrix} \kappa_x \\ \kappa_y \\ \kappa_{xy} \end{bmatrix} \qquad 2\text{-}24$$

Although the strains and the curvature in equation 2-22 are unknown, equation 2-24 gives the stresses in each layer based on these unknowns. Therefore the stresses in each lamina can be integrated through the laminate thickness to give resultant forces and moments. By having the forces and moments, the strains and curvature at mid-surface of the laminate can also be calculated as will be described below:

The thickness of the whole laminate is considered (h) and the plies number is (n), as illustrated in figure 2-3.

*Figure 2-3: positions of plies in a laminate*
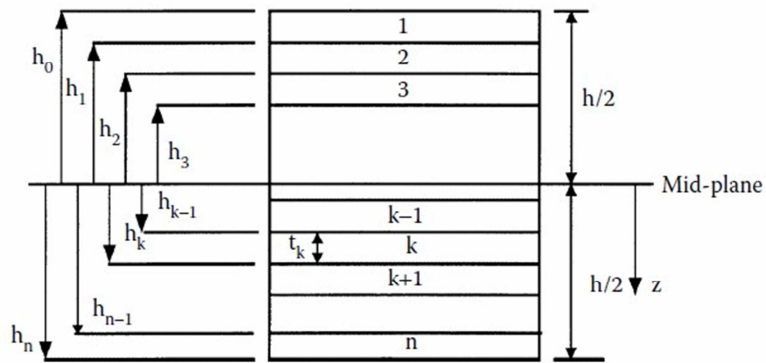


$$h = \sum_{k=1}^{n} t_k \qquad\qquad 2\text{-}25$$

In equation 2-17 the thickness of the laminate h is the sum of all the plies thicknesses $t_k$ (k from 1 to n). The mid-surface position in z direction is h/2 and the upper and

lower surfaces of $k^{th}$ layer position in z direction have been defined below in equations 2-26 and 2-27 $(k = 2,...,n-1)$.

$$h_{k-1} = -\frac{h}{2} + \sum_1^{k-1} t \quad \text{Upper surface} \qquad \text{2-26}$$

$$h_k = -\frac{h}{2} + \sum_1^{k} t \quad \text{Lower surface} \qquad \text{2-27}$$

Integrating the whole plies stresses gives the forces per length (N) in the x-y surface, and in the same way, integrating the whole plies stresses multiply to thickness parameter Z gives the moments per length (M) as shown below:

$$N_x = \int_{-h/2}^{h/2} \sigma_x dz \quad ; \text{Normal force per unit length} \qquad \text{2-28-1}$$

$$N_y = \int_{-h/2}^{h/2} \sigma_y dz \quad ; \text{Norma force per unit length} \qquad \text{2-28-2}$$

$$N_{xy} = \int_{-h/2}^{h/2} \tau_{xy} dz \quad ; \text{Shear force per unit length} \qquad \text{2-28-3}$$

$$M_x = \int_{-h/2}^{h/2} \sigma_x z dz \quad ; \text{Bending moment per unit length} \qquad \text{2-28-4}$$

$$M_y = \int_{-h/2}^{h/2} \sigma_y z dz \quad ; \text{Bending moment per unit length} \qquad \text{2-28-5}$$

$$M_{xy} = \int_{-h/2}^{h/2} \tau_{xy} z dz \quad ; \text{Twisting moment per unit length} \qquad \text{2-28-6}$$

The 2-28 equations can be written in the matrix form like:

$$\begin{bmatrix} N_x \\ N_y \\ N_{xy} \end{bmatrix} = \int_{-h/2}^{h/2} \begin{bmatrix} \sigma_x \\ \sigma_y \\ \tau_{xy} \end{bmatrix} dz \qquad \text{2-29-1}$$

$$\begin{bmatrix} M_x \\ M_y \\ M_{xy} \end{bmatrix} = \int\limits_{-h/2}^{h/2} \begin{bmatrix} \sigma_x \\ \sigma_y \\ \tau_{xy} \end{bmatrix} z\,dz \qquad\qquad\qquad\qquad 2\text{-}29\text{-}2$$

And considering the whole thickness of the laminate (see equation 2-25) will give:

$$\begin{bmatrix} N_x \\ N_y \\ N_{xy} \end{bmatrix} = \sum_{k=1}^{n} \int\limits_{h_{k-1}}^{h_k} \begin{bmatrix} \sigma_x \\ \sigma_y \\ \tau_{xy} \end{bmatrix}_k dz \qquad\qquad\qquad\qquad 2\text{-}30\text{-}1$$

$$\begin{bmatrix} M_x \\ M_y \\ M_{xy} \end{bmatrix} = \sum_{k=1}^{n} \int\limits_{h_{k-1}}^{h_k} \begin{bmatrix} \sigma_x \\ \sigma_y \\ \tau_{xy} \end{bmatrix}_k z\,dz \qquad\qquad\qquad\qquad 2\text{-}30\text{-}2$$

Now to create a relation between the strains and stresses, it is necessary to insert equation 2-30 into equation 2-24, which gives:

$$\begin{bmatrix} N_x \\ N_y \\ N_{xy} \end{bmatrix} = \sum_{k=1}^{n} \int\limits_{h_{k-1}}^{h_k} \begin{bmatrix} \overline{Q}_{11} & \overline{Q}_{12} & \overline{Q}_{16} \\ \overline{Q}_{12} & \overline{Q}_{22} & \overline{Q}_{26} \\ \overline{Q}_{16} & \overline{Q}_{26} & \overline{Q}_{66} \end{bmatrix}_k \begin{bmatrix} \varepsilon_x^0 \\ \varepsilon_y^0 \\ \gamma_{xy}^0 \end{bmatrix} dz + \sum_{k=1}^{n} \int\limits_{h_{k-1}}^{h_k} \begin{bmatrix} \overline{Q}_{11} & \overline{Q}_{12} & \overline{Q}_{16} \\ \overline{Q}_{12} & \overline{Q}_{22} & \overline{Q}_{26} \\ \overline{Q}_{16} & \overline{Q}_{26} & \overline{Q}_{66} \end{bmatrix}_k \begin{bmatrix} \kappa_x \\ \kappa_y \\ \kappa_{xy} \end{bmatrix} z\,dz \qquad 2\text{-}31\text{-}1$$

$$\begin{bmatrix} M_x \\ M_y \\ M_{xy} \end{bmatrix} = \sum_{k=1}^{n} \int\limits_{h_{k-1}}^{h_k} \begin{bmatrix} \overline{Q}_{11} & \overline{Q}_{12} & \overline{Q}_{16} \\ \overline{Q}_{12} & \overline{Q}_{22} & \overline{Q}_{26} \\ \overline{Q}_{16} & \overline{Q}_{26} & \overline{Q}_{66} \end{bmatrix}_k \begin{bmatrix} \varepsilon_x^0 \\ \varepsilon_y^0 \\ \gamma_{xy}^0 \end{bmatrix} z\,dz + \sum_{k=1}^{n} \int\limits_{h_{k-1}}^{h_k} \begin{bmatrix} \overline{Q}_{11} & \overline{Q}_{12} & \overline{Q}_{16} \\ \overline{Q}_{12} & \overline{Q}_{22} & \overline{Q}_{26} \\ \overline{Q}_{16} & \overline{Q}_{26} & \overline{Q}_{66} \end{bmatrix}_k \begin{bmatrix} \kappa_x \\ \kappa_y \\ \kappa_{xy} \end{bmatrix} z^2\,dz \qquad 2\text{-}31\text{-}2$$

As mentioned in section 2-3-2-1 the strains and curvatures of the mid-surface are independent of the Z axis. Also the reduced transformed stiffness matrixes $\begin{bmatrix} \overline{Q} \end{bmatrix}$ are constant for each ply, hence they could get out of integrations. Equation 2-31 can then be rewritten as:

$$\begin{bmatrix} N_x \\ N_y \\ N_{xy} \end{bmatrix} = \left\{ \sum_{k=1}^{n} \begin{bmatrix} \overline{Q}_{11} & \overline{Q}_{12} & \overline{Q}_{16} \\ \overline{Q}_{12} & \overline{Q}_{22} & \overline{Q}_{26} \\ \overline{Q}_{16} & \overline{Q}_{26} & \overline{Q}_{66} \end{bmatrix}_k \int\limits_{h_{k-1}}^{h_k} dz \right\} \begin{bmatrix} \varepsilon_x^0 \\ \varepsilon_y^0 \\ \gamma_{xy}^0 \end{bmatrix} + \left\{ \sum_{k=1}^{n} \begin{bmatrix} \overline{Q}_{11} & \overline{Q}_{12} & \overline{Q}_{16} \\ \overline{Q}_{12} & \overline{Q}_{22} & \overline{Q}_{26} \\ \overline{Q}_{16} & \overline{Q}_{26} & \overline{Q}_{66} \end{bmatrix}_k \int\limits_{h_{k-1}}^{h_k} z\,dz \right\} \begin{bmatrix} \kappa_x \\ \kappa_y \\ \kappa_{xy} \end{bmatrix}$$

$$2\text{-}32\text{-}1$$

$$\begin{bmatrix} M_x \\ M_y \\ M_{xy} \end{bmatrix} = \left\{ \sum_{k=1}^{n} \begin{bmatrix} \overline{Q}_{11} & \overline{Q}_{12} & \overline{Q}_{16} \\ \overline{Q}_{12} & \overline{Q}_{22} & \overline{Q}_{26} \\ \overline{Q}_{16} & \overline{Q}_{26} & \overline{Q}_{66} \end{bmatrix}_k \int\limits_{h_{k-1}}^{h_k} z\,dz \right\} \begin{bmatrix} \varepsilon_x^0 \\ \varepsilon_y^0 \\ \gamma_{xy}^0 \end{bmatrix} + \left\{ \sum_{k=1}^{n} \begin{bmatrix} \overline{Q}_{11} & \overline{Q}_{12} & \overline{Q}_{16} \\ \overline{Q}_{12} & \overline{Q}_{22} & \overline{Q}_{26} \\ \overline{Q}_{16} & \overline{Q}_{26} & \overline{Q}_{66} \end{bmatrix}_k \int\limits_{h_{k-1}}^{h_k} z^2\,dz \right\} \begin{bmatrix} \kappa_x \\ \kappa_y \\ \kappa_{xy} \end{bmatrix}$$

Knowing that:

$$\int_{h_{k-1}}^{h_k} dz = (h_k - h_{k-1})$$

$$\int_{h_{k-1}}^{h_k} z\,dz = \frac{1}{2}(h_k^2 - h_{k-1}^2)$$

$$\int_{h_{k-1}}^{h_k} z^2\,dz = \frac{1}{3}(h_k^3 - h_{k-1}^3)$$

And substituting in equation 2-32 will give:

$$\begin{bmatrix} N_x \\ N_y \\ N_{xy} \end{bmatrix} = \begin{bmatrix} A_{11} & A_{12} & A_{16} \\ A_{21} & A_{22} & A_{26} \\ A_{61} & A_{62} & A_{66} \end{bmatrix} \begin{bmatrix} \varepsilon_x^0 \\ \varepsilon_y^0 \\ \gamma_{xy}^0 \end{bmatrix} + \begin{bmatrix} B_{11} & B_{12} & B_{16} \\ B_{21} & B_{22} & B_{26} \\ B_{61} & B_{62} & B_{66} \end{bmatrix} \begin{bmatrix} \kappa_x \\ \kappa_y \\ \kappa_{xy} \end{bmatrix} \qquad \text{2-33-1}$$

$$\begin{bmatrix} M_x \\ M_y \\ M_{xy} \end{bmatrix} = \begin{bmatrix} B_{11} & B_{12} & B_{16} \\ B_{21} & B_{22} & B_{26} \\ B_{61} & B_{62} & B_{66} \end{bmatrix} \begin{bmatrix} \varepsilon_x^0 \\ \varepsilon_y^0 \\ \gamma_{xy}^0 \end{bmatrix} + \begin{bmatrix} D_{11} & D_{12} & D_{16} \\ D_{21} & D_{22} & D_{26} \\ D_{61} & D_{62} & D_{66} \end{bmatrix} \begin{bmatrix} \kappa_x \\ \kappa_y \\ \kappa_{xy} \end{bmatrix} \qquad \text{2-33-2}$$

Which:

$$A_{ij} = \sum_{k=1}^{n} \left[ \left( \bar{Q}_{ij} \right) \right]_k (h_k - h_{k-1}) \; ; \; i = 1, 2, 6 \; ; \; j = 1, 2, 6 \qquad \text{2-34-1}$$

$$B_{ij} = \frac{1}{2} \sum_{k=1}^{n} \left[ \left( \bar{Q}_{ij} \right) \right]_k \left( h_k^2 - h_{k-1}^2 \right) \; ; \; i = 1, 2, 6 \; ; \; j = 1, 2, 6 \qquad \text{2-34-2}$$

$$D_{ij} = \frac{1}{3} \sum_{k=1}^{n} \left[ \left( \bar{Q}_{ij} \right) \right]_k \left( h_k^3 - h_{k-1}^3 \right) \; ; \; i = 1, 2, 6 \; ; \; j = 1, 2, 6 \qquad \text{2-34-3}$$

Finally by combining equations 2-33-1 and 2-33-2 and positioning $[A]$ as the extensional stiffness matrix, $[B]$ as the coupling stiffness matrix and $[D]$ as the bending stiffness matrix, will simultaneously result in six linear equations and six unknowns, as shown below [1,2,7]:

$$\begin{Bmatrix} N_x \\ N_y \\ N_{xy} \\ - \\ M_x \\ M_y \\ M_{xy} \end{Bmatrix} = \begin{bmatrix} A_{11} & A_{12} & A_{16} & | & B_{11} & B_{12} & B_{16} \\ A_{21} & A_{22} & A_{26} & | & B_{21} & B_{22} & B_{26} \\ A_{61} & A_{62} & A_{66} & | & B_{61} & B_{62} & B_{66} \\ - & - & - & + & - & - & - \\ B_{11} & B_{12} & B_{16} & | & D_{11} & D_{12} & D_{16} \\ B_{21} & B_{22} & B_{26} & | & D_{21} & D_{22} & D_{26} \\ B_{61} & B_{62} & B_{66} & | & D_{61} & D_{62} & D_{66} \end{bmatrix} \begin{Bmatrix} \varepsilon_x^0 \\ \varepsilon_y^0 \\ \gamma_{xy}^0 \\ - \\ \kappa_x \\ \kappa_y \\ \kappa_{xy} \end{Bmatrix}$$

2-34

The extensional stiffness matrix $[A]$ relates the resultant in-plane forces $\{N\}$ to the in-plane strains $\{\varepsilon\}$, and the bending stiffness matrix $[D]$ relates the resultant bending moments $\{M\}$ to the plane curvatures $\{\kappa\}$. The coupling stiffness matrix $[B]$ couples the force terms $\{N\}$ to the mid-plane curvatures $\{\kappa\}$ and the moment terms $\{M\}$ to the mid-plane strains $\{\varepsilon\}$ [2]. In contrast with the CLT method (2.3.1), the ABD method considers the bending and twisting forces or moments and because of that the couple strains and the curvatures are considered by the software as it is illustrated in figure 2-4 [4]:

*Figure 2-4: positions of plies in a laminate*
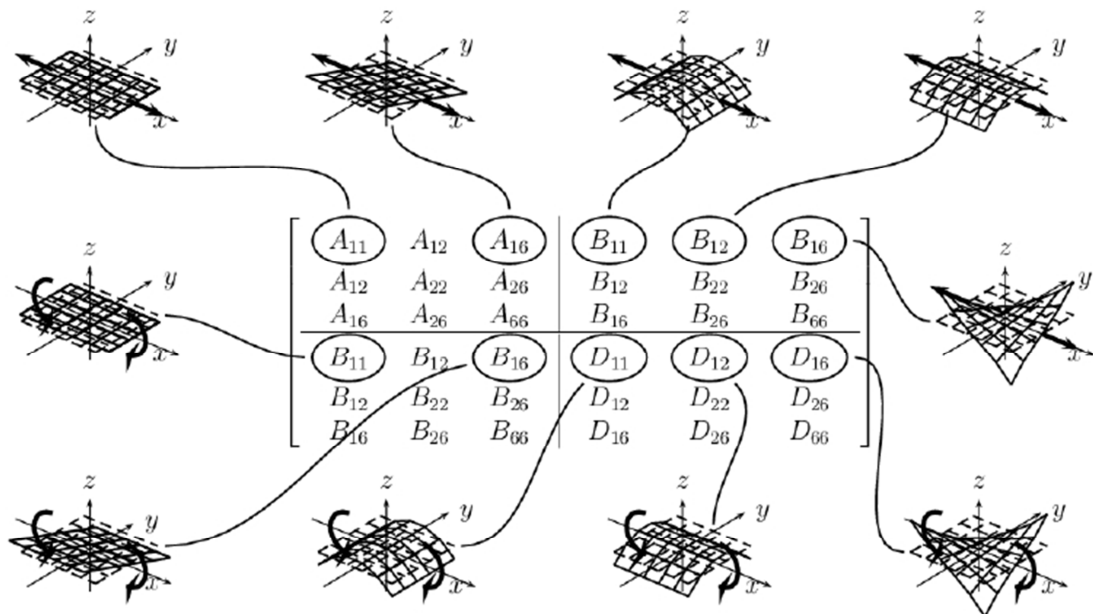


This method which, in this project, is called the ABD method is considered as the basic theoretical method for calculating the strain and the curvature of a laminate under applied forces or moments. Equation 2-34 is the final equation that will be used for the ABD method.

## 2.3.3 FEM method

In this section the Finite Element Methods (FEM) for composite Analysis have been presented. These two methods are called:

- Average method
- Complete method

### 2.3.3.1 Average method

In the average method after modeling the entire composite section in the CAD software, the neutral surface or mid-surface of the composite part should be modeled in the FEM software. In this method this surface will just be used to analyze the composite part. Therefore instead of modeling the whole plies, the average mechanical constant is used as an input for the composite material. These constants are calculated by using the CLT method (described in section 2.3.1).

In the CLT method the material properties of each ply, which are $E_1, E_2, G_{12}, v_{12}$, are available. The thickness and orientation of each ply in the laminate is also given. After using the CLT method and calculating the matrixes, the laminate average of the mechanical constants $(E_{x,Lam}, E_{y,Lam}, G_{xy,Lam}, v_{xy,Lam} = v_{yx,Lam})$ will be obtained from the flexibility matrix. These constants now should be imported into the FEM software as the composite mechanical constants. The sum of the plies thickness (laminate thickness) is considered for neutral surface thickness in the FEM software. The forces and moments and also the boundary conditions are used similar to normal FEM analysis without any special change on part.

In simple words, a surface is modeled instead of the part, and then the calculated average mechanical constants of all plies are located for the mechanical constants of the surface in the FEM software.

### 2.3.3.2 Complete method

In this method as can be seen from its name all plies are modeled ply by ply in the FEM software similar to real model layup. In the average method the angles of the plies are considered in the CLT formulation for calculating the average properties of the laminate. Hence in the average method there is no inputting of the ply angle. However at the complete simulation process, the angle of each ply is also included. In this project, the ply is considered as the smallest part of the laminate and in this method the laminate is modeled ply by ply with their angles. And the mechanical constants of each ply are inputted at the FEM software without any pre-calculation. That is why this method is called the complete method.

The best way to have the overview of the strength and the weakness of each method is to use all methods available for a sample and compare their results. These modellings and compartments have been described in chapter 3 for two samples.

# 3 Comparing the Methods in Simple Samples

In chapter 2, two theoretical methods (CLT, ABD) and two FEM methods (the average and complete method) were described. These methods could be used independently such as in the case of ABD or complete methods, or they could use each other's data like in the CLT method which create input for the average method. In this chapter all these methods have been applied for two simple samples to:

- Introduce each model in a real example
- Compare these methods to each other
- Realize the advantage and disadvantage of each method

In this chapter four methods have been applied for one sample and the results have been compared to each other. The $3^{rd}$ and $4^{th}$ methods are actually the same but with different FEM software. The goal for using two FEM software for one method is to establish the precision of the FEM software. These methods are:

- Theoretical calculations with the ABD matrix
- CATIA FEM simulation with average elastic factors
- CATIA FEM simulation with complete layups modeling
- ANSYS FEM simulation with complete layup modeling

The procedure for each method has been described in chapter 2. However, they have been described here again in brief. In the theoretical method, the parameters of the ABD matrix are calculated based on material properties and layup information. Then by placing the ABD matrix in Hooke's law, the strain or curvature can be calculated. In the second method the average elasticity factors are calculated based on the quasi isotropic formulation to see how close the results of this method are to those that are obtained by the theory method. The last two methods have the same simulation strategy, but in a different FEM software. In these methods layups are created on the components, and the input factors are the properties of each layer without simplification. The goal is to estimate the accuracy of each FEM software method in composite analysis.

## 3.1 Pre-knowledge about composite

Before getting started with the samples, it is important to have prior knowledge about the composite.

### 3.1.1 Notation

The type of layup should also be clear, because in all methods the angle of the ply should be clear. For example in the CLT method the angle of each ply is converted from the local coordinate to the laminate coordinate system. In figure 3-1 different types of layups have been shown and next to each one its notation has been written. Each laminate has one notation which shows the angles and the type of layup [5].

*Figure 3-1: Laminate types and their notations*
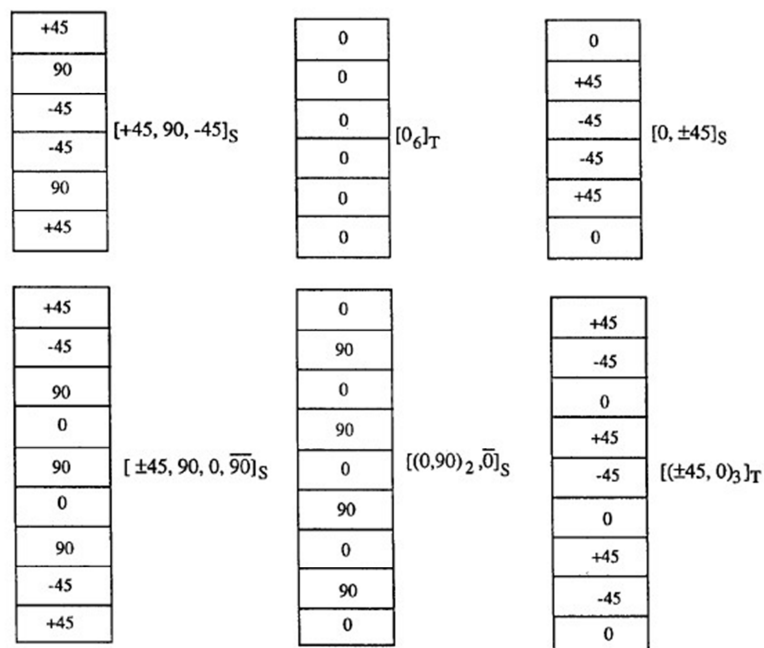


### 3.1.2 Mechanical constants

The mechanical constants are used in all methods as an input for plies properties. The ply material is a regular epoxy-carbon unidirectional, which is a very common composite material in the industry. In this chapter this material is used for both samples with the following properties [8]:

Table 3-1: Mechanical constants of epoxy carbon

| Constant | Amount |
|---|---|
| Layer thickness (ply) | $0,25\ [mm]$ |
| Longitude stiffness $E_1$ | $135000\ [N/mm^2]$ |
| Transverse stiffness $E_2$ | $9500\ [N/mm^2]$ |
| Shear stiffness $G_{12}$ | $5270\ [N/mm^2]$ |
| Poisson ratio $V_{12}$ | $0,326$ |

# 3.2 Sample1: Cylinder under Pressure

## 3.2.1 Introducing the Sample

The test component is a cylindrical tube (figure 3-1) under pressure. It is useful to mention that the theoretical calculation for the whole part is a long and complicated process. Hence by considering that the normal and shear stress are constant on the surface of the cylinder, considering one square element on the cylinder will reduce the theoretical calculation to one element instead of the whole surface. This assumption needs some pre-calculations to get to the surface forces which are acting on elements from the internal pressures of the cylinder. [6,8]

For this sample two types of layup have been applied. The first layup type is $\left[0,\ 45,-45,\ 90,\overline{0}\right]_S$ and this 9 layer layup as mentioned in figure 2-2, leads to a symmetric orthotropic laminate layup for the composite component. The second layup type is $\left[0,\ 45,-45,\ 90\right]_2$ and this 8 layer layup gives us a quasi-isotropic laminate.

Figure 3-1: sample 1 cylinder under pressure
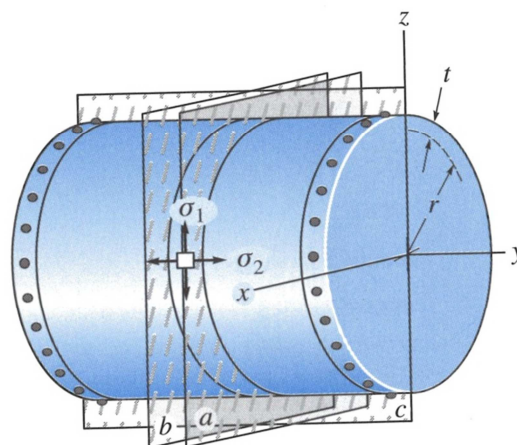
*Figure 3-2: sections on cylinder*
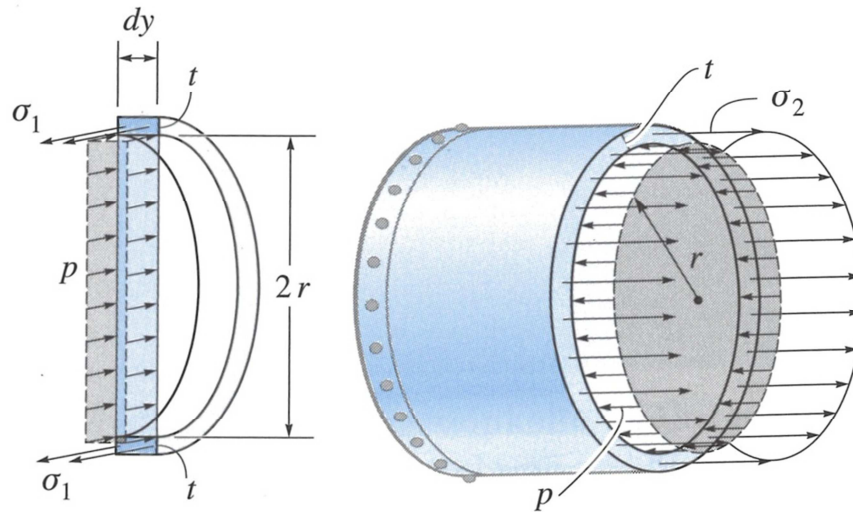
By creating a section on the cylinder (figure 3-2 [6]), a balanced equation can be written to obtain the surface stresses:

By considering:

$$\sum F_x = 0 \; ; \quad 2\left[\sigma_1\left(tdy\right)\right] - p\left(2rdy\right) = 0$$

Then we have:

$$\sigma_1 = \frac{pr}{t} \qquad\qquad\qquad 3\text{-}1$$

By considering:

$$\sum F_y = 0 \; ; \quad \sigma_2\left(2\pi rt\right) - p\left(\pi r^2\right) = 0$$

Then we have:

$$\sigma_2 = \frac{pr}{2t} \qquad\qquad\qquad 3\text{-}2$$

Table 3-2 shows the properties of the cylinder:

*Table 3-2: layup properties of cylinder*

| Properties of Cylinder | 9 layer layup | 8 layer layup |
|---|---|---|
| Pressure (p) MPa | 5 | 5 |
| Radios of cylinder (r) mm | 10 | 10 |
| Thickness of cylinder (t) mm | $(9\times0,25)=2,25$ | $(8\times0,25)=2$ |
| Thickness area of square element (A) mm² | $(2\times2,25)=4,5$ | $(2\times2)=4$ |

By incorporating the properties of the cylinder into the formulations (3-1, 3-2), both types of force for the layup can be calculated:

For the 9 layer layup:

$\sigma_1 = 22,22 \text{ MPa}$ ; $\sigma_2 = 11,11 \text{ MPa}$

For 8 layer layup:

$\sigma_1 = 25 \text{ MPa}$ ; $\sigma_2 = 12,5\text{MPa}$

The input loadings for the theoretical method are forces (ABD method); by using stress formulations the forces per surface are calculated easily:

For 9 layer layup:

$N_{1,2} = \sigma_{1,2} \times t$

$N_1 = 50 \dfrac{N}{mm}$; $N_2 = 25 \dfrac{N}{mm}$

For 8 layer layup:

$N_{1,2} = \sigma_{1,2} \times t$

$N_1 = 50 \dfrac{N}{mm}$; $N_2 = 25 \dfrac{N}{mm}$

## 3.2.2 Theoretical calculation with ABD matrix

First the ABD matrix should be calculated for the cylinder based on the material and layup properties. Then the ABD matrix and the calculated forces for the square element should be placed into Hooke's law equation. After solving the equation, strains $\left(\varepsilon_x, \varepsilon_y, \varepsilon_{xy}\right)$ will be the output.

The ABD formulation based on Hooke's law for orthotropic material has been described in section 2-3-2. The formula is re-written below.

$$\begin{Bmatrix} N_x \\ N_y \\ N_{xy} \\ - \\ M_x \\ M_y \\ M_{xy} \end{Bmatrix} = \begin{bmatrix} A_{11} & A_{12} & A_{16} & | & B_{11} & B_{12} & B_{16} \\ A_{21} & A_{22} & A_{26} & | & B_{21} & B_{22} & B_{26} \\ A_{61} & A_{62} & A_{66} & | & B_{61} & B_{62} & B_{66} \\ - & - & - & + & - & - & - \\ B_{11} & B_{12} & B_{16} & | & D_{11} & D_{12} & D_{16} \\ B_{21} & B_{22} & B_{26} & | & D_{21} & D_{22} & D_{26} \\ B_{61} & B_{62} & B_{66} & | & D_{61} & D_{62} & D_{66} \end{bmatrix} \begin{Bmatrix} \varepsilon_x^0 \\ \varepsilon_y^0 \\ \gamma_{xy}^0 \\ - \\ \kappa_x \\ \kappa_y \\ \kappa_{xy} \end{Bmatrix} \qquad 3\text{-}3$$

The ABD matrix is symmetric, and so the 3×3 submatrices (A and D) are along the main diagonal symmetric ($A_{ij} = A_{ji}$ and $D_{ij} = D_{ji}$). However the B matrix is not guaranteed to be symmetric.

The mechanical behavior of the ABD matrix has been described in figure 2-4. The symmetric layups are considered for this sample. The coupling stiffness matrix $[B]$

couples the force terms $\{N\}$ to the mid-plane curvatures $\{\kappa\}$ and the moment terms $\{M\}$ to the mid-plane strains $\{\varepsilon\}$. Symmetric layups make the B submatrix equal to zero and avoid the combination of mechanical behavior. Therefore mechanical behaviors will be more analyzable and comparable in all 4 methods.

In section 3-2-1 the surface forces $N_1$ and $N_2$ $\left(N_x, N_y\right)$ have been calculated. The next step is to obtain the ABD matrix for the whole laminate. Calculating the ABD matrix is also a long calculation process and by changing one ply property, the whole process should be repeated. However there are some software which calculate the ABD matrix for the requested layup. One of these software is eLamX2[1] [10]. For simulating the composite laminate in this software, first the mechanical constants of the ply should be defined. Note that for this sample the "stiffness properties" section is just used for calculating the ABD matrix, as has been illustrated in figure 3-3.

*Figure 3-3: Definition of mechanical constants in eLamX2 software*

| General Properies | |
|---|---|
| Name | New Material |
| Density | 1,76E-9 |
| **Stiffness Properties** | |
| $E_{\|}$ | 135000,0 |
| $E_\perp$ | 9500,0 |
| $v_{\|\perp}$ | 0,326 |
| $G_{\|\perp}$ | 5270,0 |
| **hygrothermal Properties** | |
| $\alpha^T_{\|}$ | 1,0E-6 |
| $\alpha^T_\perp$ | 3,5E-5 |
| $\beta_{\|}$ | 1,0E-2 |
| $\beta_\perp$ | 3,8E-1 |
| **Strength Properties** | |
| $X_t$ | 1500,0 |
| $X_c$ | 1000,0 |
| $Y_t$ | 180,0 |
| $Y_c$ | 240,0 |
| SC | 150,0 |

The Next step is to define the layup model and angle of each ply in the layer properties of the software. For example the 9 layers layup is modeled in figure 3-4. The "new material" in the 4th column is defined in figure 3-3. In the second row the angle of each ply is defined. And the thickness of each ply, which could even be a different value, is shown in the 3rd column. The failure criterion is another option of the software, although for the current sample the failure criterion has not been applied. These criterions could be TsaiWu, Hashin, puck and etc.

---

[1] Software website link (12.01.2015):
http://tudresden.de/die_tu_dresden/fakultaeten/fakultaet_maschinenwesen/ilr/aero/download/laminatetheory/index_html

*Figure 3-4: Definition the laminate layup*

| Name | Angle | Thickness | Material | Failure Criterion |
|---|---|---|---|---|
| New Layer | 0,0 | 0,25 | New Material | TsaiWu |
| New Layer | 45,0 | 0,25 | New Material | TsaiWu |
| New Layer | -45,0 | 0,25 | New Material | TsaiWu |
| New Layer | 90,0 | 0,25 | New Material | TsaiWu |
| New Layer | 0,0 | 0,25 | New Material | TsaiWu |
| New Layer | 90,0 | 0,25 | New Material | TsaiWu |
| New Layer | -45,0 | 0,25 | New Material | TsaiWu |
| New Layer | 45,0 | 0,25 | New Material | TsaiWu |
| New Layer | 0,0 | 0,25 | New Material | TsaiWu |

In the third step the ABD matrix of the layup has been calculated by the software and is used in the "calculation" tab of the software. In fact, the whole Hooke's equation is available in this tab. With inputting the forces or moments, strains and curvatures will be displayed as a result in the equation.

*Figure 3-5: The ABD matrix*



By having vertical forces $(N_x, N_y)$ and simulating the 9 layer layup in the eLamX2 software, the ABD matrix can be obtained as below:

$$\begin{Bmatrix} 25 \\ 50 \\ 0 \\ - \\ 0 \\ 0 \\ 0 \end{Bmatrix} = \begin{bmatrix} 150026,1 & 36587,8 & 0 & | & 0 & 0 & 0 \\ 36587,8 & 118414,7 & 0 & | & 0 & 0 & 0 \\ 0 & 0 & 41424,5 & | & 0 & 0 & 0 \\ - & - & - & - & - & - & - \\ 0 & 0 & 0 & | & 8650,2 & 15127,5 & 4939,3 \\ 0 & 0 & 0 & | & 15127,5 & 27214,2 & 4939,3 \\ 0 & 0 & 0 & | & 4939,3 & 4939,3 & 17168 \end{bmatrix} \begin{Bmatrix} \varepsilon_x \\ \varepsilon_y \\ \varepsilon_{xy} \\ - \\ \kappa_x \\ \kappa_y \\ \kappa_{xy} \end{Bmatrix}$$

And for calculating the equation, the ABD matrix should be reversed (equation 3-4):

$$
\left\{\begin{array}{c} \varepsilon_x \\ \varepsilon_y \\ \gamma_{xy} \\ - \\ \kappa_x \\ \kappa_y \\ \kappa_{xy} \end{array}\right\} =
\left[\begin{array}{ccc|ccc}
A_{11} & A_{12} & A_{16} & B_{11} & B_{12} & B_{16} \\
A_{21} & A_{22} & A_{26} & B_{21} & B_{22} & B_{26} \\
A_{61} & A_{62} & A_{66} & B_{61} & B_{62} & B_{66} \\
\hline
B_{11} & B_{12} & B_{16} & D_{11} & D_{12} & D_{16} \\
B_{21} & B_{22} & B_{26} & D_{21} & D_{22} & D_{26} \\
B_{61} & B_{62} & B_{66} & D_{61} & D_{62} & D_{66}
\end{array}\right]^{-1}
\left\{\begin{array}{c} N_x \\ N_y \\ N_{xy} \\ - \\ M_x \\ M_y \\ M_{xy} \end{array}\right\}
\qquad 3\text{-}4
$$

$$
\left\{\begin{array}{c} \varepsilon_x \\ \varepsilon_y \\ 0 \\ 0 \\ 0 \\ 0 \end{array}\right\} =
\left[\begin{array}{cccccc}
7,209\times10^{-6} & -2,227\times10^{-6} & 0 & 0 & 0 & 0 \\
-2,227\times10^{-6} & 9,133\times10^{-6} & 0 & 0 & 0 & 0 \\
0 & 0 & 2,414\times10^{-5} & 0 & 0 & 0 \\
0 & 0 & 0 & -0,018 & 0,01 & 0,002 \\
0 & 0 & 0 & 0,01 & -0,005 & -0,001 \\
0 & 0 & 0 & 0,002 & -0,001 & -2,713\times10^{-4}
\end{array}\right]
\left\{\begin{array}{c} 25 \\ 50 \\ 0 \\ 0 \\ 0 \\ 0 \end{array}\right\}
$$

The strain parameters '$\varepsilon_x$ and $\varepsilon_y$' have been obtained from the above equation for the 9 layer layup and the normal strain $(\varepsilon)$ can be obtained as below:

$$
\varepsilon = \sqrt{\varepsilon_x^{\,2}+\varepsilon_y^{\,2}} = \sqrt{\left(6,9\times10^{-5}\right)^2+\left(4,01\times10^{-4}\right)^2} = 3,267\times10^{-4}
$$

Through the same procedure and by simulating the 8 layer layup in the eLamX2 software the ABD matrix will be calculated.

$$
\left\{\begin{array}{c} 25 \\ 50 \\ 0 \\ - \\ 0 \\ 0 \\ 0 \end{array}\right\} =
\left[\begin{array}{ccc|ccc}
116021,8 & 35807,7 & 0 & 0 & 0 & 0 \\
35807,7 & 116021,8 & 0 & 0 & 0 & 0 \\
0 & 0 & 40107 & 0 & 0 & 0 \\
\hline
0 & 0 & 0 & 16813,3 & 1088 & 3951,4 \\
0 & 0 & 0 & 10088 & 64230,4 & 3951,4 \\
0 & 0 & 0 & 3951,4 & 3951,4 & 11521,1
\end{array}\right]
\left\{\begin{array}{c} \varepsilon_x \\ \varepsilon_y \\ \varepsilon_{xy} \\ - \\ \kappa_x \\ \kappa_y \\ \kappa_{xy} \end{array}\right\}
$$

$$
\left\{\begin{array}{c} \varepsilon_x \\ \varepsilon_y \\ 0 \\ 0 \\ 0 \\ 0 \end{array}\right\} =
\left[\begin{array}{cccccc}
9,526\times10^{-6} & -2,94\times10^{-6} & 0 & 0 & 0 & 0 \\
-2,94\times10^{-6} & 9,526\times10^{-6} & 0 & 0 & 0 & 0 \\
0 & 0 & 2,493\times10^{-5} & 0 & 0 & 0 \\
0 & 0 & 0 & 6,454\times10^{-5} & 2,743\times10^{-7} & -2,223\times10^{-5} \\
0 & 0 & 0 & -8,963\times10^{-6} & 1,587\times10^{-5} & -2,368\times10^{-6} \\
0 & 0 & 0 & -1,906\times10^{-6} & -5,536\times10^{-6} & 9,523\times10^{-5}
\end{array}\right]
\left\{\begin{array}{c} 25 \\ 50 \\ 0 \\ 0 \\ 0 \\ 0 \end{array}\right\}
$$

The strain parameters '$\varepsilon_x$ and $\varepsilon_y$' have been obtained from the above equation for the 8 layer layup and the normal strain $(\varepsilon)$ can be obtained as described below:

$$\varepsilon = \sqrt{\varepsilon_x^2 + \varepsilon_y^2} = \sqrt{\left(9,1 \times 10^{-5}\right)^2 + \left(4,03 \times 10^{-4}\right)^2} = 4,131 \times 10^{-4}$$

The results of this method are considered as the basic theoretical results and the strain results of the remaining three methods will be compared with the results of this method. This means the ABD method is the reference method in this project and the accuracy of each method can be obtained by comparison with the ABD method.

The deformations of the square element appear in X and Y directions, which has been illustrated in the figure 3-5.

*Figure 3-6: Deformation the element at the ABD method*
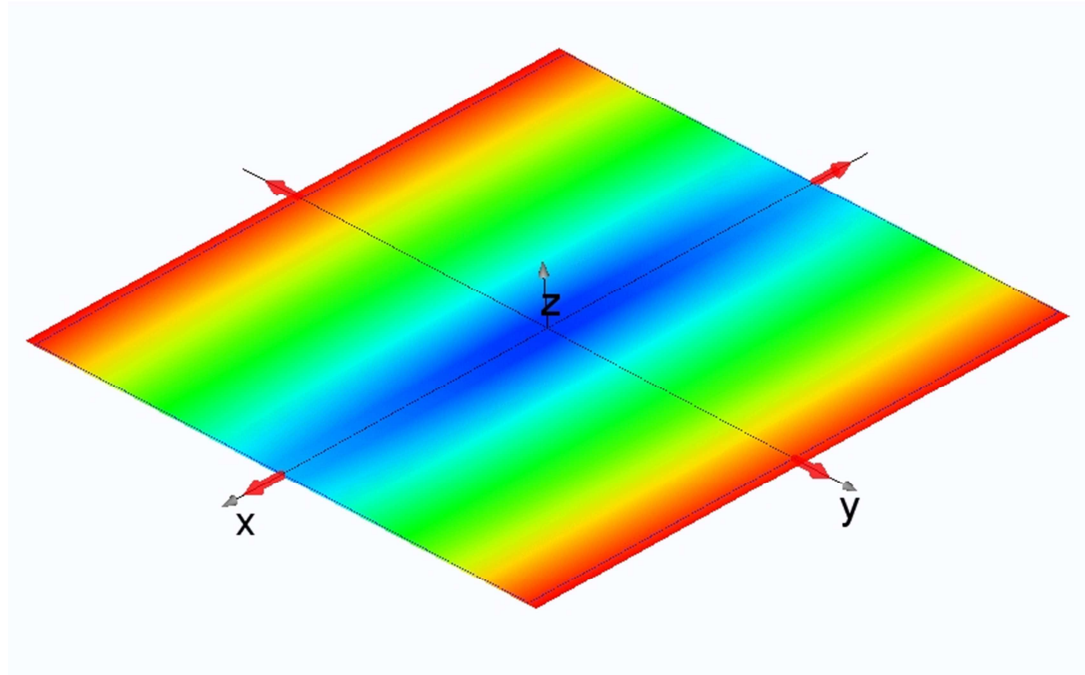


## 3.2.3 CATIA FEM simulation with the average elastic factors input

In chapter 2, in section 2.3.3.1 the average method has been introduced. It has also been mentioned that the CLT method (more information in 2.3.1) creates the input for the FEM software here. The CATIA here, is the FEM software for modeling the square element. First the plies rigidities $[Q]_k$ for orthotropic plies at the ply coordinate system should be calculated. The CLT formulations are described in 2.3.1. According to the equation 2-6 and table 3-1, this can be written as:

$$[Q]_k = \begin{bmatrix} \dfrac{E_1}{1-v_{12}^2 \cdot \dfrac{E_2}{E_1}} & \dfrac{v_{12} \cdot E_2}{1-v_{12}^2 \cdot \dfrac{E_2}{E_1}} & 0 \\ \dfrac{v_{12} \cdot E_2}{1-v_{12}^2 \cdot \dfrac{E_2}{E_1}} & \dfrac{E_2}{1-v_{12}^2 \cdot \dfrac{E_2}{E_1}} & 0 \\ 0 & 0 & G_{12} \end{bmatrix} = \begin{bmatrix} 1,36 \cdot 10^{11} & 3,12 \cdot 10^9 & 0 \\ 3,12 \cdot 10^9 & 9,572 \cdot 10^9 & 0 \\ 0 & 0 & 5,27 \cdot 10^9 \end{bmatrix}$$

Second the rigidities [Q]$_{PlyCS,k}$ of each ply are transformed from the local ply coordinate system (PlyCS) to the global coordinate system of the laminate (LamCS) in accordance with the transformation laws (equations 2-7,2-8).

Based on the material properties (table 3-1), in the third step, the rigidity matrixes $[Q]_k$ for all layup angles, which are [0, 45,-45, 90], should be calculated. The transformed rigidities of all plies, weighted according to their cross sectional ratios, are added together to yield a homogeneous laminate rigidity. The result is the laminate rigidity matrix $[A]$:

$$[A] = \sum_k \frac{t_k}{t_{Lam}} \cdot [Q]_{LamCS,k} = \frac{3 \cdot 0,25}{2,25} \cdot [Q]_{lam,1} + \frac{2 \cdot 0,25}{2,25} \cdot [Q]_{lam,2} + \frac{2 \cdot 0,25}{2,25} \cdot [Q]_{lam,3} +$$

$$\frac{2 \cdot 0,25}{2,25} \cdot [Q]_{lam,4}$$

$$[A] = \begin{bmatrix} 6,668 \cdot 10^{10} & 1,626 \cdot 10^{10} & 0 \\ 1,626 \cdot 10^{10} & 5,263 \cdot 10^{10} & -1,907 \cdot 10^{-6} \\ 0 & -1,907 \cdot 10^{-6} & 1,841 \cdot 10^{10} \end{bmatrix}$$

In the fourth step before determining the distortions in the laminate, the invert of the rigidity matrix $[A]$ that is compliance matrix $[a]$ should be calculated.

$$[a] = \begin{bmatrix} 1,622 \cdot 10^{-11} & -5,012 \cdot 10^{-12} & -5,192 \cdot 10^{-28} \\ -5,012 \cdot 10^{-12} & 2,055 \cdot 10^{-11} & 2,129 \cdot 10^{-27} \\ -5,192 \cdot 10^{-28} & 2,129 \cdot 10^{-27} & 5,432 \cdot 10^{-11} \end{bmatrix}$$

The engineering constants for the laminate are obtained from elements of the compliance matrix (equations 2-12, 2-13):

$$E_{x,Lam} = \frac{1}{a_{11}} = 61652 \left( \frac{N}{mm^2} \right)$$

$$E_{y,Lam} = \frac{1}{a_{22}} = 48660 \left( \frac{N}{mm^2} \right)$$

$$G_{xy,Lam} = \frac{1}{a_{33}} = 18409 \left( N\!\!\left/\!\!{mm^2}\right.\right)$$

$$V_{xy,Lam} = V_{yx,Lam} = \frac{-a_{21}}{a_{11}} = 0,309$$

With the same calculation process for the 8 layer layup, the engineering constants can be calculated as below:

$$E_{x,Lam} = \frac{1}{a_{11}} = 52493 \left( N\!\!\left/\!\!{mm^2}\right.\right)$$

$$E_{y,Lam} = \frac{1}{a_{22}} = 52493 \left( N\!\!\left/\!\!{mm^2}\right.\right)$$

$$G_{xy,Lam} = \frac{1}{a_{33}} = 18409 \left( N\!\!\left/\!\!{mm^2}\right.\right)$$

$$V_{xy,Lam} = V_{yx,Lam} = \frac{-a_{21}}{a_{11}} = 0,309$$

It should be noted that for the quasi-isotropic laminate layups (8 layer layup) $E_x = E_y$ , but when this method is used for the symmetric orthotropic laminate layups (9 layer layup) $E_x \neq E_y$. Since there is just one input for the E modulus in the average method, the elasticity modulus in the X direction $E_x$ is considered as an input for the elasticity modulus in the 9 layer layup method.

The engineering constants are available now for both 8 and 9 layer layups. These constants can be used as material properties for the CATIA model.

The cylinder is modeled (figure 3-7) according to the geometry properties of table 3-2 in the CATIA software. The boundary conditions are placed at the two sides of the cylinder (two circles marked by red color) that make a uniform deformation on the cylinder surface. The meshing on the surface of the cylinder should be square and with specific size (2mm), in this case the strains of one square element on the cylinder surface (2x2 mm$^2$) will be appropriate for comparison with the theoretical result (figure3-8). Inside pressure and thickness (table 3-2) of the cylinder are also considered for the model in software.

*Figure 3-7: cylinder with boundary condition*
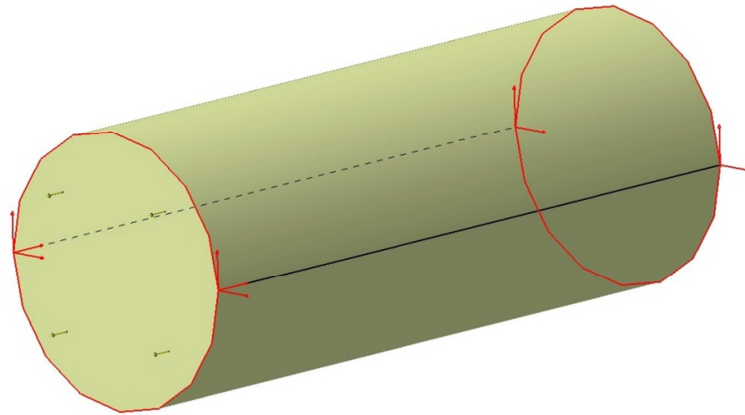


*Figure 3-8: cylinder square mesh (2 mm)*
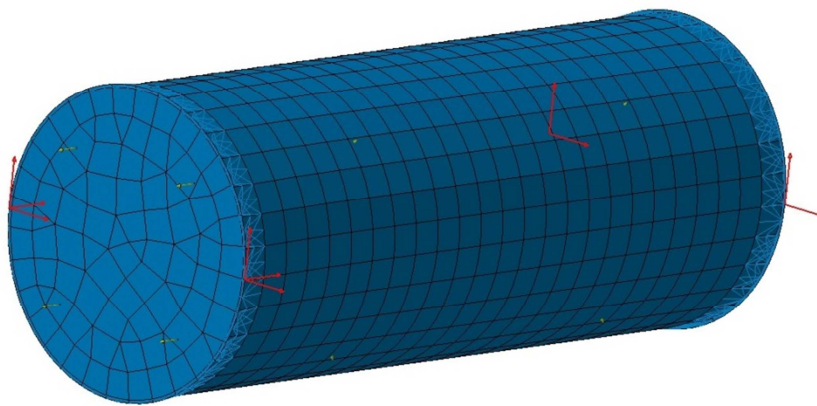


After modeling and calculating the results in the CATIA software, the strain and stress of the cylinder will be available:

*Figure 3-9: Strain of the cylinder ($\varepsilon_{x}$ in the left side and $\varepsilon_{y}$ in the right side) for the 9 layer layup*
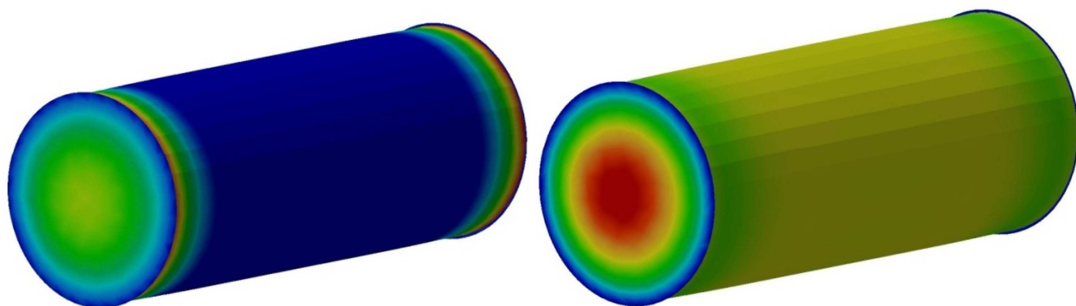
And for the 8 layer layup this would be:

*Figure 3-10: Strain of the cylinder (Ɛx in the left side and Ɛy in the right side) for the 8 layer layup*
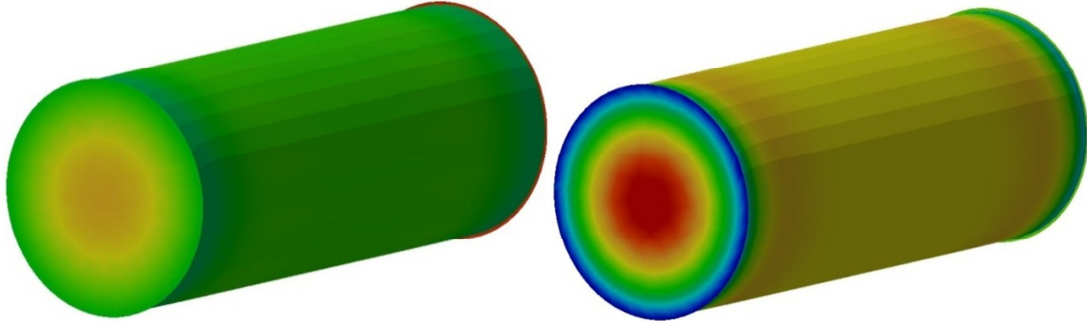


Although all of the strains on the surface of the cylinder have almost the same quantity, only one square element should be selected to establish the amounts of the strain. In figures 3-9 and 3-10 the elements' strains that are located near the edges are quite different from the elements' strains that are located on other positions of the surface. It is suggested that the element be selected from the middle of the cylinder surface. This selection will avoid the effect of the boundary conditions 'which are located on the edges' to the strain of the element. By selecting the element on the surface of the cylinder, the following amounts are obtained:

For the 9 layer layup (using $E_x$ as input):

$\varepsilon_x \approx 7,75 \times 10^{-5}$ And $\varepsilon_y \approx 3,23 \times 10^{-4}$ so $\varepsilon$ will be: $\varepsilon = \sqrt{\varepsilon_x^2 + \varepsilon_y^2} \approx 3,32 \times 10^{-4}$

For the 8 layer layup:

$\varepsilon_x \approx 4,33 \times 10^{-4}$ And $\varepsilon_y \approx 1,02 \times 10^{-4}$ so $\varepsilon$ will be: $\varepsilon = \sqrt{\varepsilon_x^2 + \varepsilon_y^2} \approx 4,446 \times 10^{-4}$

## 3.2.4 FEM simulation with complete layup modeling (CATIA, ANSYS)

In chapter 2 section 2.3.3.2 the complete method has been introduced. In this method theoretical calculation is not necessary, because the laminate is modeled ply by ply in the FEM software. The cylinder is modeled with two different FEM software (CATIA, ANSYS) in this simulation; therefore there will be two types of result for one sample model. The question that comes to mind here is: why should this simulation be done with two FEM software? This is done because of two reasons. First if the results of both FEM software were nearly the same, it would prove that this method is acceptable. Second the comparison of the results of the two software will lead to a better overview over the precision of each FEM software. As these two methods have the same modeling procedure, they are studied together in this chapter.

The sample of the simulation is the same as figure 3-7 with the same properties. in this method all layers are modeled ply by ply on the sample surface, and the orthotropic composite properties of regular epoxy carbon is considered for each layer, which are illustrated in table 3-2.

As the 2D properties of orthotropic material are used for the surface layup of the current sample, some properties of the table 3-3 ($v_{yz}$, $v_{xz}$, $G_{yz}$ and $G_{xz}$) are not used for this layup.

Table 3-3: mechanical constants for orthotropic layup

| Constant | Amount |
|---|---|
| Number of the layers | $8 or 9$ |
| Each layer thickness | $0,25 \ [mm]$ |
| Young's Modulus in X direction $E_1$ | $135000 \ [N/mm^2]$ |
| Young's Modulus in Y direction $E_2$ | $9500 \ [N/mm^2]$ |
| Young's Modulus in Z direction $E_{12}$ | $9500 \ [N/mm^2]$ |
| Poisson ratio $v_{xy}$ | $0,326$ |
| Poisson ratio $v_{yz}$ | $0,4$ |
| Poisson ratio $v_{xz}$ | $0,4$ |
| Shear modulus $G_{xy}$ | $5270 \ [N/mm^2]$ |
| Shear modulus $G_{yz}$ | $3100 \ [N/mm^2]$ |
| Shear modulus $G_{xz}$ | $3100 \ [N/mm^2]$ |

The FEM model is the same as figure 3-7, but in this method after modeling, the laminate layup should be also built up on the model. In the CATIA each ply angle is represented by a color as has been illustrated in figure 3-11 (0 degree –yellow, 45 degree–blue, -45 degree –green, 90 degree– red).

*Figure 3-11: Composite layup in CATIA*
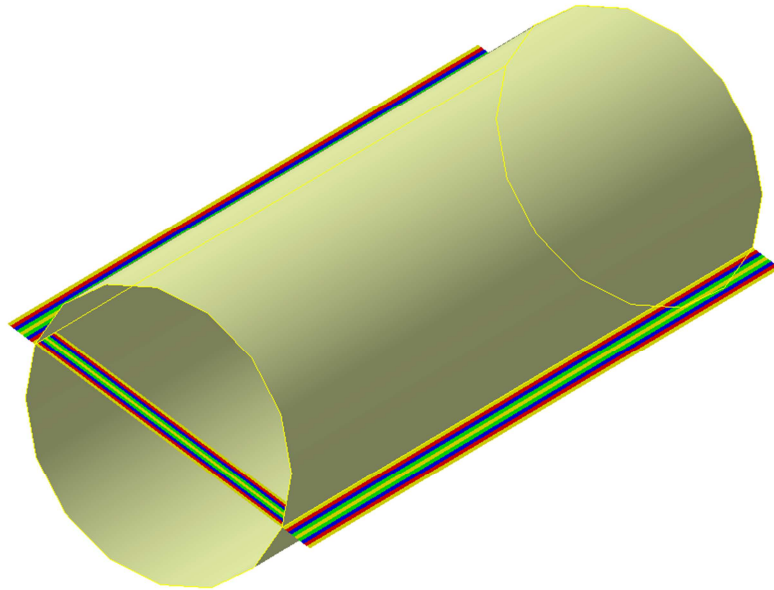


Note that the layup modeling for the 8 layer and the 9 layer layups are different, as it is visible in figure 3-12:

*Figure 3-12: Different between 8 layer and 9 layer layup in CATIA*
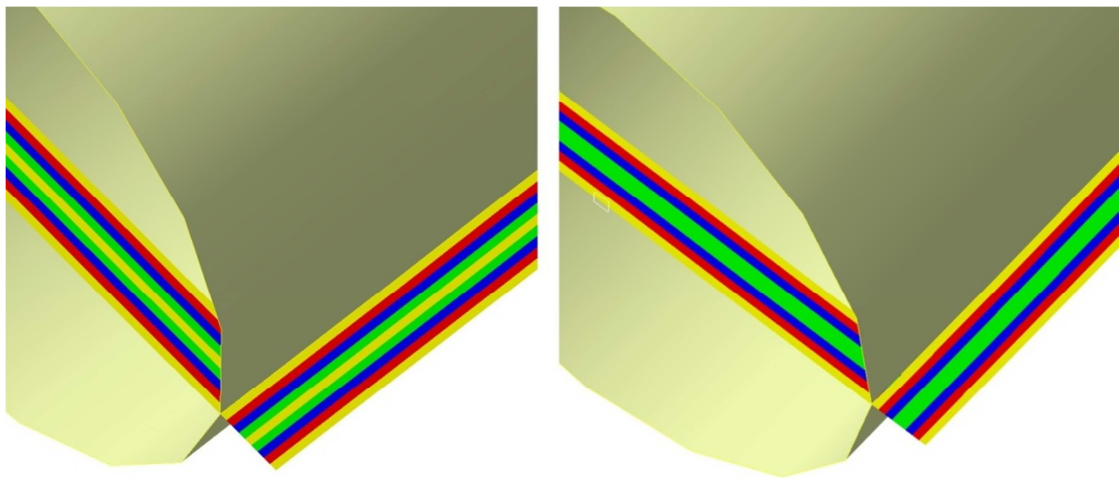


The ANSYS PrePost (the composite area of ANSYS for preprocessing and post processing of the composite layups) shows each layer by its own angle on the surface. In figure 3-13 all types of the ply angles have been illustrated (0,45,-45,90).

*Figure 3-13: Composite layup angles in ANSYS PrePost*
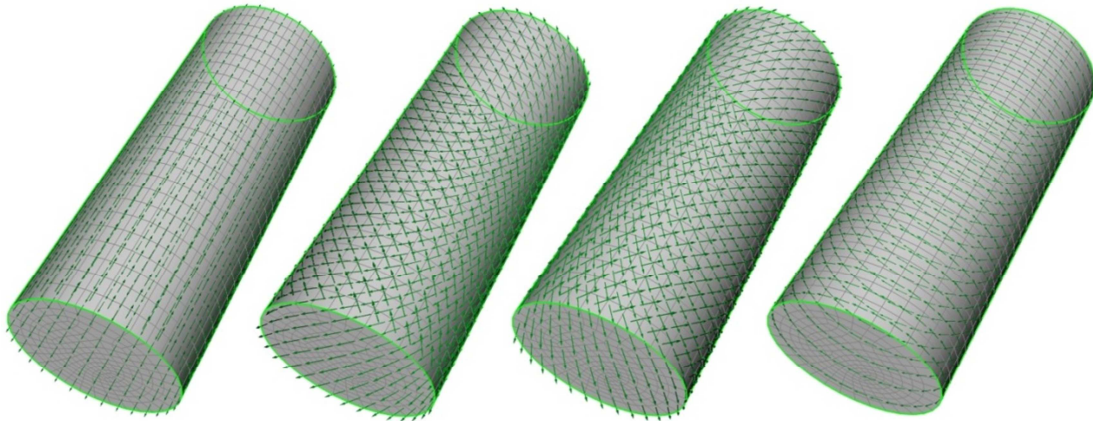
The mesh size is 2 mm and the mesh type is 2nd order square similar to the average method. The pressure amount is also based on table 3-2, and boundary conditions are similar to the average method. In this technique one square element (2×2 mm$^2$) on the surface of the cylinder is also selected to establish the results. There is a useful option in the ANSYS software which allows the user to see the finished model with the mesh and also the laminate thickness (figure 3-14).

*Figure 3-14: Cylinder after mesh and layup (In ANSYS software)*
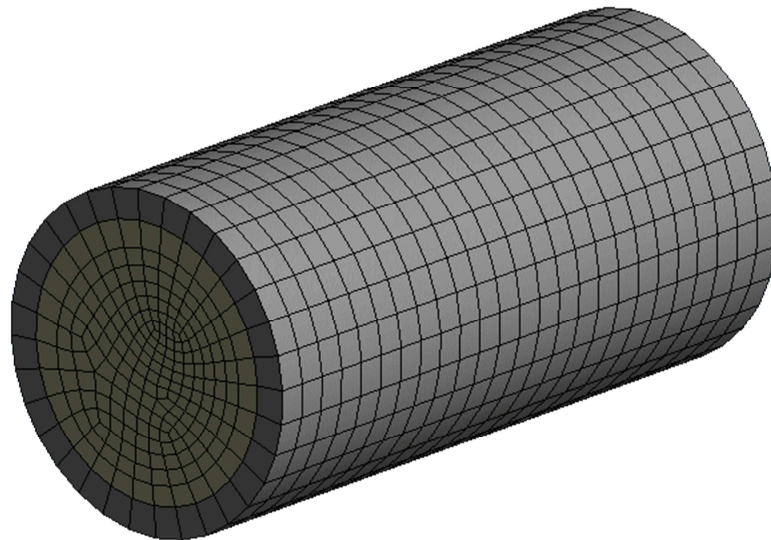


After calculating the model with the described layups and meshes, the results will be ready. Same as in the two previous methods, the strain factors in X and Y directions should be extracted. The sample is one square element (2×2 mm$^2$) on the surface of the cylinder. For CATIA models there are:

For the 9 layer layup (figure 3-15):
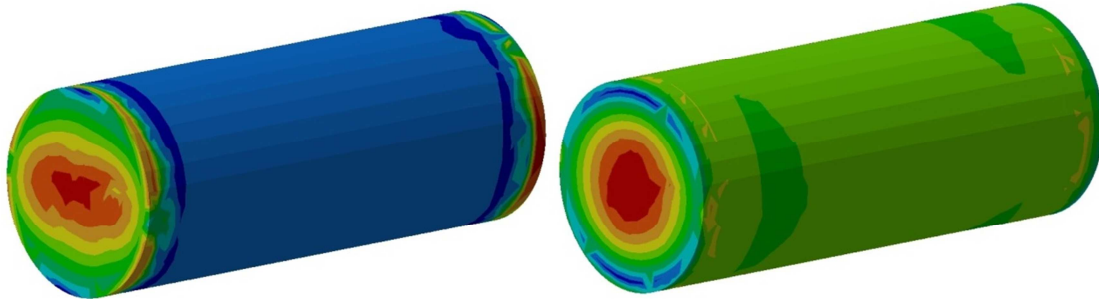
$\varepsilon_x \approx 9,2{\times}10^{-5}$ And $\varepsilon_y \approx 3,4{\times}10^{-4}$ so $\varepsilon$ will be: $\varepsilon = \sqrt{\varepsilon_x^{\ 2}+\varepsilon_y^{\ 2}} \approx 3,52{\times}10^{-4}$

And for the 8 layer layup (figure 3-16):
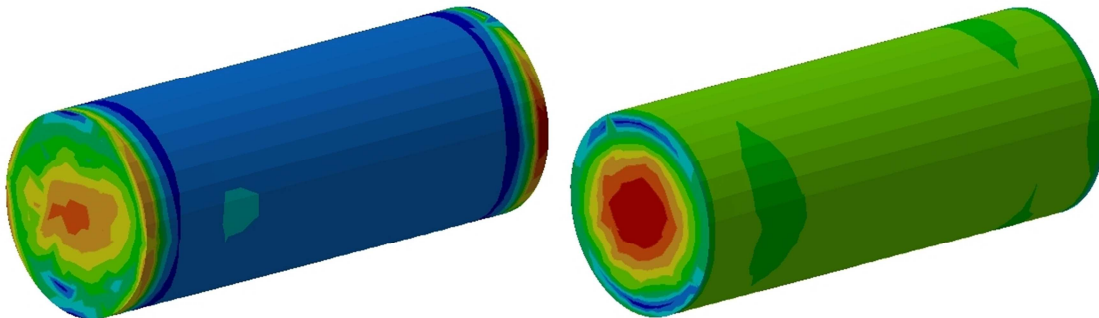
$\varepsilon_x \approx 7,19{\times}10^{-5}$ And $\varepsilon_y \approx 4,41{\times}10^{-4}$ so $\varepsilon$ will be: $\varepsilon = \sqrt{\varepsilon_x^{\ 2}+\varepsilon_y^{\ 2}} \approx 4,46{\times}10^{-4}$

In the ANSYS software the process of getting to the strain is somehow easier, because there is an option in the software called equivalent elastic strain. By using this option the equivalent strain $\varepsilon$ will be illustrated (figure 3-17 and 3-18).

*Figure 3-17: Equivalent elastic strain in ANSYS for 9 layer layup*
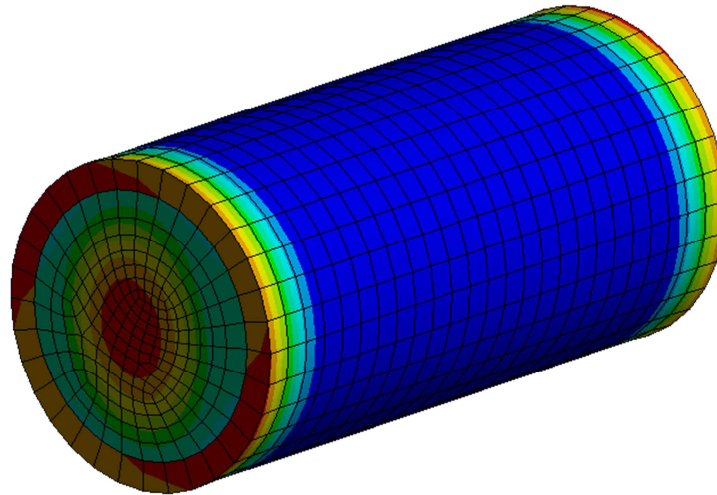


For the 9 layer layup (figure 3-17): $\varepsilon = \sqrt{\varepsilon_x^{\,2} + \varepsilon_y^{\,2}} \approx 3,70 \times 10^{-4}$

Note that like the average method, in this method the sample should also be selected from the middle of the cylinder surface and not near the edges to avoid the influence of boundary conditions and have a correct sample.

*Figure 3-18: Equivalent elastic strain in ANSYS for 8 layer layup*
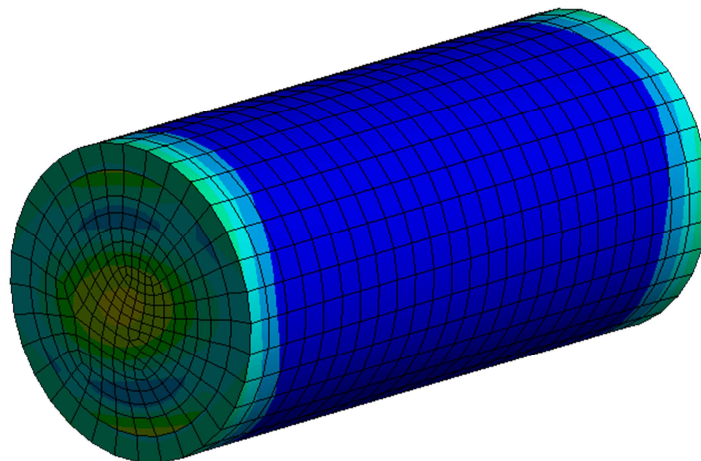


For the 8 layer layup (figure 3-18): $\varepsilon = \sqrt{\varepsilon_x^{\,2} + \varepsilon_y^{\,2}} \approx 4,54 \times 10^{-4}$

In the composite post processing of the FEM software, it is also possible to have a plot of the strain and stress for each ply separately. With this possibility the stress distribution at each ply of the 9 layer and 8 layer layup are established and compared with theoretical results to make sure about the validity of the calculations.

The left side figures (figure 3-19, 3-20) are theoretical stress distribution values in each layer for the 9 layer and the 8 layer in X and Y directions (established by eXlam2 software). On the right side, there are the values for two FEM software is also in the X and Y directions. As it can be seen from the figures, both FEM software have a good adaptation with each other and with the theoretical stress distributions.

*Figure 3-19: stress distribution in each layer in X and Y directions (9 layer layup)*
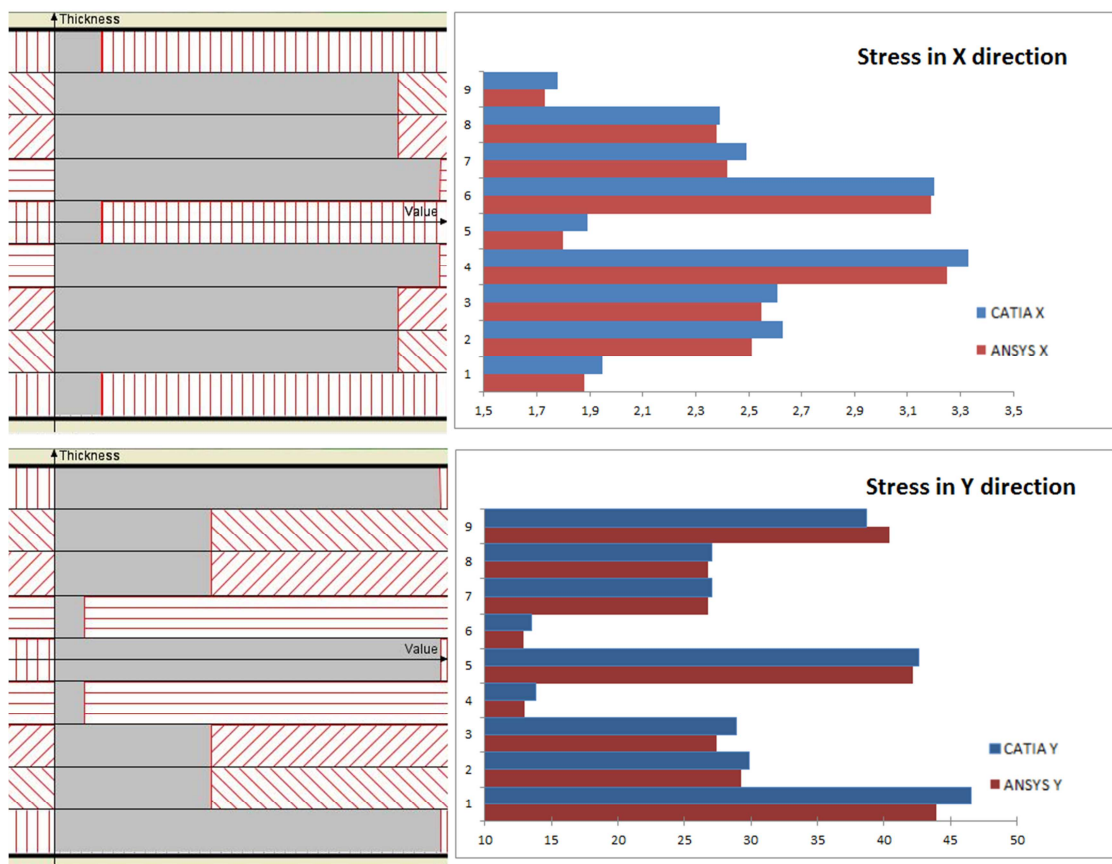


The theoretical stress distribution figures come from eLamX2 software. Although in picture 3-20 the FEM figure (right side, stress in X direction) shows the maximum stress at the middle layer (90 degree), the theoretical figure (left side) shows the maximum value at 45 and -45 degree which is not correct. Hence this would be a mistake by the eLamX2 software in displaying the theoretical stress distribution figures.

*Figure 3-20: stress distribution in each layer in X and Y directions (8 layer layup)*
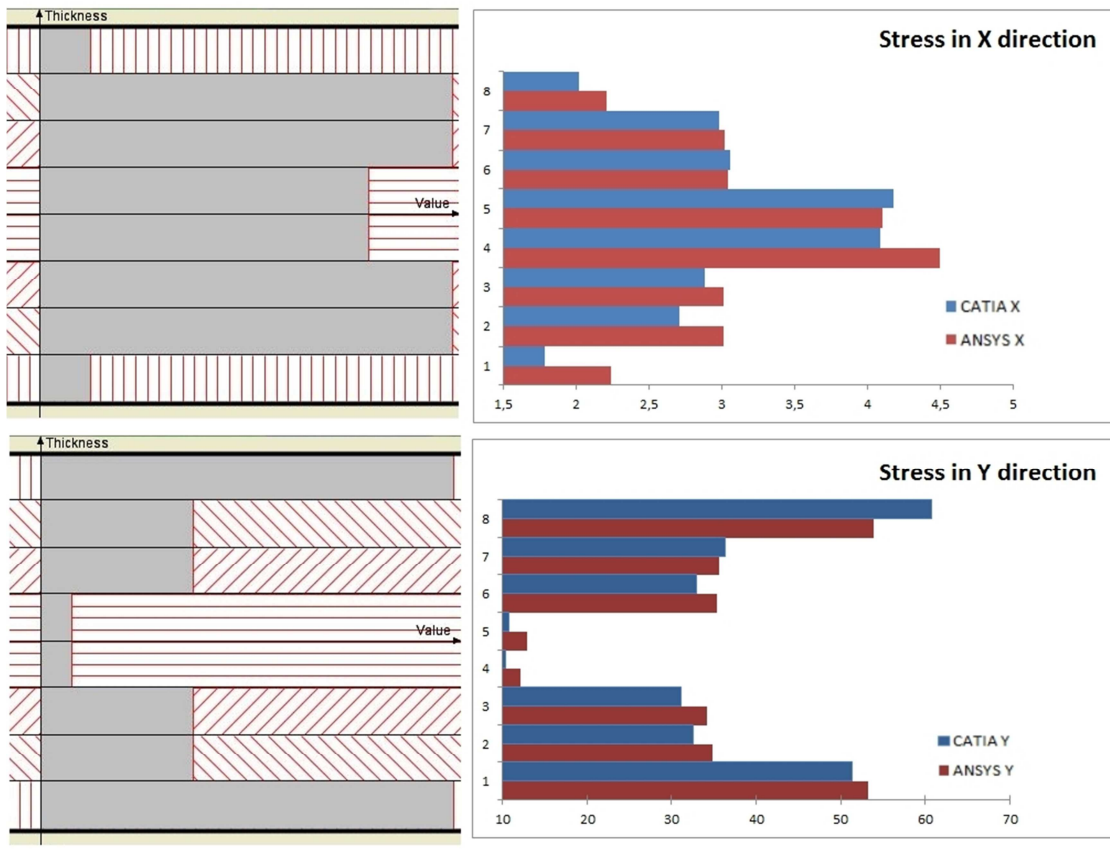


## 3.2.5 Comparison

Based on what has been calculated in the previous sections for all methods (3.2.2 to 3.2.4), it is possible now to compare the results. In the table 3-4 all of the strains which are

*Table 3-4: Strain results for all methods*

| Comparison of strain results | 9 layer layup | 8 layer layup |
|---|---|---|
| Theoretical calculation | $3,267 \times 10^{-4}$ | $4,131 \times 10^{-4}$ |
| CATIA simulation with average factors | $3,32 \times 10^{-4}$ | $4,44 \times 10^{-4}$ |
| CATIA simulation with complete layup modeling | $3,52 \times 10^{-4}$ | $4,46 \times 10^{-4}$ |
| ANSYS simulation with complete layup modeling | $3,70 \times 10^{-4}$ | $4,54 \times 10^{-4}$ |

The basic method is theoretical calculation. It is precise and trustable because it is based on proven formulations. Yet some questions still continue to arise. For example, how far can the theoretical calculation be used? What should be done for complicated composite parts? How much time and energy should be used for

calculation of even a simple part like the sample? And the most important question is whether the theoretical calculation is even possible in complicated cases? The answer is clear and that's why in recent years the FEM simulation is improved and used much more than before, and because composite material calculations are even more complicated, the FEM simulation is more required.

The average method especially for the quasi isotropic layups is quiet useful and applicable as it is shown in this sample. It saves a lot of time and energy of simulation. Instead of a long layups simulation process, the average input amounts are just calculated. This method has even been tested and used in industry for layups or layups with honeycomb, and the results were quite satisfactory and passed the industry test results. For example the average method answer is a good compromise between time consumption and quality of results for quasi isotropic layups like $\left[0,\ 45,-45,\ 90\right]_n$ and even for the simulations where a honeycomb exists between the layup. Although the average method shows better results compared to other methods in the current layup samples, when the force and moments have a bending and buckling effect, the analysis of this method is not precise anymore (will be described in sample 2). In fact, in the buckling analysis the position of each layer orientation is quiet important but the average method does not consider the position of the oriented layer.

The complete layup simulation as it comes from its name is of course more precise and also time consuming process for the orthotropic laminates. If the layup type is symmetrical orthotropic or when there is a bending moment acting on a component and the precision of the answer is important, there will be no choice but the complete simulation method. But here in sample 1 there is no difference between using the average method or the complete method. In section 2.3.1 and 2.3.2 some assumptions have been introduced for calculating the "CLT" and "ABD matrix". These assumptions simplify the procedure of the theoretical calculation and also neglect some boundaries of calculation precision. For instance in section 2.3.2.1 it has been mentioned that: a line straight and perpendicular to the middle surface remains straight and perpendicular to the middle surface during deformation. The assumption is not necessarily considered by the FEM calculation; therefore the complete method has more realistic results. This is the reason the average method shows more conformity with theoretical results [8].

## 3.3 Sample 2: Surface with bending moment

### 3.3.1 Introducing the sample

The test component of this sample is a square surface (100x100 mm$^2$) with a bending momentum at the two side of it (figure 3-21). In contrast with previous sample, there will be no simplification, because the model is quite simple. The momentum amount on each side of the surface is 5 Nxm in the y direction.

For this sample one type of layup is applied. The symmetric orthotropic laminate layup (the 9 layer layup $\left[ 0, \ 45, -45, \ 90, \overline{0} \right]_s$ ) is considered for this sample [8].

*Figure 3-21: sample 2 surface with momentum*
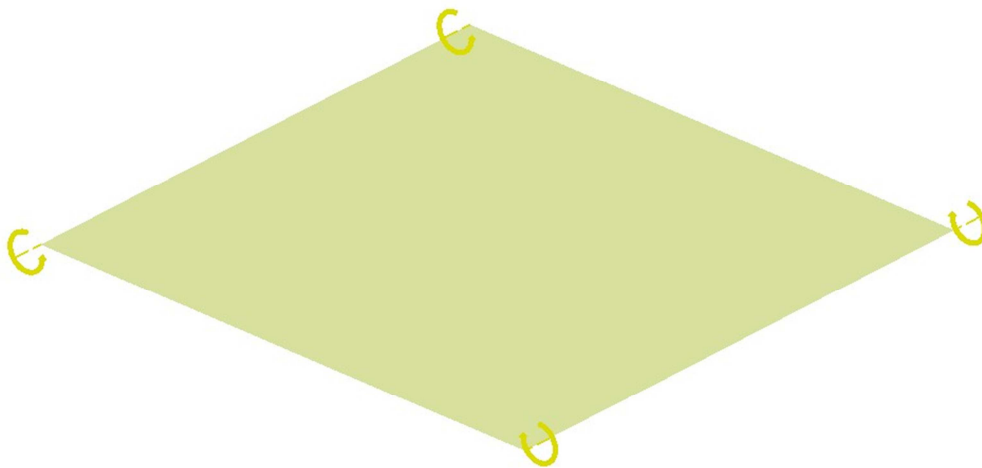


### 3.3.2 Theoretical calculation with ABD matrix

In this sample the ABD matrix should be calculated for the surface based on the mechanical constants of the table 3-1. Instead of forces in this sample the momentum $M_y$ is acted on the ages of surface and it should be placed into the Hooke's law equation (2-34). After solving the equation the curvatures $\left( \kappa_x, \kappa_y, \kappa_{xy} \right)$ will be the output.

To get more familiar with the phrase curvature, it would be useful to describe the curvature in geometrical way. Based on the "Math world" definition[2], it is natural to define the curvature of a straight line to be identically zero. The curvature of a circle of radius R should be large if R is small and small if R is large. Thus the curvature of a circle is defined to be the reciprocal of the radius [11]. The curvature can be defined as below:

---

[2] Website link : http://mathworld.wolfram.com/RadiusofCurvature.html

$$\kappa = \frac{1}{R}$$

It should be noticed that in the section 2.3.2 (equations 2-28-4 and 2-28-5) the unit of the bending moments in X and Y directions are moment per unit length, therefore the moment amount dimension should be changed to moment per length and then can be used in the ABD matrix. so it could be written:

$$M_y = 5N \times m / 0,05m = 100$$

After having the input moment, the ABD matrix should be calculated. The eLamX2 software is also used here for obtaining the ABD matrix. The general material properties of plies are the same as sample 1 and figure 3-3.

The type of the layup should be defined in the software, for this sample the 9 layer layup is illustrated in figure 3-22:

*Figure 3-22: laminate layup definition for surface sample*

| Name | Angle | Thickness | Material |
|---|---|---|---|
| New Layer | 0,0 | 0,25 | New Material |
| New Layer | 45,0 | 0,25 | New Material |
| New Layer | -45,0 | 0,25 | New Material |
| New Layer | 90,0 | 0,25 | New Material |
| New Layer | 0,0 | 0,25 | New Material |
| New Layer | 90,0 | 0,25 | New Material |
| New Layer | -45,0 | 0,25 | New Material |
| New Layer | 45,0 | 0,25 | New Material |
| New Layer | 0,0 | 0,25 | New Material |

In this sample like what has been done in sample 1, the ABD matrix should also be calculated with the software as it illustrated in figure 3-23.

*Figure 3-23: ABD matrix for sample 2*

| | nm mech. | + | nm hygrotherm. | = | ABD-Matrix | | | | | | * | εκ | |
|---|---|---|---|---|---|---|---|---|---|---|---|---|---|
| $n_x$ = | 0,0 | | 0,0 | | 150026,1 | 36587,8 | 0,0 | 0,0 | -0,0 | 0,0 | | -0,0 | $= \varepsilon_x$ |
| $n_y$ = | 0,0 | | 0,0 | | 36587,8 | 118414,7 | 0,0 | -0,0 | 0,0 | 0,0 | | 0,0 | $= \varepsilon_y$ |
| $n_{xy}$ = | 0,0 | | 0,0 | | 0,0 | 0,0 | 41424,5 | 0,0 | 0,0 | 0,0 | | -0,0 | $= \gamma_{xy}$ |
| $m_x$ = | 0,0 | + | 0,0 | = | 0,0 | -0,0 | 0,0 | 86650,2 | 15127,5 | 4939,3 | * | 0,000682 | $= \kappa_x$ |
| $m_y$ = | -100,0 | | 0,0 | | -0,0 | 0,0 | 0,0 | 15127,5 | 27214,2 | 4939,3 | | -0,004239 | $= \kappa_y$ |
| $m_{xy}$ = | 0,0 | | 0,0 | | 0,0 | 0,0 | 0,0 | 4939,3 | 4939,3 | 17168,0 | | 0,001024 | $= \kappa_{xy}$ |

After calculating the ABD matrix in the software and having the momentum $M_y$, the Hooke's law equation can be rewritten for this sample.

$$
\begin{Bmatrix} 0 \\ 0 \\ 0 \\ - \\ 0 \\ -100 \\ 0 \end{Bmatrix} = \left[\begin{array}{ccc|ccc} 150026,1 & 36587,8 & 0 & 0 & 0 & 0 \\ 36587,8 & 118414,7 & 0 & 0 & 0 & 0 \\ 0 & 0 & 41424,5 & 0 & 0 & 0 \\ - & - & - & - & - & - \\ 0 & 0 & 0 & 8650,2 & 15127,5 & 4939,3 \\ 0 & 0 & 0 & 15127,5 & 27214,2 & 4939,3 \\ 0 & 0 & 0 & 4939,3 & 4939,3 & 17168 \end{array}\right] \begin{Bmatrix} \varepsilon_x \\ \varepsilon_y \\ \varepsilon_{xy} \\ - \\ \kappa_x \\ \kappa_y \\ \kappa_{xy} \end{Bmatrix}
$$

To obtain the curvature the equation should be reversed, so it could be written as below:

$$
\begin{Bmatrix} 0 \\ 0 \\ 0 \\ - \\ \kappa_x \\ \kappa_y \\ \kappa_{xy} \end{Bmatrix} = \left[\begin{array}{ccc|ccc} 7,209{\times}10^{-6} & -2,227{\times}10^{-6} & 0 & 0 & 0 & 0 \\ -2,227{\times}10^{-6} & 9,133{\times}10^{-6} & 0 & 0 & 0 & 0 \\ 0 & 0 & 2,414{\times}10^{-5} & 0 & 0 & 0 \\ - & - & - & - & - & - \\ 0 & 0 & 0 & -0,018 & 0,01 & 0,002 \\ 0 & 0 & 0 & 0,01 & -0,005 & -0,001 \\ 0 & 0 & 0 & 0,002 & -0,001 & -2,713{\times}10^{-4} \end{array}\right] \begin{Bmatrix} 0 \\ 0 \\ 0 \\ - \\ 0 \\ -100 \\ 0 \end{Bmatrix}
$$

As the result for the curvature it can be written:

$$
\begin{Bmatrix} \kappa_x \\ \kappa_y \\ \kappa_{xy} \end{Bmatrix} = \begin{Bmatrix} 6,82{\times}10^{-4} \\ -4,239{\times}10^{-3} \\ 1,024{\times}10^{-3} \end{Bmatrix}
$$

These obtained curvatures are considered as the theoretical result of the ABD method. The ABD method is considered as the reference method also for the sample 2 and the accuracy of each method can be obtained by comparison with the ABD method.

The curvature of the square element for this sample has been illustrated in the figure 3-24:

*Figure 3-24: ABD matrix for sample 2*
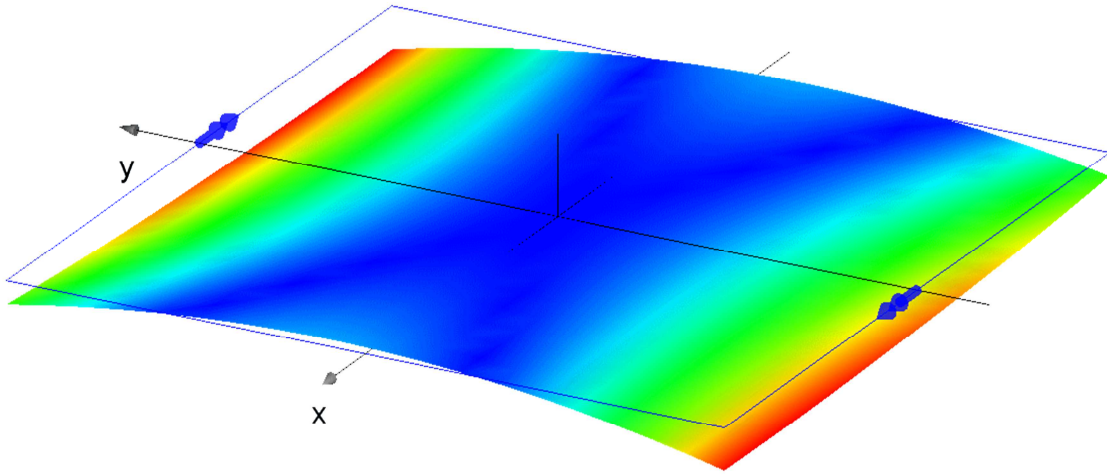


### 3.3.3 CATIA FEM simulation with the average elastic factors input

The whole calculation process of this method is similar to section 3.2.3 of the sample 1. The material properties are also similar to the sample 1 properties. Therefore the rigidity matrix for this sample can be re-written as below:

$$[Q]_k = \begin{bmatrix} \dfrac{E_1}{1-v_{12}^2 \cdot \dfrac{E_2}{E_1}} & \dfrac{v_{12} \cdot E_2}{1-v_{12}^2 \cdot \dfrac{E_2}{E_1}} & 0 \\[2em] \dfrac{v_{12} \cdot E_2}{1-v_{12}^2 \cdot \dfrac{E_2}{E_1}} & \dfrac{E_2}{1-v_{12}^2 \cdot \dfrac{E_2}{E_1}} & 0 \\[2em] 0 & 0 & G_{12} \end{bmatrix} = \begin{bmatrix} 1,36 \cdot 10^{11} & 3,12 \cdot 10^9 & 0 \\ 3,12 \cdot 10^9 & 9,572 \cdot 10^9 & 0 \\ 0 & 0 & 5,27 \cdot 10^9 \end{bmatrix}$$

Based on the material properties (table 3-1), the rigidity matrixes $[Q]_k$ for all layup angels, which are (0, 45,-45, 90), should be calculated. The transformed rigidities of all plies, weighted according to their cross sectional ratios, are added together to yield a homogeneous laminate rigidity. The result is the laminate rigidity matrix $[A]$:

$$[A] = \begin{bmatrix} 6,668 \cdot 10^{10} & 1,626 \cdot 10^{10} & 0 \\ 1,626 \cdot 10^{10} & 5,263 \cdot 10^{10} & -1,907 \cdot 10^{-6} \\ 0 & -1,907 \cdot 10^{-6} & 1,841 \cdot 10^{10} \end{bmatrix}$$

Before determining the distortions in the laminate, the invert of the rigidity matrix $[A]$ that is compliance matrix $[a]$ should be calculated.

$$[a] = \begin{bmatrix} 1,622 \cdot 10^{-11} & -5,012 \cdot 10^{-12} & -5,192 \cdot 10^{-28} \\ -5,012 \cdot 10^{-12} & 2,055 \cdot 10^{-11} & 2,129 \cdot 10^{-27} \\ -5,192 \cdot 10^{-28} & 2,129 \cdot 10^{-27} & 5,432 \cdot 10^{-11} \end{bmatrix}$$

The engineering constants for the laminate are obtained from elements of the compliance matrix (equations 2-12, 2-13):

$$E_{x,Lam} = \frac{1}{a_{11}} = 61652 \left( N \middle/ mm^2 \right)$$

$$E_{y,Lam} = \frac{1}{a_{22}} = 48660 \left( N \middle/ mm^2 \right)$$

$$G_{xy,Lam} = \frac{1}{a_{33}} = 18409 \left( N \middle/ mm^2 \right)$$

$$\nu_{xy,Lam} = \nu_{yx,Lam} = \frac{-a_{21}}{a_{11}} = 0,309$$

The engineering constants are calculated and available. Now the CATIA model should be created and these constant will be used as material properties for the CATIA model.

The square surface of sample 2 is modeled in figure 3-25. The moments are positioned on two edge of the surface (5 N×m). It should be noticed that, for the boundary condition first the surface should have a pure bending and second the surface should be fixed in the way that it cannot be moved in any direction. Therefore three fix points are considered for the boundary condition on the middle of the surface. The mesh type is the normal quadrat mesh but the mesh size is important in this sample. As this surface model simulates the theoretical square element, the mesh size should be as large as possible. Therefore the mesh size is considered 25 mm, which divides the whole surface to 16 elements and the quantity of curvature will be more realistic. According to the laminate layup definition in figure 3-22, the thickness of each ply is considered 0,25 mm and the number of layup is 9, therefore the thickness of the surface will be 2,25 mm.

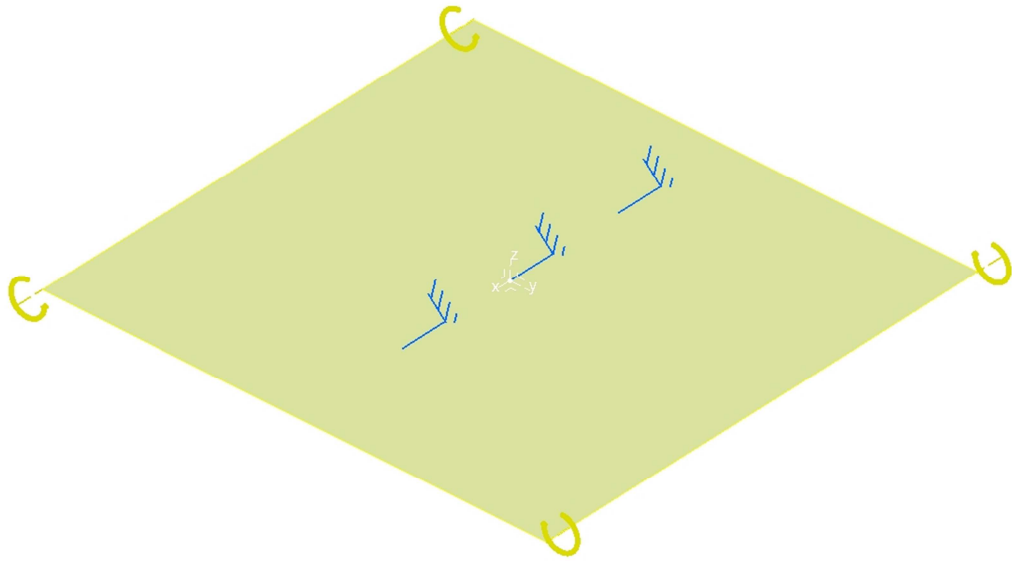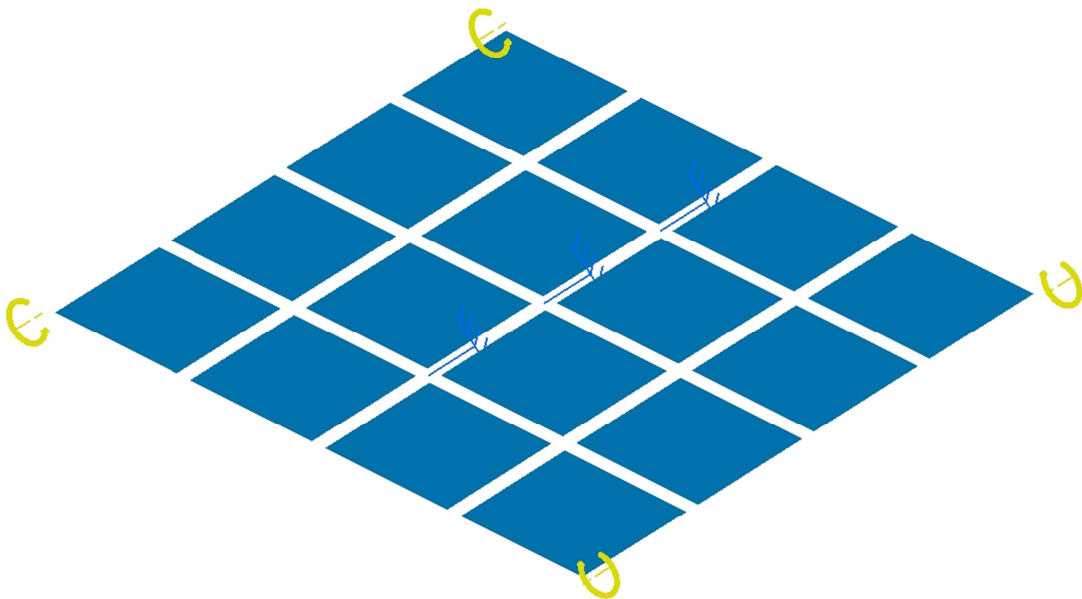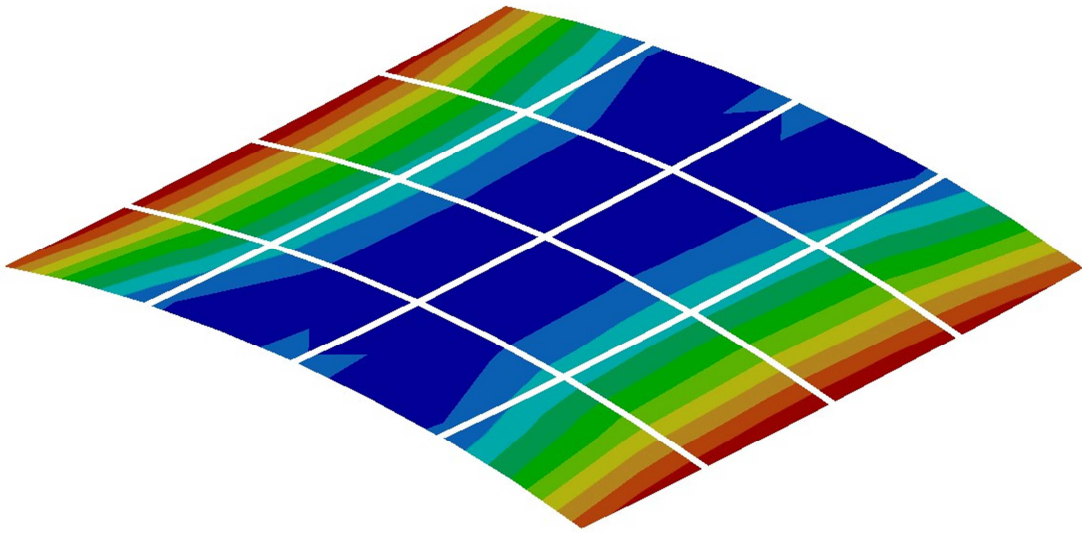*Figure 3-25: Square surface with boundary conditions and moment*



*Figure 3-26: Square surface with quadrat mesh*



After modeling and calculation the results in the CATIA software, the deformation of the surface will be available as it is illustrated in figure 3-27:

*Figure 3-27: sample 2 deformation*



The maximum displacement amount is 1,05 mm on the red edges of the surface.

In fact the factor that should be extracted in this sample is the curvature in X and Y directions. There is an option in the CATIA software which shows the curvature quantity of composite part in all directions as it is illustrated in figure 3-28. Otherwise the radius of deformation should be calculated and by reversing the radius, the curvature will be obtained.

Therefore the curvature of surface will be:

$$\left\{ \begin{matrix} \kappa_x \\ \kappa_y \end{matrix} \right\} = \left\{ \begin{matrix} 4,5 \times 10^{-4} \\ -1,33 \times 10^{-3} \end{matrix} \right\}$$

*Figure 3-28: curvature in X (upside) and Y (downside) directions*
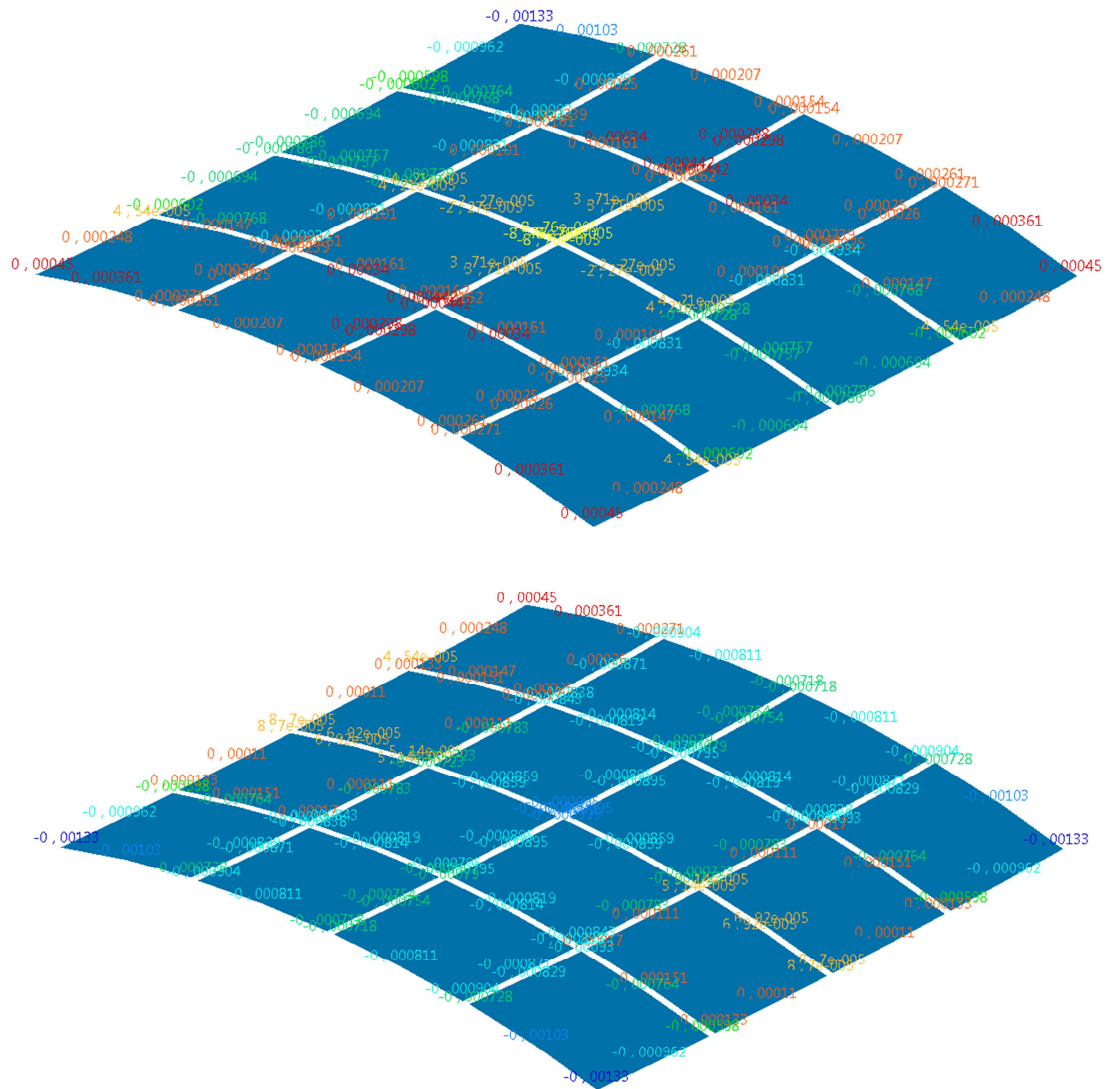


### 3.3.3.1 Position of Ply

To investigate the importance of ply position in this sample the theoretical ABD calculation for $\left[ 90,\ 45, -45,\ 0, \overline{0} \right]_s$ instead of $\left[ 0,\ 45, -45,\ 90, \overline{0} \right]_s$ is presented:

After calculating the ABD matrix in the eLamX2 software and having the moment $M_y$ (same as section 3.3.1) the Hooke's law equation can be rewritten for this sample.

46

$$
\left\{\begin{array}{c} 0 \\ 0 \\ 0 \\ - \\ 0 \\ -100 \\ 0 \end{array}\right\} = \left[\begin{array}{cccccc} 150026,1 & 36587,8 & 0 & | & 0 & 0 & 0 \\ 36587,8 & 118414,7 & 0 & | & 0 & 0 & 0 \\ 0 & 0 & 41424,5 & | & 0 & 0 & 0 \\ - & - & - & + & - & - & - \\ 0 & 0 & 0 & | & 27378,8 & 15127,5 & 4939,3 \\ 0 & 0 & 0 & | & 15127,5 & 86485,6 & 4939,3 \\ 0 & 0 & 0 & | & 4939,3 & 4939,3 & 17168 \end{array}\right] \left\{\begin{array}{c} \varepsilon_x \\ \varepsilon_y \\ \varepsilon_{xy} \\ - \\ \kappa_x \\ \kappa_y \\ \kappa_{xy} \end{array}\right\}
$$

Like section 3.3.2 to obtain the curvature the equation should be reversed, so it could be written as below:

$$
\left\{\begin{array}{c} 0 \\ 0 \\ 0 \\ - \\ \kappa_x \\ \kappa_y \\ \kappa_{xy} \end{array}\right\} = \left[\begin{array}{cccccc} 7,209\times10^{-6} & -2,227\times10^{-6} & 0 & | & 0 & 0 & 0 \\ -2,227\times10^{-6} & 9,133\times10^{-6} & 0 & | & 0 & 0 & 0 \\ 0 & 0 & 2,414\times10^{-5} & | & 0 & 0 & 0 \\ - & - & - & + & - & - & - \\ 0 & 0 & 0 & | & 4.211\times10^{-5} & -6.785\times10^{-6} & -1.016\times10^{-5} \\ 0 & 0 & 0 & | & -6.785\times10^{-6} & 1,285\times10^{-5} & -1.745\times10^{-6} \\ 0 & 0 & 0 & | & -1.016\times10^{-5} & -1.745\times10^{-6} & 6,167\times10^{-5} \end{array}\right] \left\{\begin{array}{c} 0 \\ 0 \\ 0 \\ - \\ 0 \\ -100 \\ 0 \end{array}\right\}
$$

As the result for the curvature of $\left[90,\ 45,-45,\ 0,\overline{0}\right]_S$ can be written:

$$
\left\{\begin{array}{c} \kappa_x \\ \kappa_y \\ \kappa_{xy} \end{array}\right\} = \left\{\begin{array}{c} 6,78\times10^{-4} \\ -1,285\times10^{-3} \\ 1,74\times10^{-4} \end{array}\right\}
$$

The result which has been calculated for $\left[0,\ 45,-45,\ 90,\overline{0}\right]_S$ is:

$$
\left\{\begin{array}{c} \kappa_x \\ \kappa_y \\ \kappa_{xy} \end{array}\right\} = \left\{\begin{array}{c} 6,82\times10^{-4} \\ -4,239\times10^{-3} \\ 1,024\times10^{-3} \end{array}\right\}
$$

The simple comparisons between these two results demonstrate the change on the quantity of curvatures by changing the position of ply (with different orientation) in layup. On the other hand, Reviewing the CLT formulation in section 2.3.1 and also the CLT calculation for sample 2 in section 3.3 reveals this fact that the CLT formulation output (mechanical constants) for both $\left[0,\ 45,-45,\ 90,\overline{0}\right]_S$ and $\left[90,\ 45,-45,\ 0,\overline{0}\right]_S$ are the same. As these mechanical constants are used as input for the FEM software, the software output (curvature) will be similar, while according to the ABD method the curvature quantity should be different. more detail of this difference will be discussed in section 3.3.5.

### 3.3.4 FEM simulation with complete layup modeling (CATIA, ANSYS)

In this method as it has been described in section 3.2.4, the laminate is modeled ply by ply in the FEM software. The sample2 (surface) similar to sample 1 (cylinder) is also modeled with two different FEM software (CATIA, ANSYS) in this simulation.

In case that all method could be compared to each other, they should have a same model and same mesh size. Therefore the sample model is similar to the average method model (figure 3-25) with the same properties; and the mesh size is considered 25 mm similar to the average method (figure 3-26). The layup procedure on the surface is ply by ply, the orthotropic composite properties of regular epoxy carbon are considered for each ply according to the table 3-3.

The 9 layer layup laminate is modeled in the CATIA software, the surface after modeling is illustrated in the figure 3-29 (0 degree–yellow, 45 degree–blue, -45 degree–green, 90 degree– red).

*Figure 3-29: composite layup in CATIA*
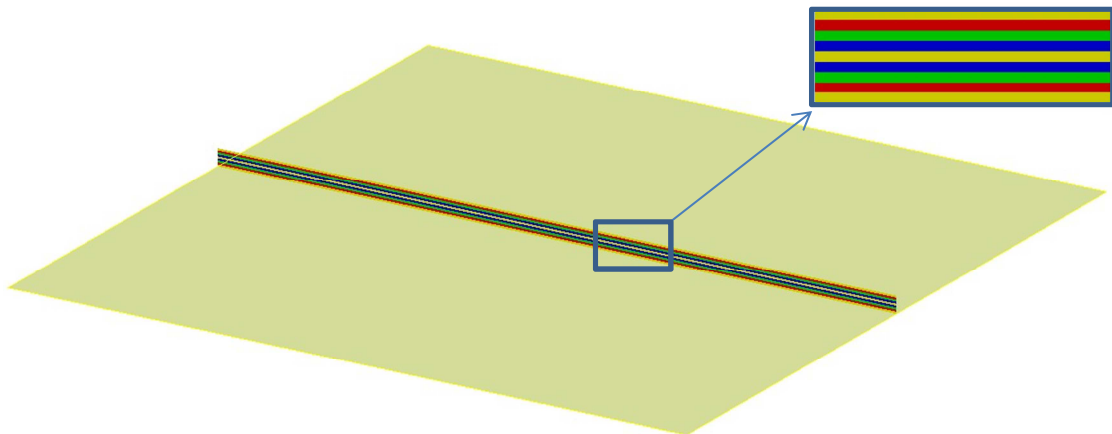


As it has been described in section 3.2.4, the ANSYS PrePost shows each layer by its own angle on the surface. In figure 3-30 all types of the ply angles have been illustrated (0, 45, -45, and 90).

*Figure 3-30: composite layup in ANSYS*
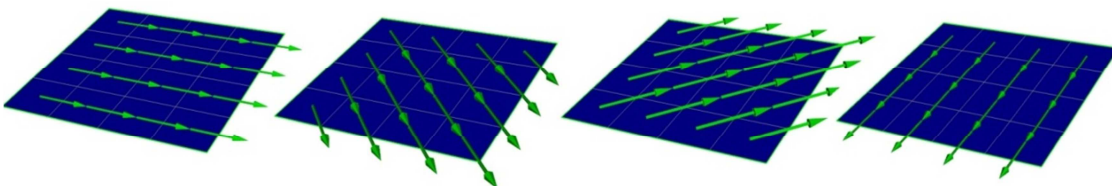
The moments and boundary conditions are similar to the average method (figure 3-25). The surface thickness after layup will be 2,25 mm (0,25mm for each ply). The outer edge of the red element in the figure 3-31 is considered for extracting the curvature of the surface. In fact the maximum curvature occurs at this place.

*Figure 3-31: surface after layup*
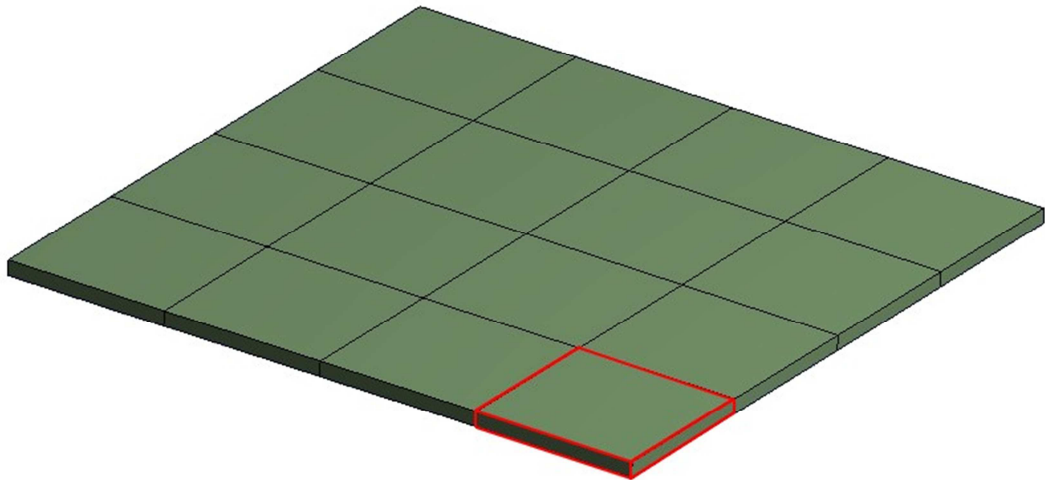


After calculating the model with the following laminate layup and mesh properties, the result will be accessible. The deformation of the surface in the CATIA software is illustrated in figure 3-32.

*Figure 3-32: surface deformation in CATIA*
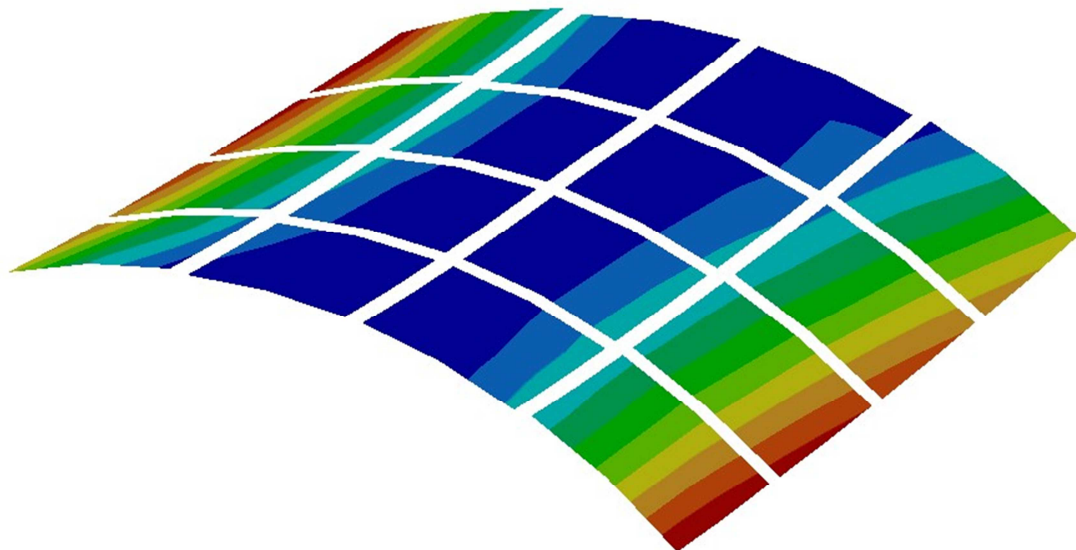
The maximum deformation amount is 2,9 mm on the red edge of the surface. And similar to the average method curvatures can be extracted from CATIA software as it shown in the figure 3-32.

*Figure 3-33: surface curvature in Y direction*
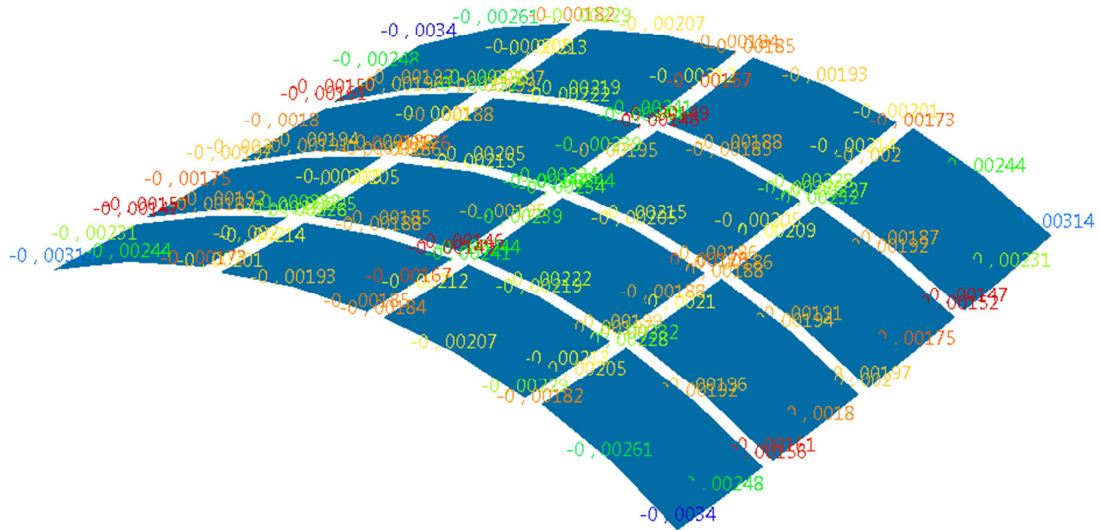


Therefore the curvature vector of the CATIA model can be written as below:

$$\begin{Bmatrix} \kappa_x \\ \kappa_y \\ \kappa_{xy} \end{Bmatrix} = \begin{Bmatrix} 4,69 \times 10^{-4} \\ -3,4 \times 10^{-3} \\ 1,21 \times 10^{-3} \end{Bmatrix}$$

In the ANSYS software the procedure of calculating the curvature factors is somehow harder, because there is no option for showing the curvature factors. Therefore in this case some calculations should be done first deformation should be calculated, second radius should be measured from the deformation in each direction, third the radius should be reversed until the curvature can be obtained. (Equation 3-5)

The maximum deformation as it illustrated in figure 3-34 is 2,95 mm which also occurs on the outer edge of the element. It should be noticed that this amount expresses the total deformation. Hence the deformation which should be used for calculating the curvature has different amount in each direction.

Figure 3-34: surface deformation in ANSYS
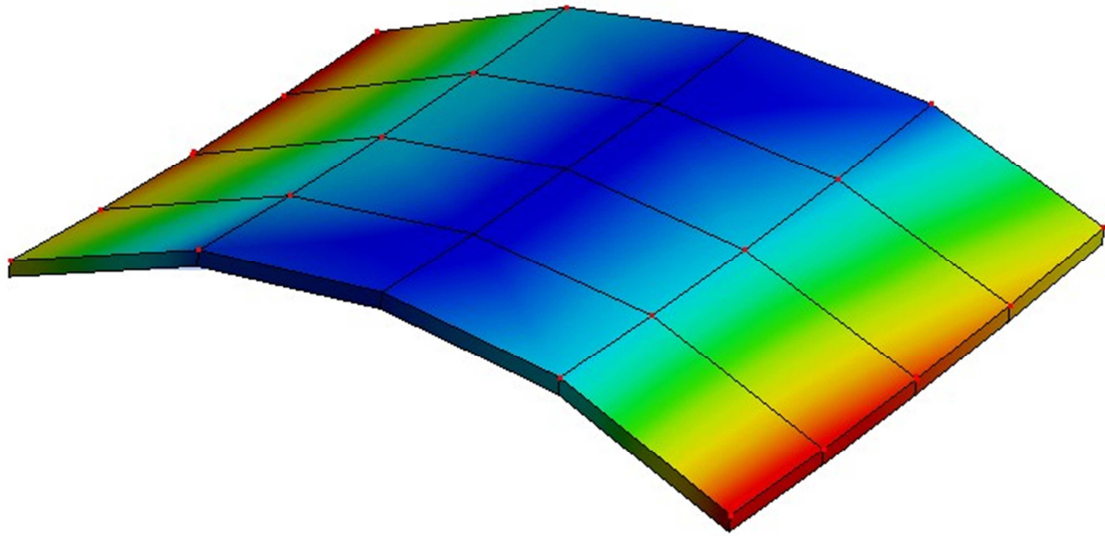


After calculating the curvature based on the deformation in each direction, the curvature vector of ANSYS software can be written:

$$\begin{Bmatrix} \kappa_x \\ \kappa_y \\ \kappa_{xy} \end{Bmatrix} = \begin{Bmatrix} 5,75 \times 10^{-4} \\ -3,51 \times 10^{-3} \\ 1,21 \times 10^{-3} \end{Bmatrix}$$

## 3.3.5 Comparison

Based on what have been obtained in the previous sections (3.3.2 to 3.3.4), it is possible now to compare the results. In the table 3-5 all of the curvatures (four methods) in X and Y directions are gathered for this sample.

Table 3-4: Strain results for all methods

| Curvature of surface | In X direction | In Y direction |
|---|---|---|
| **Theoretical calculation** | $6,82 \times 10^{-4}$ | $-4,239 \times 10^{-3}$ |
| **CATIA simulation with average factors** | $4,5 \times 10^{-4}$ | $-1,33 \times 10^{-3}$ |
| **CATIA simulation with complete layup modeling** | $4,69 \times 10^{-4}$ | $-3,4 \times 10^{-3}$ |
| **ANSYS simulation with complete layup modeling** | $5,75 \times 10^{-4}$ | $-3,51 \times 10^{-3}$ |

In this sample (similar to the sample1) the theoretical method is also the reference method, and the three other methods are compared to this method in case the precision of each be evaluated. As it has been described in section 3.2.5, this difference between the theoretical and the complete methods results is also visible in sample 2, and that could be related to the assumption which has been made for the theoretical calculation in ABD matrix.

In contrast with sample 1 where the average method had good results for both layups, the average method outcomes for the sample 2 are really weak and non-acceptable. In this method the maximum deformation occurs in the middle of surface edges as it is illustrated in figure 2-27. But as it displayed in figure 3-35 the maximum deformation should be at the end of the edges. That means the shape of deformation and also its quantity in the average method is not correct. According to the table 3-4, the major curvature occurs in Y direction. By the simple comparison between the average method amount and the theoretical amount, it would be realized that the average method curvature is lower than even half of the theoretical method amount. Therefore when the force and moments have a bending and buckling effect, the position of plies will play an effective role on the precision of the result. Since in the average method the position of the ply is not considered (described in section 3.3.3.1), its results are not precise enough.

*Figure 3-35: surface deformation of all four methods*
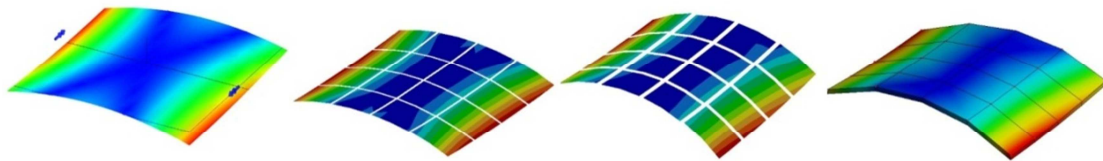


*1-Theoretical method   2-Average method   3-Complete method (CATIA)   4-Complete method (ANSYS)*

According to the table 3-4 both complete methods (with CATIA and ANSYS) have a good coverage of the results in compare to the theoretical results.  After comparing the figures of 3-35, it would be clear that the complete method has a correct distribution of deformation over the surface of sample.  Hence in case that the bending or buckling loadings act on the composite structure, the complete layup simulation would be a good choice for analyzing the structure and the result will be more realistic. Having the stress, strain and failure data of each layer separately is another advantage of this method. In the post processing section of FEM software it is possible to check out the deformation and also stress distribution of each ply separately. This option is really useful for finding the failure plies, after identifying these plies their position could be changed or the number of plies could be increased to avoid the failure of the laminate.

With all of these benefits reaching complete simulation is not always simple, Imagine the layer thicknesses are less than 0.1 mm and the number of layers exceed to 100 with the orthotropic orientation (for example $\left[45, -45\right]_n$ ). In these cases, simulation with the CATIA takes lots of time and is sometimes even impossible, but there are some options in ANSYS that help the user simulate the model easier and faster. That is why the complete simulation is made for two different FEM software, to show the similarity of results in one method using different FEM software. However the possibility of simulation depends on the software facilities. In the next chapter (4-2) a composite spiral spring will be modeled with the complete method and these subjects (orthotropic orientation and software ability) will be discussed there [8].

# 4 Application of FEM Methods in Industrial Projects with Composite Material

In chapter 2 the theoretical and FEM methods have been introduced. After comparing these methods with the theoretical approach in chapter 3, it has been concluded that these methods are precise enough to be used in industrial projects but with some considerations. In this chapter FEM methods will be used in two industrial projects which have composite material.

In recent years the FEM has had vast applications in all fields of mechanical engineering and especially in solid design. The FEM is used for simulation and analysis of those parts which are complicated to solve theoretically. This saves a great deal of time, money and energy, because it helps designers optimize their design easier and faster before getting involved in the production procedure. When an analysis deals with composite structures, it becomes even more complicated to do theoretical calculations. However composite design in mechanical engineering is still young. Many FEM software companies like ANSYS, CATIA, ABAQUS, SIEMENS NX, and HAYPER WORKS have added composite simulation in their new software releases due to increasing composite design applications in industrial products.

In this chapter for each FEM method one practical example has been provided to make each FEM method more tangible. For each method, the benefits and limitations have been described. All the examples used in this chapter have come from real models in industry and are compared with practical results.

## 4.1 Average Method

In this method as it has been described in chapter 2 section 2.3.3.1, the neutral or middle surface of the composite part should be modeled in the FEM software. The mechanical constants should be calculated from the CLT method as it has been described in chapter 2 (2.3.1).

### 4.1.1 Exploring an Example

For the average method one part of the internal body of a medical helicopter has been considered as an example, which should be replaced with the composite laminate layups. The goal of this project is to first have an appropriate environment on the internal wall of the helicopter for placing medical boxes and oxygen capsules. Second, it is to possibly move and replace them on different wall positions, and third, which is the most important part, is to evaluate how the internal body can tolerate the pressure of helicopter maneuvers in different axis or directions. The CATIA is used as the FEM software for this example. The sample parts are modeled in the environment

of surface design and have been illustrated in figure 4-1. Since describing the procedure for analyzing the entire model in this example would be too time consuming and unnecessary, considering only one part of the model would be enough. Therefore the part in figure 4-2 is considered as the selected part.

*Figure 4-1: internal wall of helicopter*



Connection to Body

Connection to Body
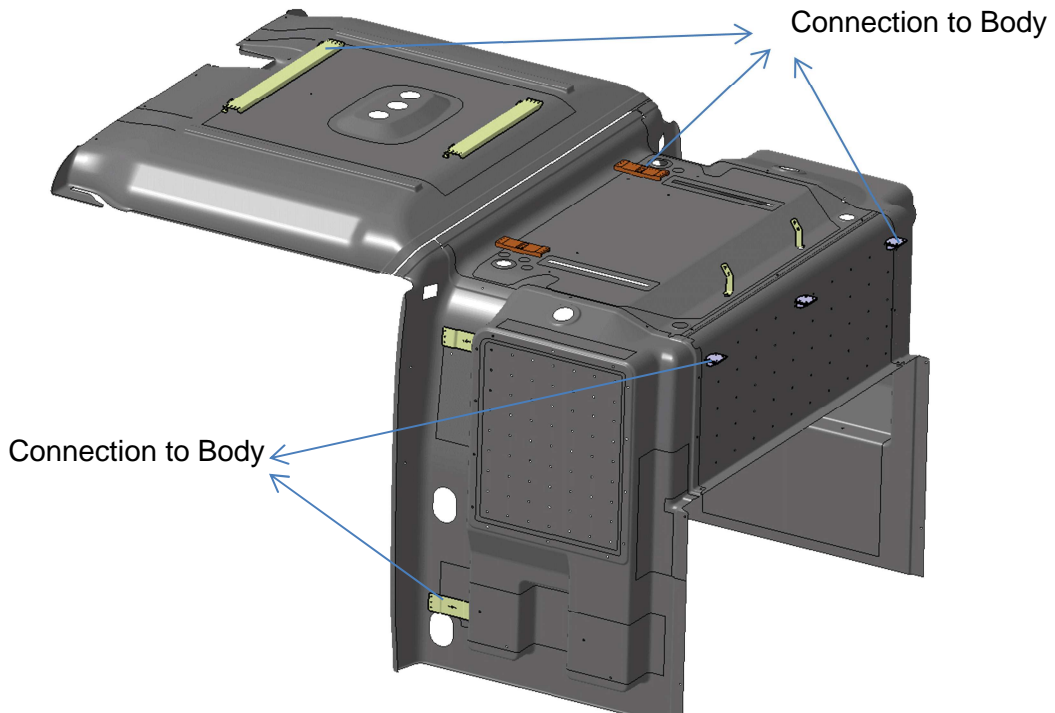
The surface bodies have been fixed to the body of the helicopter by screws and rivets as has been shown in image 4-1 in yellow, blue and orange colors. There are some parts which have been cut down since they have different types of layup compared to other parts in that section. As mentioned in chapter 2, in the CLT method the smallest part of a laminate is a ply. Here, the ply material is the epoxy carbon with long homogenized fiber direction, the mechanical constants of which have been shown in table 4-1[9].

*Table 4-1: Mechanical constants of epoxy carbon*

| Constant | Amount |
| --- | --- |
| $E_1$ | $135000 \ [N/mm^2]$ |
| $E_2$ | $9500 \ [N/mm^2]$ |
| $G_{12}$ | $5270 \ [N/mm^2]$ |
| $v_{12}$ | $0,326$ |

Figure 4-2: sample part
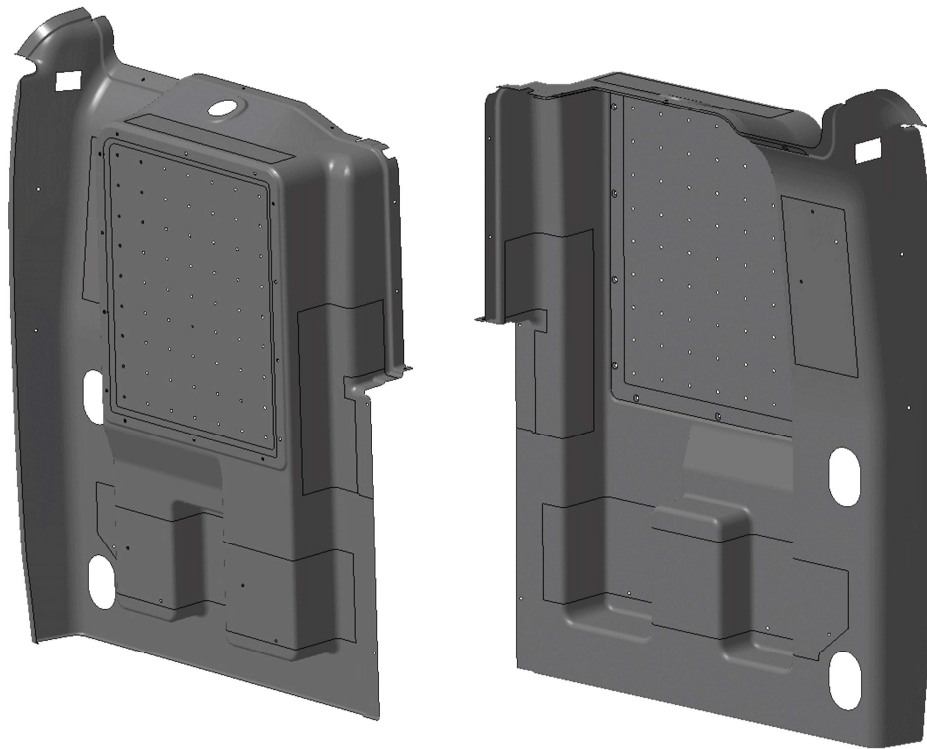


The type of the layup should be also clear, because the CLT method use angle of each ply and convert it from local coordinate to laminate coordinate system. In chapter 3 section 3.1.1 the laminate type and their notations have been described. The basic layup notation for this example part is $[0,\ 45, -45,\ 90]_n$ , but "n" which is the number of layup is not the same in each section of the sample as it illustrated in figure 4-4 and table 4-2. In some sections of the sample (for instance section B) there is a honeycomb which is placed between the layups.

In table 2-4 the number of plies, notations and thickness of the laminate for each section of the sample shown in figure 4-4 has been presented:

Table 4-2: part section layup notations and thicknesses

| Part Section | Notation | Number of plies | Honeycomb thickness (mm) | Thickness of plies + honeycomb (mm) |
|---|---|---|---|---|
| $A, D, F$ | $[0,\ 45, -45,\ 90]_2$ | 8 layer | - | 2 |
| $B$ | $[0,\ 45, -45,\ 90]_2$ | 8 Layer +Honeycomb | 8 | 2+8=10 |
| $C$ | $[0,\ 45, -45,\ 90]_4$ | 16 Layer+ Honeycomb | 4 | 4+4=8 |
| $E, G$ | $[0,\ 45, -45,\ 90]_2$ | 8 Layer + Honeycomb | 4 | 2+4=6 |

*Figure 4-4: Separating part to section based on their layups*
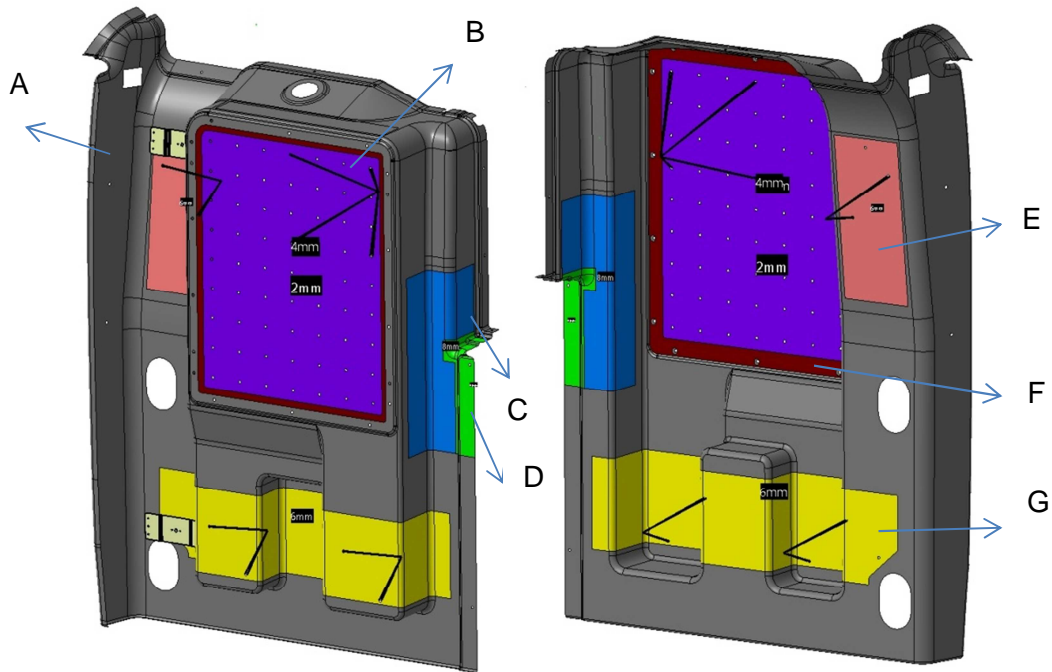


## 4.1.2 CLT Calculation

According to chapter 2 section 2-3-1, the CLT formulations are available. The mechanical constants of plies of this sample can be obtained from table 4-1. The calculation is described for section B as an example. Although the calculation process for other sections is similar, calculation for section B because of the existence of honeycomb in layup would be interesting.

In this section "k" as the number of plies is 8 and the thickness of each ply is 0,25mm which means:

$$t_k = 0,25mm \quad k = 1,\ldots,8$$

$$\sum t_k = 8 \times 0,25 = 2mm$$

In section B there is a honeycomb in layup, the layup sections with the honeycomb have similar calculation processes to layup without honeycomb, because the quantity of honeycomb stiffness is neglectable, however its thickness should be considered in the laminate thickness ($t_{Lam}$).

$$t_{Lam} = 2 + 8 = 10mm$$

By using equation 2-6, this can be written as:

$$[Q]_k = \begin{bmatrix} Q_{21} & Q_{12} & 0 \\ Q_{21} & Q_{22} & 0 \\ 0 & 0 & Q_{33} \end{bmatrix} = \begin{bmatrix} \dfrac{E_1}{1-v_{12}^2 \cdot \dfrac{E_2}{E_1}} & \dfrac{v_{12} \cdot E_2}{1-v_{12}^2 \cdot \dfrac{E_2}{E_1}} & 0 \\ \dfrac{v_{12} \cdot E_2}{1-v_{12}^2 \cdot \dfrac{E_2}{E_1}} & \dfrac{E_2}{1-v_{12}^2 \cdot \dfrac{E_2}{E_1}} & 0 \\ 0 & 0 & G_{12} \end{bmatrix} =$$

$$\begin{bmatrix} 1,36\times10^{11} & 3,12\times10^9 & 0 \\ 3,12\times10^9 & 9,572\times10^9 & 0 \\ 0 & 0 & 5,27\times10^9 \end{bmatrix}$$

The layup type is $[0,\ 45, -45,\ 90]_2$, therefore the Transformer matrix $[T]_k$ should be calculated for all current four degrees. The next step is to use formulation 2-7 to convert the rigidity matrix $[Q]_k$ from the ply coordinate system to the laminate coordinate system. In this sample, the rigidity of the plies are the same, therefore $[Q]_k$ will be the same for all plies:

For $\theta_1 = 0$:

$$[T]_1 = \begin{bmatrix} \cos^2 & \sin^2 & 2\sin\cos \\ \sin^2 & \cos^2 & -2\sin\cos \\ -\sin\cos & \sin\cos & \cos^2-\sin^2 \end{bmatrix} = \begin{bmatrix} 1 & 0 & 0 \\ 0 & 1 & 0 \\ 0 & 0 & 1 \end{bmatrix}$$

$$[Q]_{LamCS,1} = [T]_1 \cdot [Q]_{PlyCS,k} \cdot [T]_1^T = \begin{bmatrix} 1,36\times10^{11} & 3,12\times10^9 & 0 \\ 3,12\times10^9 & 9,572\times10^9 & 0 \\ 0 & 0 & 5,27\times10^9 \end{bmatrix} Pa$$

For $\theta_2 = 45$:

$$[T]_2 = \begin{bmatrix} \cos^2 & \sin^2 & 2\sin\cos \\ \sin^2 & \cos^2 & -2\sin\cos \\ -\sin\cos & \sin\cos & \cos^2-\sin^2 \end{bmatrix} = \begin{bmatrix} 0,5 & 0,5 & 1 \\ 0,5 & 0,5 & -1 \\ -0,5 & 0,5 & 0 \end{bmatrix}$$

$$[Q]_{LamCS,2} = [T]_2 \cdot [Q]_{PlyCS,k} \cdot [T]_2^T = \begin{bmatrix} 4,323\times10^{10} & 3,269\times10^{10} & -3,161\times10^{10} \\ 3,269\times10^{10} & 4,323\times10^{10} & -3,161\times10^{10} \\ -3,161\times10^{10} & -3,161\times10^{10} & 3,484\times10^{10} \end{bmatrix} Pa$$

For $\theta_3 = -45$:

$$[T]_3 = \begin{bmatrix} \cos^2 & \sin^2 & 2\sin\cos \\ \sin^2 & \cos^2 & -2\sin\cos \\ -\sin\cos & \sin\cos & \cos^2-\sin^2 \end{bmatrix} = \begin{bmatrix} 0,5 & 0,5 & -1 \\ 0,5 & 0,5 & 1 \\ 0,5 & -0,5 & 0 \end{bmatrix}$$

$$[Q]_{LamCS,3} = [T]_3 \cdot [Q]_{PlyCS,k} \cdot [T]_3^T = \begin{bmatrix} 4,323\times10^{10} & 3,269\times10^{10} & 3,161\times10^{10} \\ 3,269\times10^{10} & 4,323\times10^{10} & 3,161\times10^{10} \\ 3,161\times10^{10} & 3,161\times10^{10} & 3,484\times10^{10} \end{bmatrix} Pa$$

For $\theta_4 = 90$:

$$[T]_4 = \begin{bmatrix} \cos^2 & \sin^2 & 2\sin\cos \\ \sin^2 & \cos^2 & -2\sin\cos \\ -\sin\cos & \sin\cos & \cos^2-\sin^2 \end{bmatrix} = \begin{bmatrix} 0 & 1 & 0 \\ 1 & 0 & 0 \\ 0 & 0 & -1 \end{bmatrix}$$

$$[Q]_{LamCS,4} = [T]_4 \cdot [Q]_{PlyCS,k} \cdot [T]_4^T = \begin{bmatrix} 9,572\times10^9 & 3,12\times10^9 & -2,504\times10^{-7} \\ 3,12\times10^9 & 1,36\times10^{11} & -7,492\times10^{-6} \\ -2,504\times10^{-7} & -7,492\times10^{-6} & 5,27\times10^9 \end{bmatrix} Pa$$

In order to obtain the laminate stiffness matrix $[A]$, it is necessary to apply equation 2-10. It should be noted that there are two plies for each angle; therefore the number of plies with the same angle should be included in this calculation:

$$[A] = \sum_k \frac{t_k}{t_{lam}}\cdot[Q]_{LamCS,k} = \frac{2t_1}{t_{Lam}}Q_{LamCS,1} + \frac{2t_2}{t_{Lam}}Q_{LamCS,2} + \frac{2t_3}{t_{Lam}}Q_{LamCS,3} + \frac{2t_4}{t_{Lam}}Q_{LamCS,4}$$

After inputting the rigidity matrices into the equation it could be written:

$$[A] = \frac{0,5}{10}\begin{bmatrix} 1,36\times10^{11} & 3,12\times10^9 & 0 \\ 3,12\times10^9 & 9,572\times10^9 & 0 \\ 0 & 0 & 5,27\times10^9 \end{bmatrix} + \frac{0,5}{10}\begin{bmatrix} 4,323\times10^{10} & 3,269\times10^{10} & -3,161\times10^{10} \\ 3,269\times10^{10} & 4,323\times10^{10} & -3,161\times10^{10} \\ -3,161\times10^{10} & -3,161\times10^{10} & 3,484\times10^{10} \end{bmatrix} +$$

$$\frac{0,5}{10}\begin{bmatrix} 4,323\times10^{10} & 3,269\times10^{10} & 3,161\times10^{10} \\ 3,269\times10^{10} & 4,323\times10^{10} & 3,161\times10^{10} \\ 3,161\times10^{10} & 3,161\times10^{10} & 3,484\times10^{10} \end{bmatrix} + \frac{0,5}{10}\begin{bmatrix} 9,572\times10^9 & 3,12\times10^9 & -2,504\times10^{-7} \\ 3,12\times10^9 & 1,36\times10^{11} & -7,492\times10^{-6} \\ -2,504\times10^{-7} & -7,492\times10^{-6} & 5,27\times10^9 \end{bmatrix}$$

And the $[A]$ matrix will be:

$$A = \begin{bmatrix} 1,16\times10^{10} & 3,581\times10^9 & 0 \\ 3,581\times10^{10} & 1,16\times10^{10} & -4,768\times10^{-7} \\ 0 & -4,768\times10^{-7} & 4,011\times10^9 \end{bmatrix} Pa$$

And the flexibility matrix $[a]$ which is the reverse of the $[A]$ matrix will be (according to equation 2-11):

$$[a]=[A]^{-1}=\begin{bmatrix} 9,526\times10^{-11} & -2,94\times10^{-11} & -3,496\times10^{-27} \\ -2,94\times10^{-11} & 9,526\times10^{-11} & 1,133\times10^{-26} \\ -3,496\times10^{-27} & 1,133\times10^{-26} & 2,493\times10^{-10} \end{bmatrix}$$

Based on equation 2-13 the laminate mechanical constants can be obtained from elements of the flexibility matrix:

$$E_{x,Lam}=\frac{1}{a_{11}}=10,498\ Gpa$$

$$E_{y,Lam}=\frac{1}{a_{22}}=10,498\ Gpa$$

$$G_{xy,Lam}=\frac{1}{a_{33}}=4,011\ Gpa$$

$$v_{xy,Lam}=v_{yx,Lam}=\frac{-a_{21}}{a_{11}}=0,309$$

These constants are used as an input for mechanical constants of sample sections in figure 4-4. It is important to mention that in this method the thickness of each section should be allocated separately according to table 4-3 as 2D mechanical properties. After finishing all these steps, each section of the sample will have its own laminate thickness as well as its average mechanical constant instead of the laminate layup.

Note that as mentioned earlier, the procedure for other layup calculations in table 4-3 is similar to the current calculation. The only difference is that the number of same angle plies should also be taken into account in equation 2-10, and thereinafter the $[A]$ matrix should be calculated again. If a honeycomb exists in the layup, the thickness of it will be considered just in the laminate thickness.

### 4.1.3 Load Cases, Mesh and Boundary Conditions

A load case is the type of forces and moments acting on the model based on the different conditions. These conditions would be related to different accelerations, increasing the load by time and etc. In this model the load cases are dependent on the acceleration in different directions which occur by the maneuver of the helicopter and would vary based on required safety factors of the factory. For this analysis the 11 load cases in all 4 flight directions have been applied. The situations for the load cases are considered to be where the helicopter has 16g (g is the gravity) acceleration forward or 20g downward. These two load cases which are the most critical cases are selected, because more deformation details would be visible on the part.

The forces are obtained from the acceleration which acts on the center of gravity of the medical boxes or capsules. These boxes are attached on the part surface and their weight should also be considered in the load case. In figure 4-5 medical boxes are shown by blue colors and their center of gravity by yellow points. As can be seen in figure 4-5, there are some holes embedded on the part which are used for attaching the medical boxes on the part wall. The virtual point tool in CATIA is applied to make a connection between the holes and the center of gravity in the box.

*Figure 4-5: loading positions*
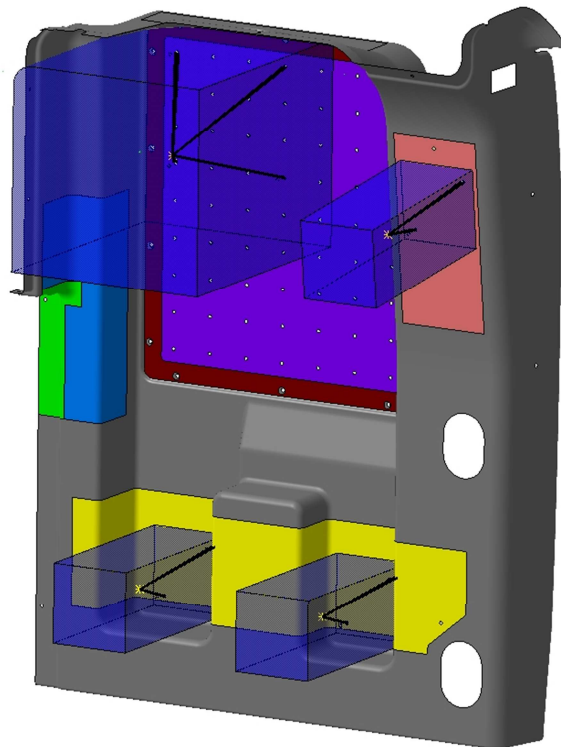


The surface mesh type is a triangle and the element is $2^{nd}$ order parabolic. There are two important points in the meshing procedure which should be noticed. First the sections which are cut down should be connected to the other parts with a mesh capture option. Otherwise the software considers them as separate parts and they should be connected manually which takes a lot of time and work. Second, all of the wholes on the part should be recognized by the mesh. Because these holes have two kinds of application, some of them are used for fixing the part to the helicopter body by using the rivets and screws (figure 4-1), and others are used for attaching the boxes to the part on the FEM software. Figure 4-6 illustrates the part after meshing by considering the mentioned points.

*Figure 4-6: mesh*
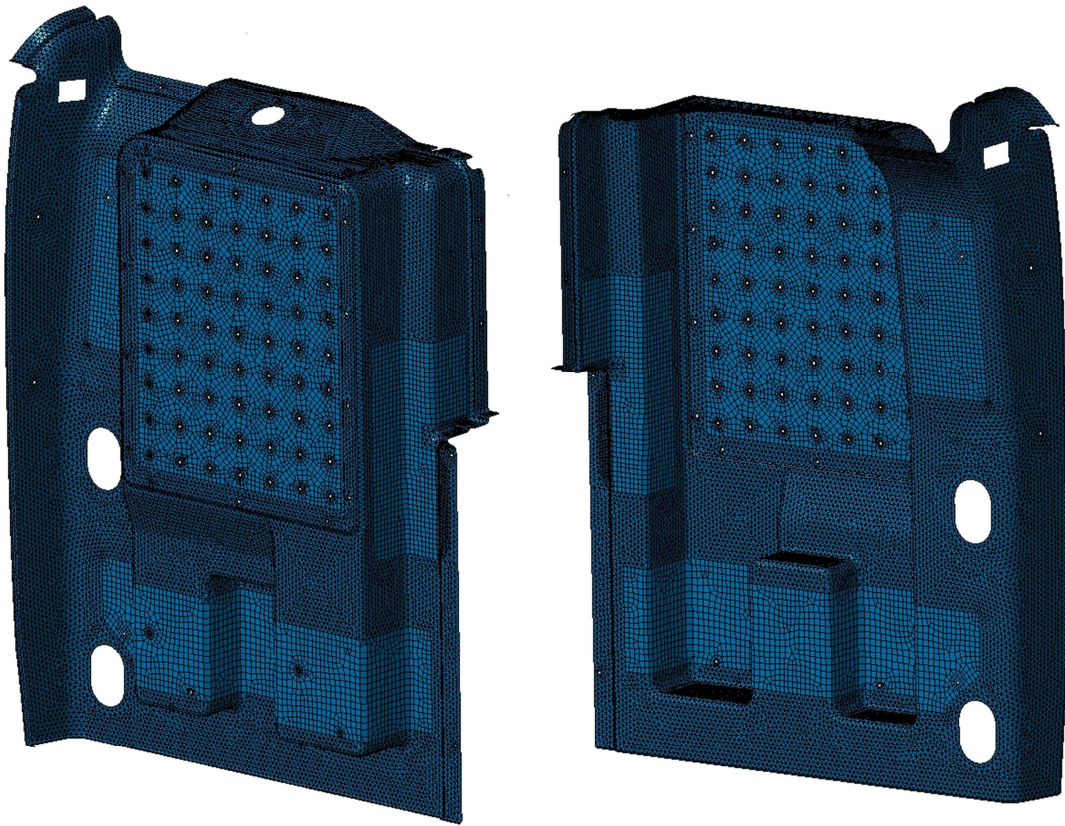


The boundary condition is a very important part of the simulation in this sample. The first type, as illustrated in picture 4-1, are the holes on the part which should be screwed or riveted to the connection bodies. The connection bodies are connected with the inner side and then fixed to the outer side of the helicopter body. The second type of boundary condition involves connecting the parts of the sample to each other. The type of connection depends on the position but is mostly a rigid connection. The third type, are the holes which fix the part directly. These holes are mostly located on the edge of the part. As an example, one sample has been shown for each type in figure 4-7.

*Figure 4-7: Boundary conditions*
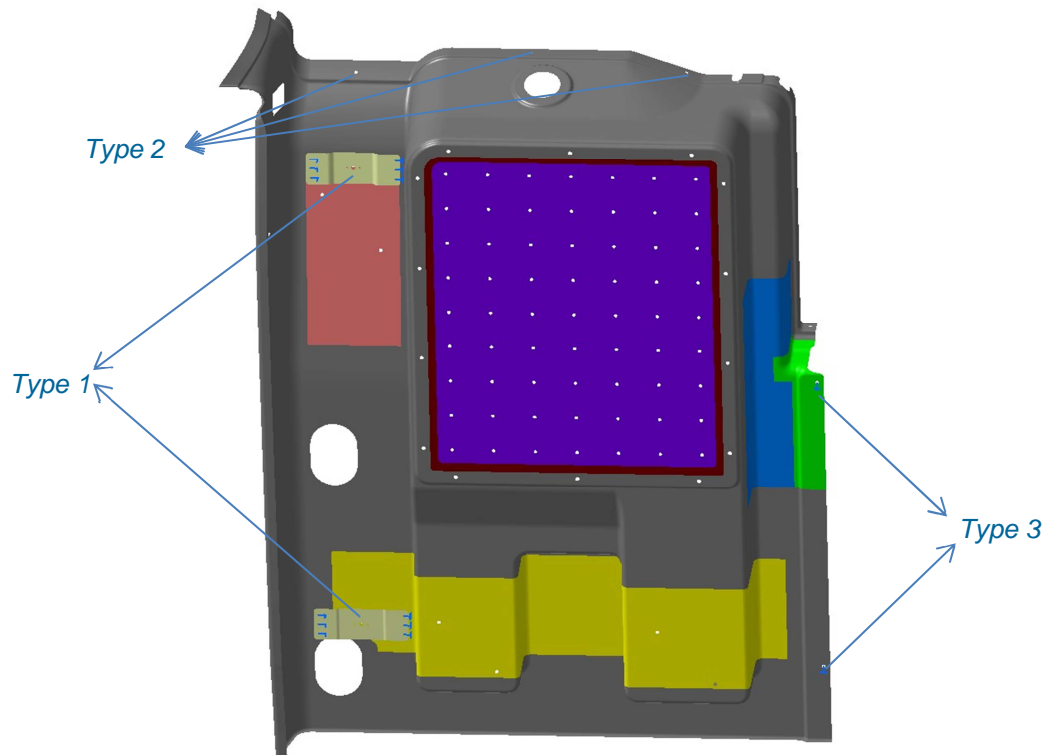


## 4.1.4 Results

After applying all the mentioned points in section 4.1.3 (mesh, load cases, boundary conditions), virtual forces in the FEM software (CATIA) and eventually calculation, the deformation of the part will be ready as has been illustrated in figure 4-8.

The important result from this is the maximum deformation of the body which should not exceed a certain limit (20mm for this sample). It should be noted that in all normal load cased (the normal load cases happen when the helicopter has a normal maneuver), the deformation amounts are quite acceptable. These results have been accepted by the "Eurocopter" company and have been used in the production procedure.

In figure 4-8 the two most critical maneuvers have been illustrated, although the deformation of the considered part is not critical, the other parts of the body have critical deformations. Hence after each critical maneuver the body should be changed due to large deformations. However, the question which comes to mind is why these critical situations which happen for instance during emergency landings should also be simulated. The answer is that if the maximum amount of deformation exceeds the specified limit, it will cause harm to the passengers. In Figure 4-9 the stress distribution of two following maneuvers are also illustrated. Studying the stress distribution helps the designer to apply a stiffer layup for the critical areas.

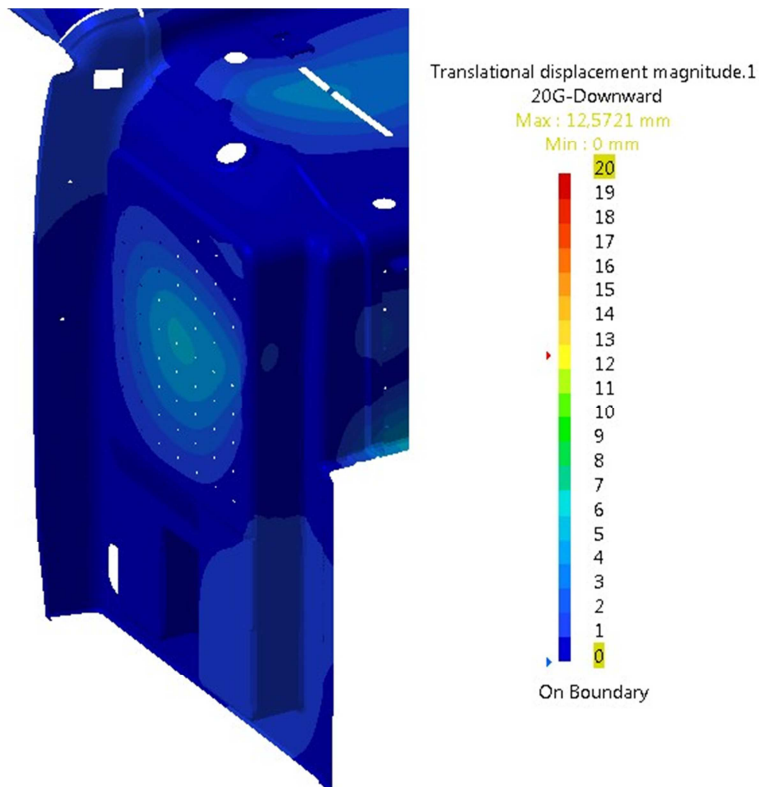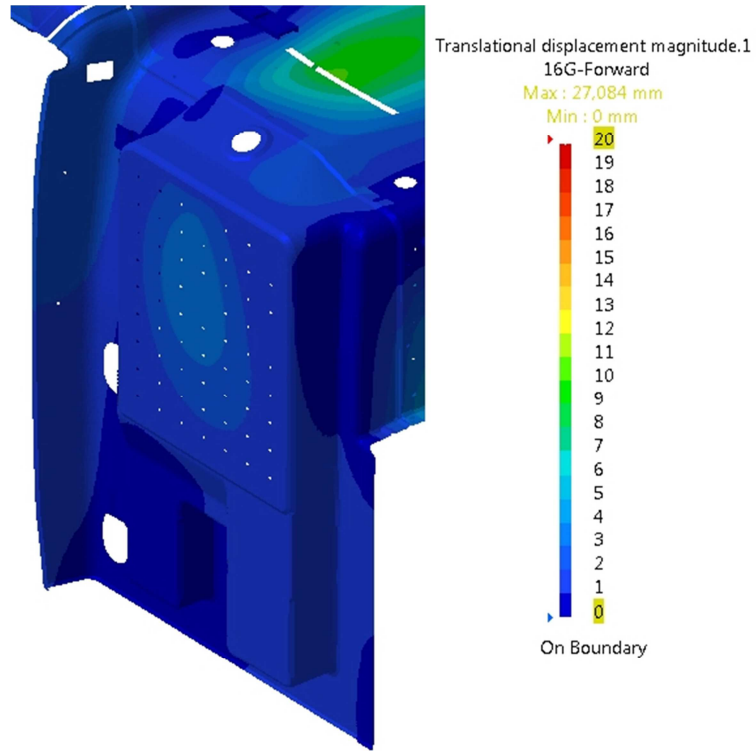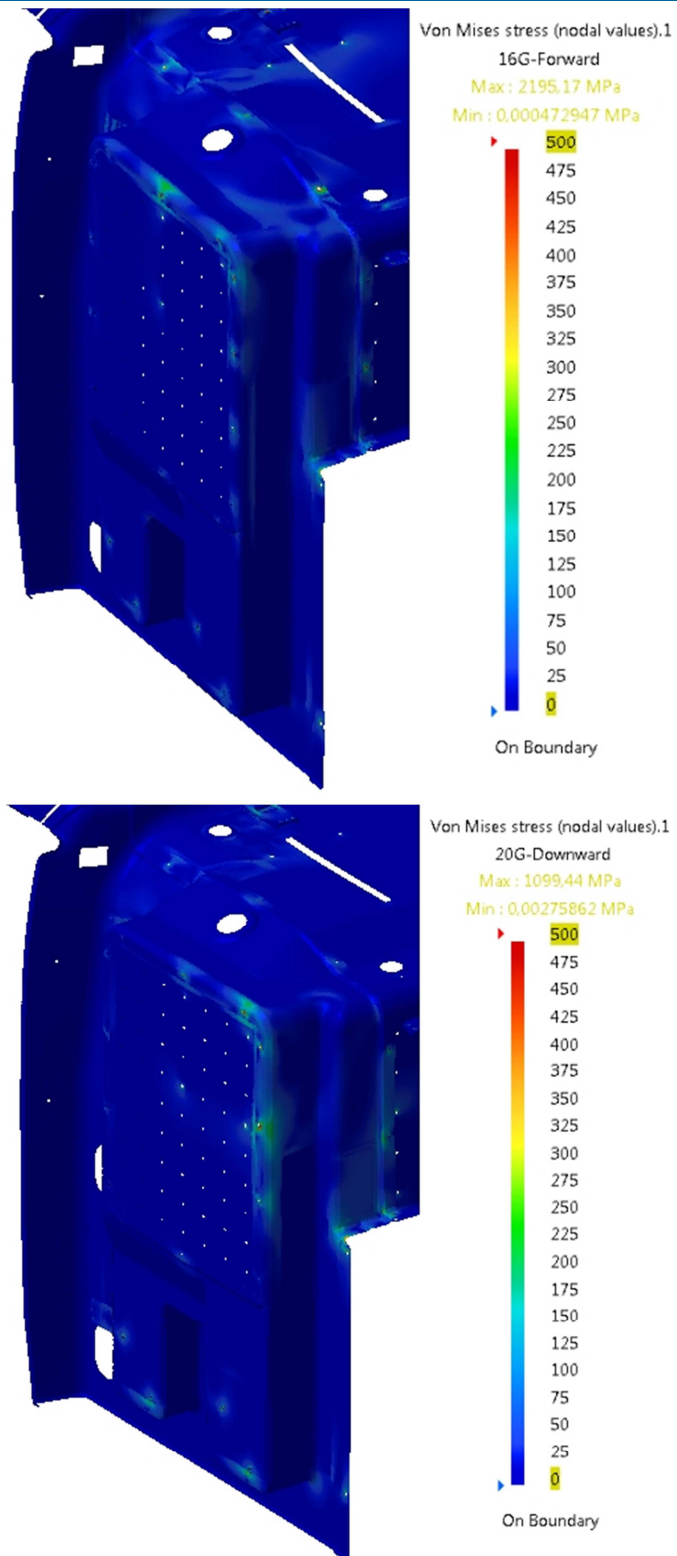*Figure 4-8: part deformations in 16 g forward and 20 g downward*

*Figure 4-9: part stress distribution in 16 g forward and 20 g downward*

## 4.1.5 Advantage and disadvantage of average method

In chapter 3 section 3.2.5 it has been described that the average method is considered as a fast and time saving method. If all the plies in this example had been modeled ply by ply, it would have taken a great deal of time. Therefore the time saving factor and the simplified simulation process can be considered as the advantages of this method. Although this method is an approximate technique, it can be used for many simulation projects while producing an acceptable precision of results if some observations are attended to.

The CLT method (chapter 2, section 2.3.1) does not consider the position of the ply in the laminate layup and it only takes into account the plies with their angles and converts them to the coordinate system of the laminate. Also, chapter 3.3 uses sample 2 to describe when the main loadings are bending or twisting on the laminate, and points out that considering the position of the ply in the laminate is very important and even critical. Although in this example the bending and twisting of the loads exist, the main loads are compressive and tensional. That's why the results are acceptable.

This method can be used for the quasi-isotropic layup, but in the orthotropic laminate layup this method should be replaced with a more precise one, because the average method in this case does not work properly. For instance the mechanical constants ($E_1$, E2, and $G_{12}$) of the two laminates (the first one is a quasi-isotropic laminate [0, 45, -45, 90]$_s$ and the second one is an orthotropic laminate [45,-45]$_n$) have been shown in polar properties in figure 4-10 and 4-11.

The mechanical constants of the quasi-isotropic laminate (figure 4-10) are nearly the same in each angle of the laminate because there is a ply in each 45 degree angle. But in the orthotropic laminate (figure 4-11) the amounts of the mechanical constants are not the same in each angle. For instance elasticity modulus has a maximum quantity at 45 and -45 directions and near to zero at the other directions [4].

*Figure 4-10: quasi-isotropic constants in polar view*
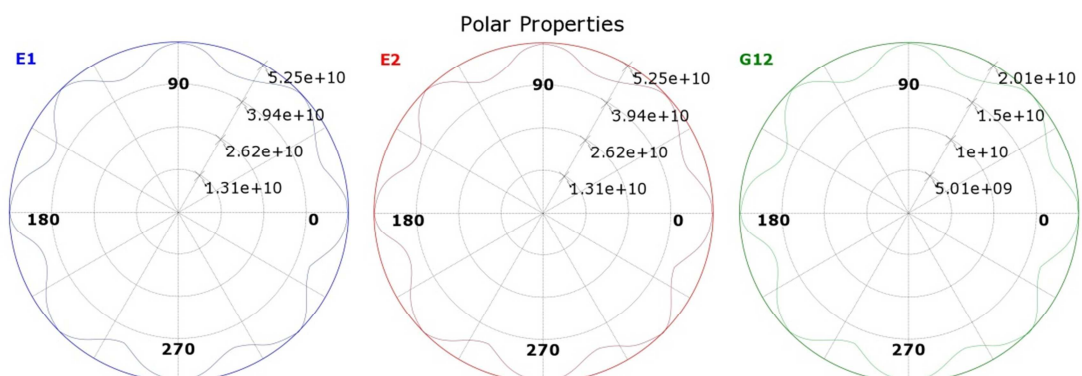
Note that the polar view for the quasi-isotropic laminate is illustrated with two types of curves (One with a circle and another with a curve) in figure 4-10. The curve shows more detail of polar view with the maximum quantity in each 45 degree, but as it visible in figure 4-10 the amounts in each angle are nearly the same therefore they could be approximately illustrated on the circle.

*Figure 4-11: orthotropic constants in polar view*
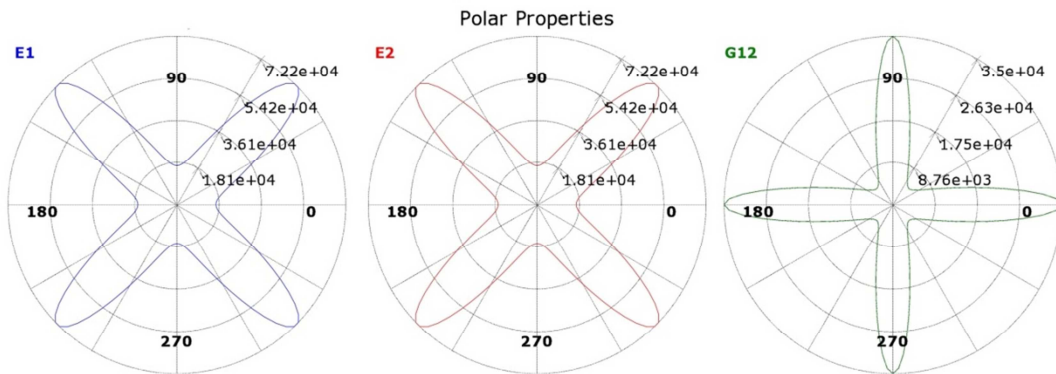


Therefore in order to use the average method the type of layup should also be taken into account. For some orthotropic layups however, the average method cannot be a good solution. Figure 4-12 compares these two types of layups. It should be noted that the amount of $E_1$ and $E_2$ are the same, therefore they cannot be seen separately in figure 4-12.

*Figure 4-12: orthotropic constants in polar view*
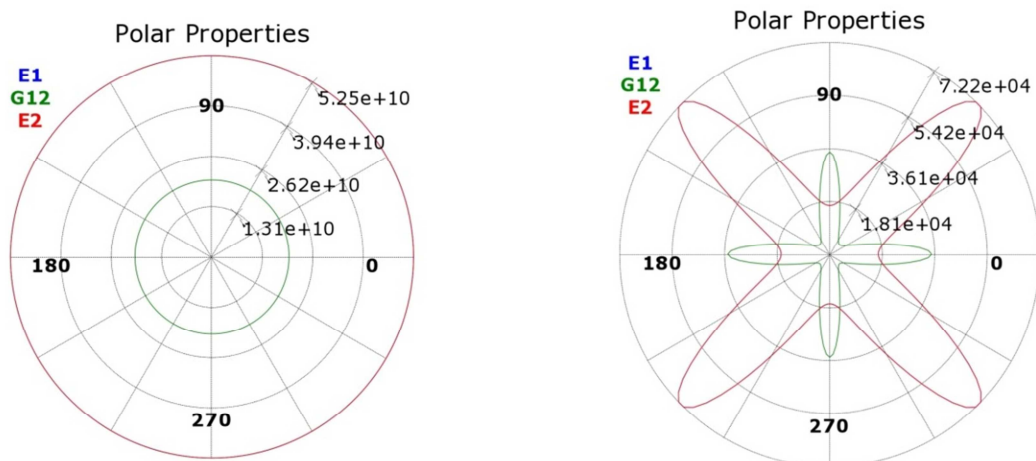
## 4.2 Complete layup simulation

In chapter 2 section 2.3.3.2 the complete method has been introduced. This method has been applied for 2 samples in chapter 3 and has been compared with the other methods. This example creates an overview of the complete method for a part with orthotropic laminate layup, when the average method result is not accurate. The assumption for this method is that the smallest part of the laminate is a ply, therefore in the complete method each ply should be modeled with its mechanical constants and of courses its orientation in the FEM software.

### 4.2.1 Exploring an Example

The example model for this section is a spring made of composite structure, which means that laminate layups form the body of the spring instead of the metals. The goal of this project is to simulate the FEM model of the spring like the real sample with the complete method; and in the next step study the simulation to see if it can cover the practical results. Although the spring is produced and tested in the factory, the simulation is still necessary. Different layup angles need to be applied, so that the best layup angles for obtaining the highest spring stiffness can be found. For this example ANSYS is applied as the FEM simulator and PrePost as the composite module for modeling the laminate layup ply by ply.

In figure 4-13 (left side) the solid model of the spring has been illustrated. The procedure of modeling in the complete method is to model the neutral surface and accumulate the plies on the neutral surface. In figure 4-13 (right side) the surface design of the spring has been illustrated. For a better preview of the surfaces the spring has been sectioned. The spring has been modeled through three surfaces called the outer, middle and inner surfaces. The thickness between the outer and inner surfaces is filled with the composite laminate layup. The quantity of the thickness is about 2,16 mm. The thickness of each fiber is 0,007mm and the type of layup is $\left[45, -45\right]_n$ orthotropic layup. With a simple calculation it will be clear that about 308 layers are required for this layup which means the quantity of "n" in the notation is equal to 154. It should be noted that in a general case, the smallest part of the laminate is a ply, but in this example the smallest part of the laminate is a fiber, because the procedure for producing the spring is special. In the real model, fibers with the thickness of 0,007 are stacked together with a machine to create a one ply layer. Therefore in this special case the fibers layup are modeled in the FEM software.

It has been described in chapter 2 section 2-3-2 that the ABD matrix calculates the entire properties of the laminate layup on the neutral surface (mid-surface). Hence for getting a better calculation result, the middle surface is considered as the neutral surface (figure 4-13 right side) while the two other surfaces should be neglected. In the next step, the laminate layups should be modeled on the upper and lower side of the neutral surface. The layup will fill the thickness between the upper and the neutral (middle) surfaces and the lower and neutral (middle) surfaces. The neutral surface is illustrated with red circles on one spine of the spring in figure 4-13.

*Figure 4-13: spring model and spring section for layup*
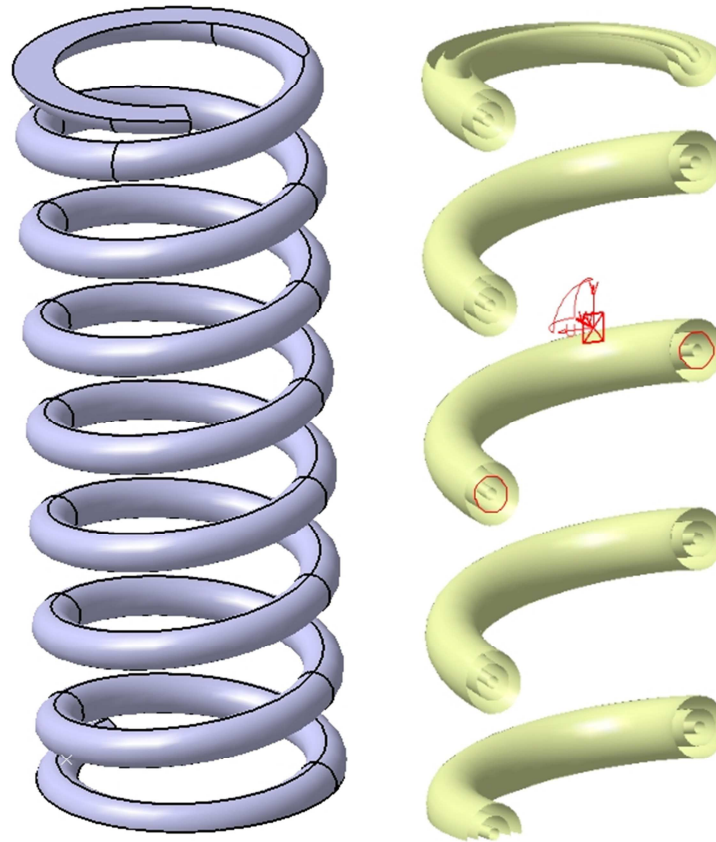


Modeling 306 layers in the FEM software is not an ordinary simulation, therefore a shortcut strategy should be applied in order to have a faster and simpler simulation. In this example three steps have been applied for modeling the whole layup as shown in figure 4-14. In step 1 five ply groups on the outer side of the neutral surface and four ply groups on the inner side of the neutral surface have been defined. Each ply group in step1 consists of 17 subgroups which are illustrated in step 2 (In ANSYS software there is a possibility to define the number of subgroups, which helps the user reduce the procedure of modeling). Each subgroup is made of a stack up, in the stack up two fibers one in the 45 degree direction and the other in the -45 degree direction have been defined as shown in step3. In the "fabrics" option of ANSYS the thickness of each fiber should be defined as 0,007mm, therefore with a simple calculation it will be written as:

Thickness of laminate: $9 \times 17 \times 2 \times 0,007 = 2,142$

As a result the desired thickness of the laminate is obtained through using this shortcut strategy. In the "fabrics" option, the material of the fiber also needs to be defined. The Epoxy carbon unidirectional is considered as the fiber material for the spring. The mechanical constants of the fiber as the smallest part of the laminate are defined in composite material options (ANSYS material properties). In table 4-3 all

mechanical constants of Epoxy carbon unidirectional have been mentioned, these amounts are imported for fiber mechanical constants [12].

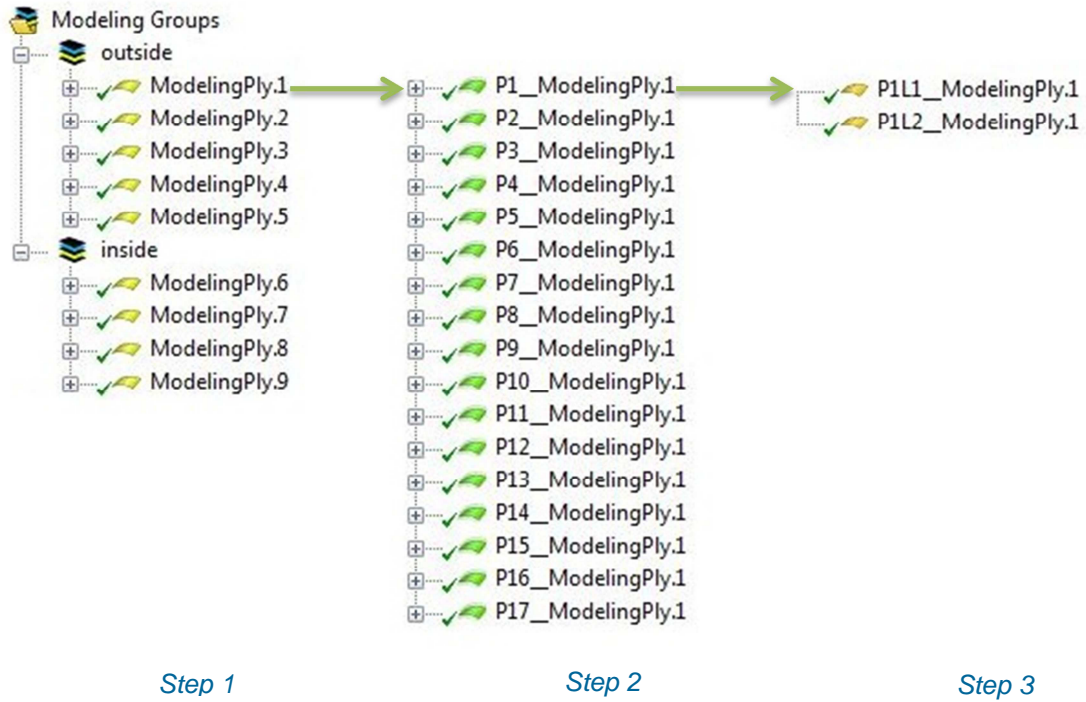*Figure 4-14: procedure of layup in ANSYS*



|  |  |  |
| :---: | :---: | :---: |
| *Step 1* | *Step 2* | *Step 3* |

*Table 4-3: Mechanical constants of Epoxy carbon UD*

| Constant | Amount |
| :---: | :--- |
| $E_x$ | $135000 \ [N/mm^2]$ |
| $E_y$ | $9500 \ [N/mm^2]$ |
| $E_Z$ | $9500 \ [N/mm^2]$ |
| $v_{XY}$ | $0,27$ |
| $v_{YZ}$ | $0,3$ |
| $v_{XZ}$ | $0,27$ |
| $G_{XY}$ | $4700 \ [N/mm^2]$ |
| $G_{YZ}$ | $3100 \ [N/mm^2]$ |
| $G_{XZ}$ | $4700 \ [N/mm^2]$ |

In this example the surface layup in two directions has been modeled. Therefore all of these 3 dimensional constants in table 4-3 are not necessary. However, defining the 2D orthotropic material in the ANSYS material properties is not possible. Based on ANSYS help "For the orthotropic properties, the X, Y, and Z value must be specified for the model to solve (2-D models only use the X and Y values). Those properties which support isotropic or orthotropic behavior will be preceded by Isotropic or Orthotropic". Hence these constants should be imported, but they are not necessarily considered in the solution process.

There is an option in the material library of ANSYS where epoxy carbon can be considered woven instead of unidirectional. In the unidirectional style, fibers are positioned in one direction and in the woven style; the fibers are placed in two directions as is illustrated in figure 4-15. In this example both have been modeled and compared [13].

*Figure 4-15: Fiber direction variation (woven left side, UD right side)*
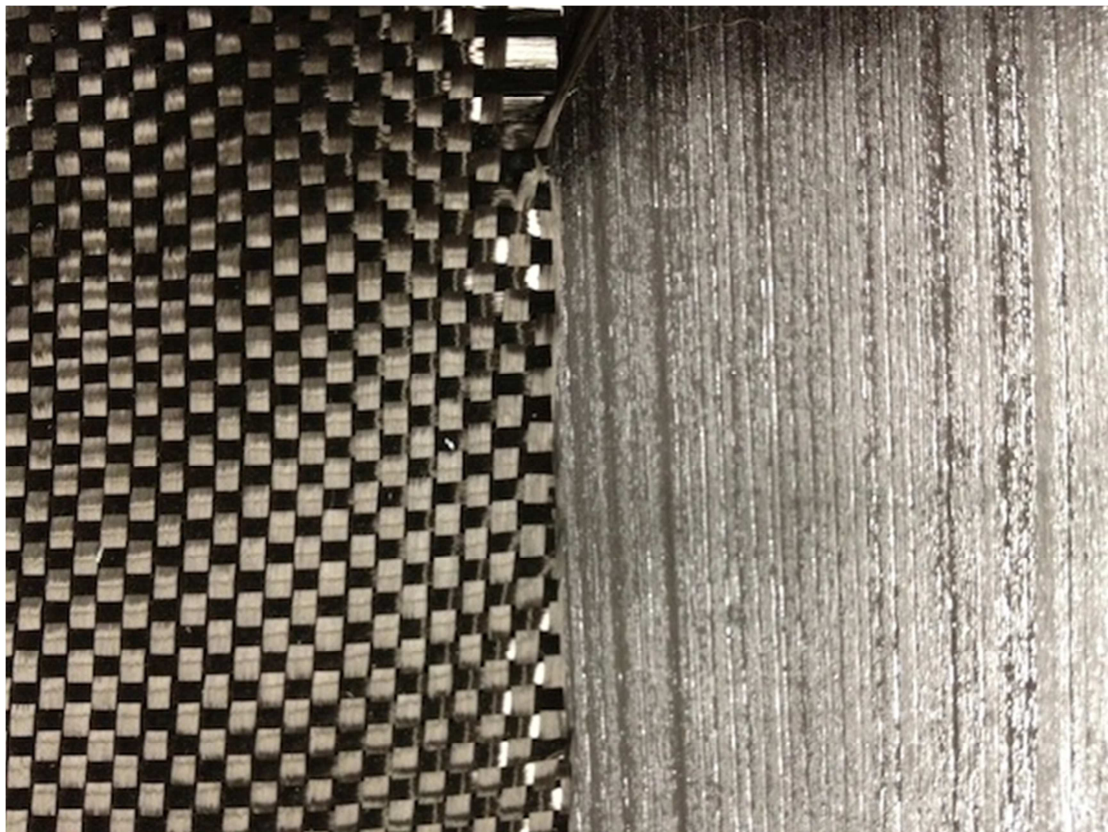


## 4.2.2 Layup process in ANSYS

In step 3 (figure 4-14) two plies one in the 45 degree and the other one in the -45 degree angle have been applied. These two ply angles have been illustrated on the model in figure 4-16. The polar properties of one layup (orthotropic layup) and its thickness are shown in lower part of figure 4-16.
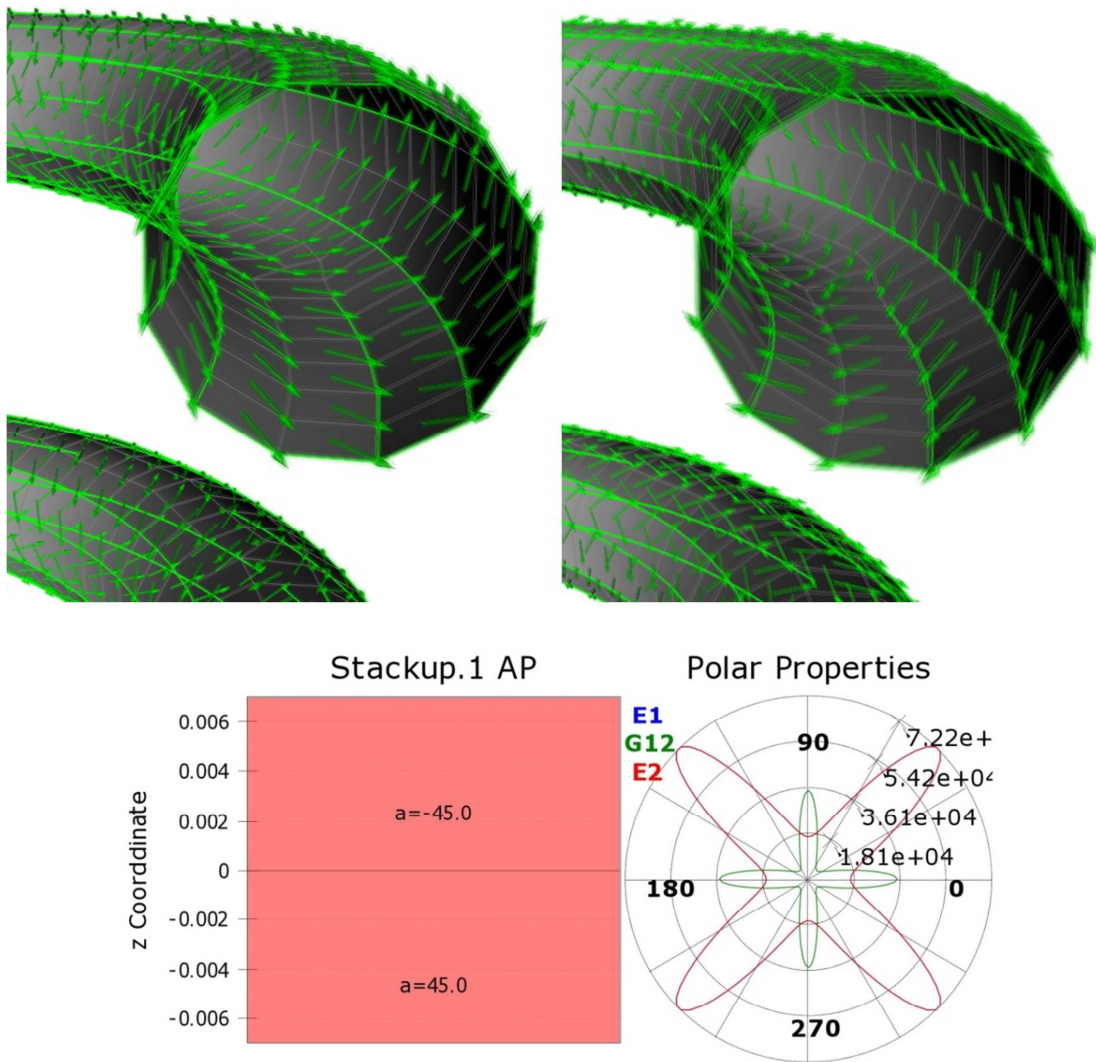
The geometry of the spring is a tube which is spun in a spiral; therefore the angle of the ply should also spin on the surface of the spring and could not be linear. For this purpose defining a reference direction in the composite simulation is necessary. The reference direction defines the rout of the ply angle on the surface in the composite layup, as has been shown in figure 4-17 (on the left side). As can be seen, the red line on the spring shows the reference direction and by selecting the current line, the plies will lie on the neutral surface in the correct format. Ply angles are also considered based on the reference direction on the ply. The reference direction has been illustrated in figure 4-17 (right side) by yellow arrows.

*Figure 4-17: Reference direction*
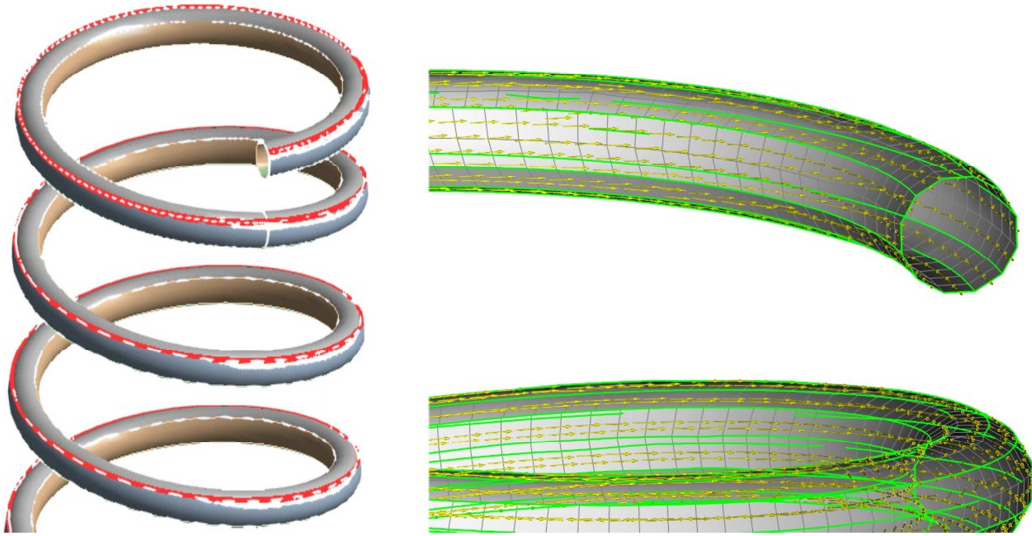


The next important composite layup modeling step which should be taken into account is the layup direction. The layup direction defines the position of the layup which can be upside or downside of the neutral surface. As it has been described in step 1 (figure 4-14), there are 5 ply groups which are modeled outside of the neutral surface and 4 ply groups which are modeled inside of the neutral surface. Hence a layup direction should be defined on the neutral surface (In ANSYS software layup direction can be defined in "oriented element set" option as it illustrated in figure 4-18).

*Figure 4-18: Orientation of element in laminate layup*
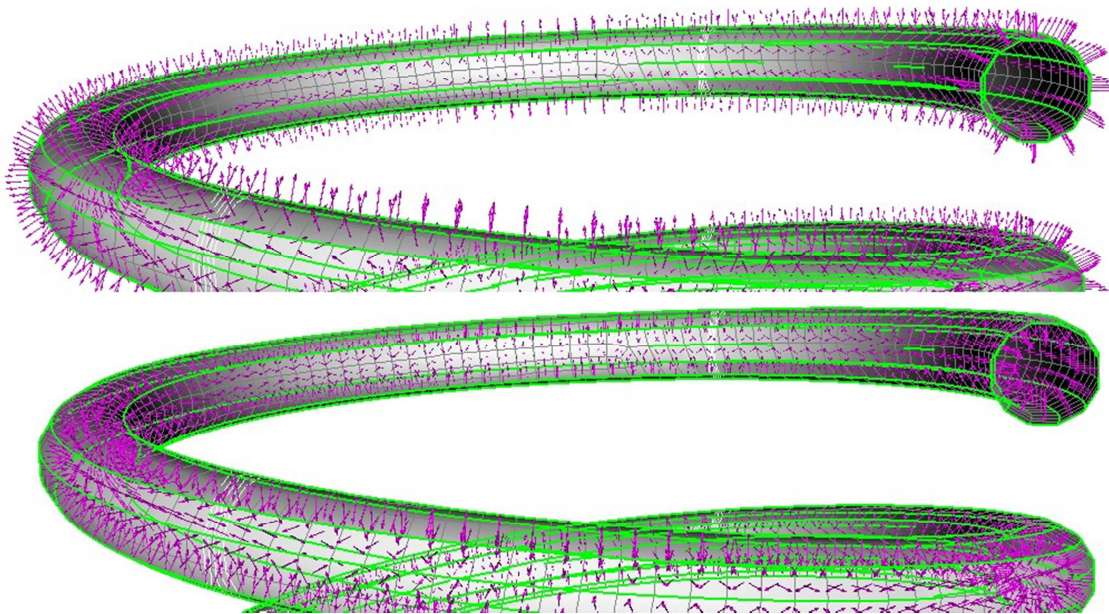
## 4.2.3 Load, mesh and boundary conditions

After all composite layup modeling steps in section 4.2.2, the mesh, boundary conditions and loads should be applied. The mesh type is the normal square mesh and software will make this for all of the layups.

The Loading acts on the spring are the step forces from 100N to 600N in six load steps (marked by A in figure 4-19). Forces act on above surface of spring (colored by red color), because a pure vertical force in y direction is required, but if the ending circle of the spring is applied as a force support, the resultant bending moment will change the deformation results.

The fixed support is the ending circle of the lower side of spring (marked by B in figure 4-19). This fixed support is fixed in all directions. In case of having a pure vertical deformation two remote displacements on the above and below surfaces of the spring have been considered. Their deformation should be avoided in the x and z directions, as well as their rotation in these directions. This action will also avoid the cone deformation of the spring (marked by C and D in figure 4-19).

*Figure 4-19: layup laminate left side and force and boundary conditions right side*
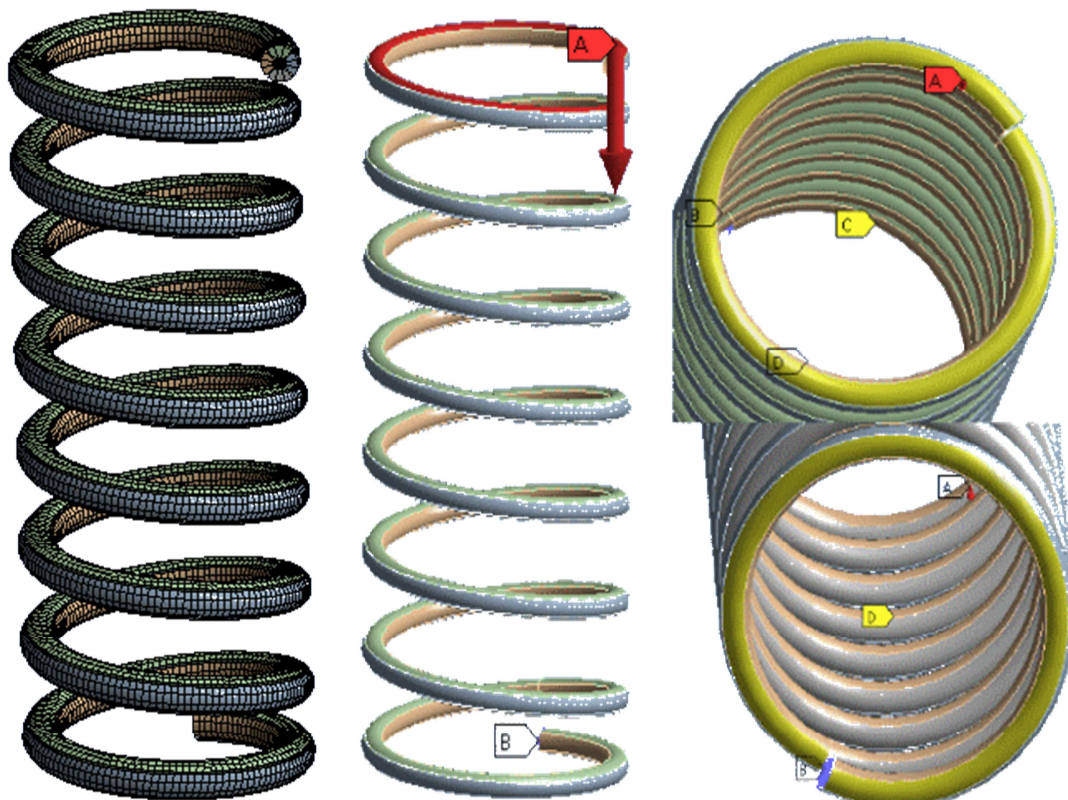
## 4.2.4 Results

After considering the boundary conditions and forces it will be possible to have the deformations of the spring for each load step. The deformation is illustrated in six steps in figure 4-20. It should be noted that only the vertical deformations are required.

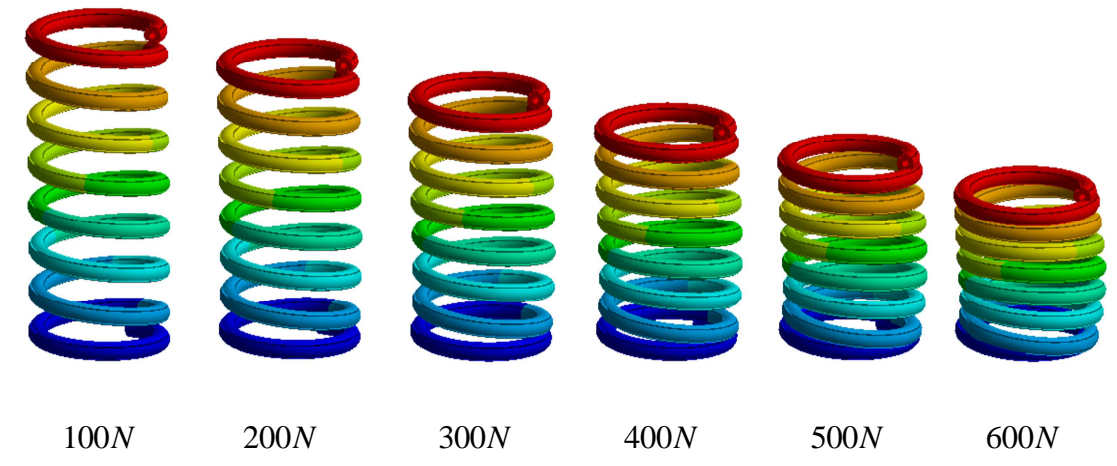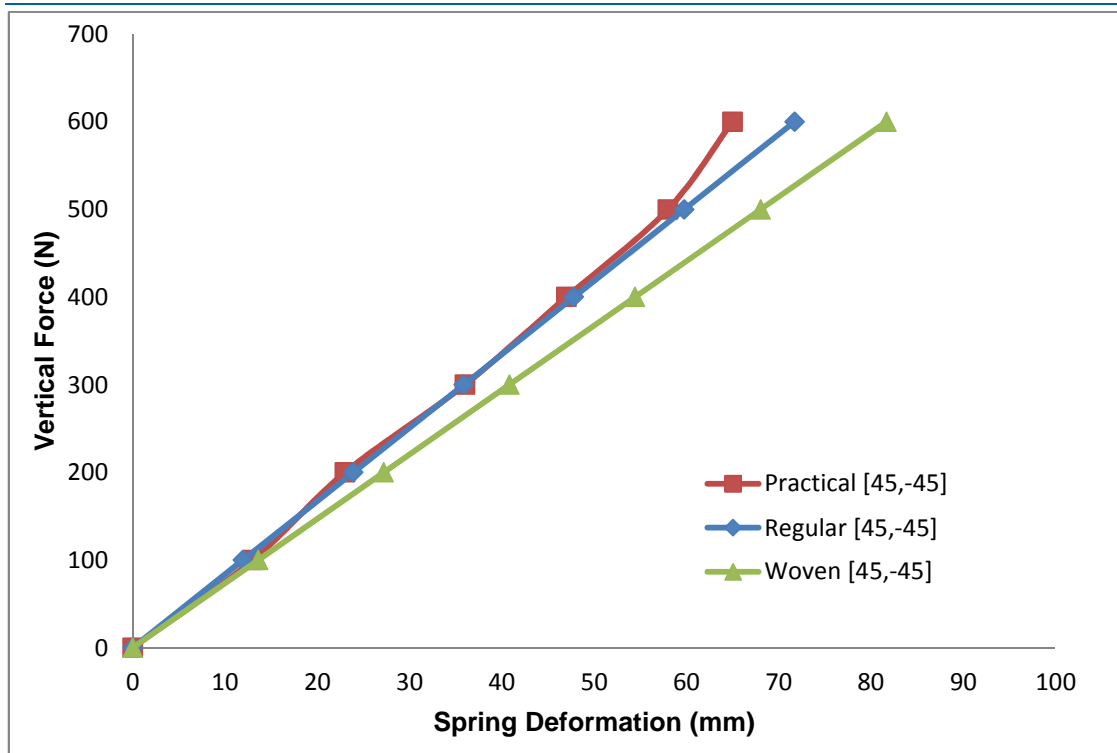*Figure 4-20: Deformation of spring for six load steps*



| 100$N$ | 200$N$ | 300$N$ | 400$N$ | 500$N$ | 600$N$ |

*Diagram 4-1: comparing the FEM deformation of spring with deformation of real deformation*

In this example as it has been mentioned earlier, the Epoxy Carbon UD (regular) and the Epoxy Carbon Woven are applied as the fiber material. The deformation comparison between these two types of material and the practical result has been shown in diagram 4-1. But why does the woven fiber have a lower strength than the UD fiber?

Deformation of the spring simulation with Regular material shows good adaptation with the practical results in diagram 4-1. There is still a difference between these two diagrams from step 5 to step 6 (500N to 600N). In figure 4-16 between load steps 500 to 600, spirals start to interfere with each other which cause more deformation in the FEM simulation. But in the real model test this interference is not possible. There is a possibility to define contact between the spirals to avoid their interference, but this is not actually the concern of this project and therefore is not dealt with here.

## 4.2.5 Optimizing the model

In section 4.2.1 the practical example for the complete layup simulation has been introduced. In the next step the procedure of modeling has been described and a simulation with acceptable deformation results has been obtained. The goal of this section is to find a better stiffness for the spring and optimize the model with the same geometry. In this case the fiber angles on the simulation process are changed and the rest of the simulation stays untouched. This action will show the effect of the fiber orientation on the stiffness of the spring. This is the advantage of the complete method that the layup model could be changed and optimized without an extra simulation.

*Figure 4-21: Ply angles on upside $[60,-60]_n$ and on downside $[30,-30]_n$ (both two ply angles shown in one figure)*



76
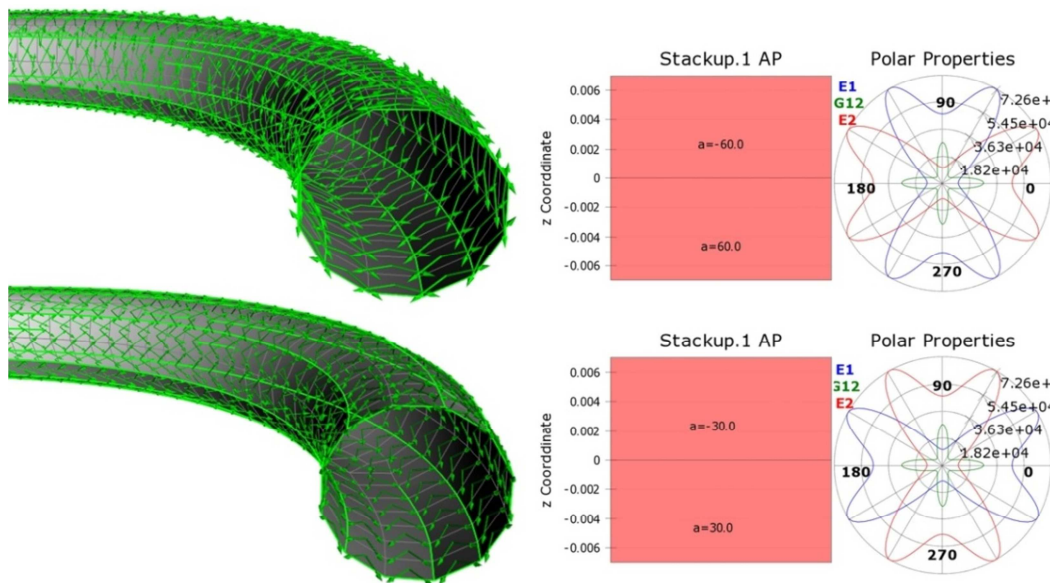
In figure 4-21 two new types of layup are introduced, the first layup type is $[60,-60]_n$ and the second layup type is $[30,-30]_n$, with "n" considered as 154, which is similar to the $[45,-45]_n$ layup. The mechanical constants which are applied for these simulations are also similar to table 4-3. As it has been mentioned the layup model stays untouched. After applying the new fiber orientation and calculations, the deformations of each new optimized model will be available. By obtaining these deformations, they can be compared to the deformations in diagram 4-1. The deformations of the spring with different fiber orientations are compared in diagram 4-2.

*Diagram 4-2: Comparing all deformations with different layup angles*
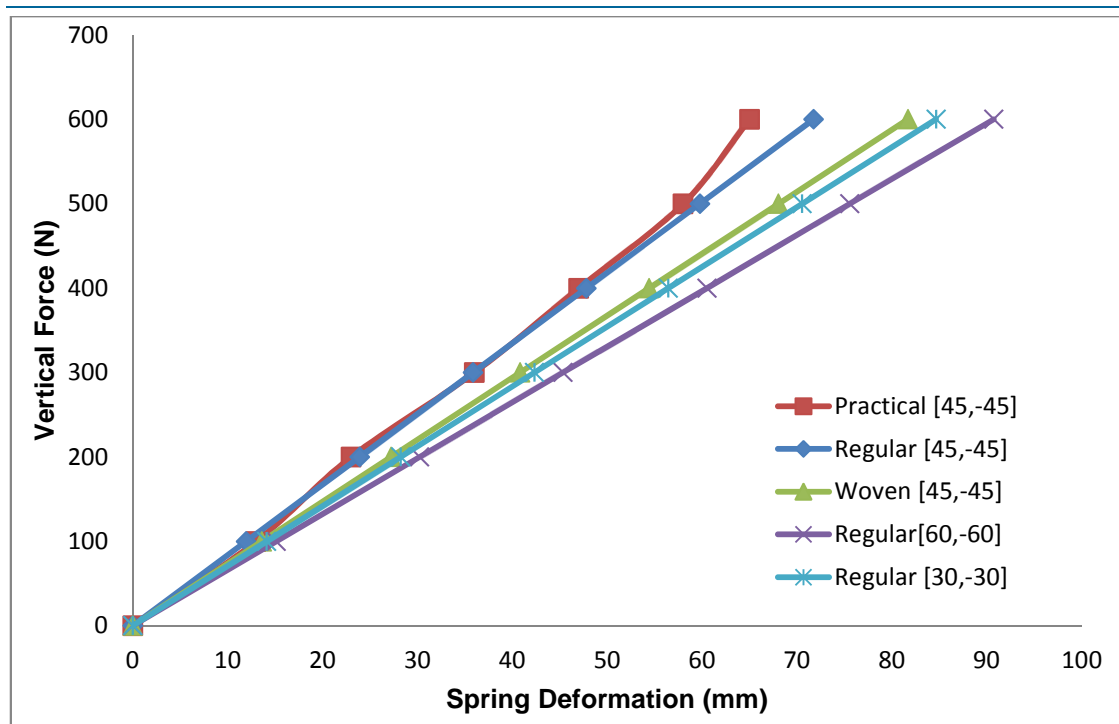


According to diagram 4-2 the new simulations cannot meet the required demands. The deformations of changed layups ($[60,-60]_n$, $[30,-30]_n$) are even more than primarily design which was $[45,-45]_n$ layup, which means the stiffness of the new layups are weaker than the practical model and cannot be considered as the optimized layup.

The question which may come to mind is why the $[45,-45]_n$ laminate has the best result? To investigate this question the principal stresses of the spring spirals should be studied. In figure 4-22 the principal stress vectors are available. The maximal vectors are shown with red arrows and minimum vectors with blue arrows (as the minimum stress vectors are quite small, they would be recognized in the zoomed part of figure 4-22. In this figure, spring spirals are rotated until they become parallel with

the X axis (global axis system) to acquire the correct angle view of the stress vectors acting on the spring. All principal stresses which act on the body of the spring are orientated in the 45 and -45 degree directions. Since the best layup should have the ply angles in the same orientation of the principal stresses to be able to better resist against the stresses and consequently have a better stiffness, the $[45, -45]_n$ layup is already the best layup for the spring.

*Figure 4-22: principal stress vectors of spring*
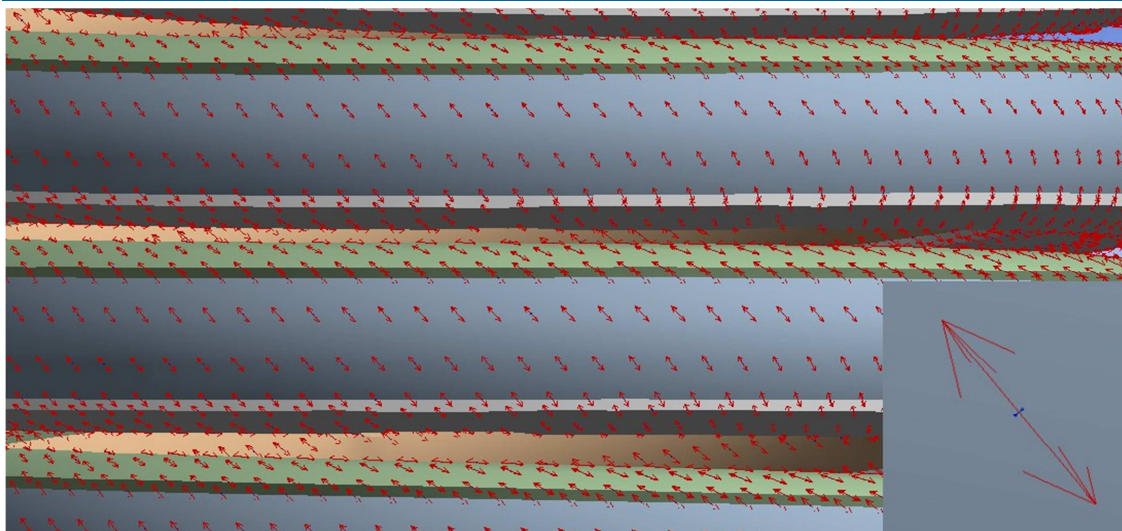


## 4.2.6 Advantage and disadvantage of complete method

The complete method used in this example provides a good estimation and acceptable results, compared to the real model, as can be seen in diagram 4-1. In section 4.1.5 it has been described that the average method is not precise when the main loadings are the bending or twisting and when considering the position of plies is important in the model. In the current example the vertical force acts on top of the spring, but because of the spirals geometry of spring the bending momentum appears on the body of the spring. Thanks to the complete method, the precise deformation results, similar to the practical result test have been obtained, regardless of the bending momentum. In this example, changing the position of the plies will change the spring stiffness; therefore the position of the plies in this example is also important. By considering all of the following conditions using the complete layup simulation is inevitable. To prove this claim, the spring is simulated with the new method.

In this method the spring is modeled in the CATIA software by using a new strategy. In fact this method is not purely an average method nor a complete method. However, it is the combination of the average method and the complete method. In the complete method (section 4.2.1) it has been described that 306 layups are required for the spring layup. The strategy of this method is modeling the 9 layer layup instead of the 306 layer layup and allocates the average mechanical constants

of each of the 34 plies to one of these 9 plies. Therefore there will be a 9 layer layup simulation where each new ply has the thickness of 34 plies in the real model .The mechanical constants of each new ply is the average mechanical constants of the 34 plies and is calculated by the CLT method. This new layup model is illustrated in figure 4-23.

*Figure 4-23: New layup model for spring*
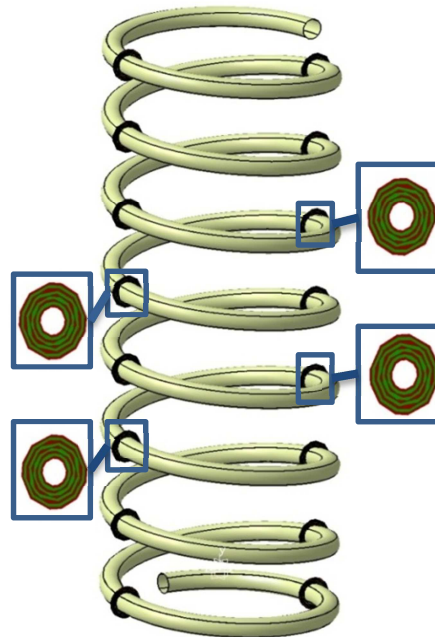


The boundary condition and loadings are the same as in the complete method (section 4.2.3). After calculating the model, the deformation results will be available. In figure 4-24 the spring deformation at the 3rd load step 300 N is illustrated. The spring at the 3rd load step is completely pressed. According to diagram 4-2 the spring in the practical test has a 36mm deformation at the load step 300 N. But in this simulation the deformation quantity of the spring is more than double that of the practical amount. In addition the spring deformation as is illustrated in figure 4-24 reaches the maximum amount. Therefore the spring in this simulate cannot tolerate more load steps. This means that this simulation is not acceptable and its results are far from the complete method results.

To realize where this huge difference between the results comes from, the layup simulation of this model should be analyzed. In figure 4-25 the 9 layer layup is presented. The red colors layups are plies with the 45 degree orientation and the green colors are considered for the plies with -45 degree. As it has been mentioned each ply in this simulation is represent with 34 plies in the complete method. These 34 plies are alternatively 45 and -45 degree in the complete method. But in this simulation one ply with the thickness of 34 plies is simulated in one orientation such as in 45 degree. Hence instead of 153 plies in 45 degrees and 153 plies in -45 degrees, there are 5 plies in 45 degrees and 4 plies in -45 degrees.

*Figure 4-24: Deformation of spring at load step 300 N*

Translational displacement magnitude.1
mm

| | |
|---|---|
| 🟥 | 74,7 |
| 🟧 | 67,3 |
| 🟧 | 59,8 |
| 🟨 | 52,3 |
| 🟨 | 44,8 |
| 🟩 | 37,4 |
| 🟩 | 29,9 |
| 🟩 | 22,4 |
| 🟦 | 14,9 |
| 🟦 | 7,47 |
| 🟦 | 0 |

On Boundary
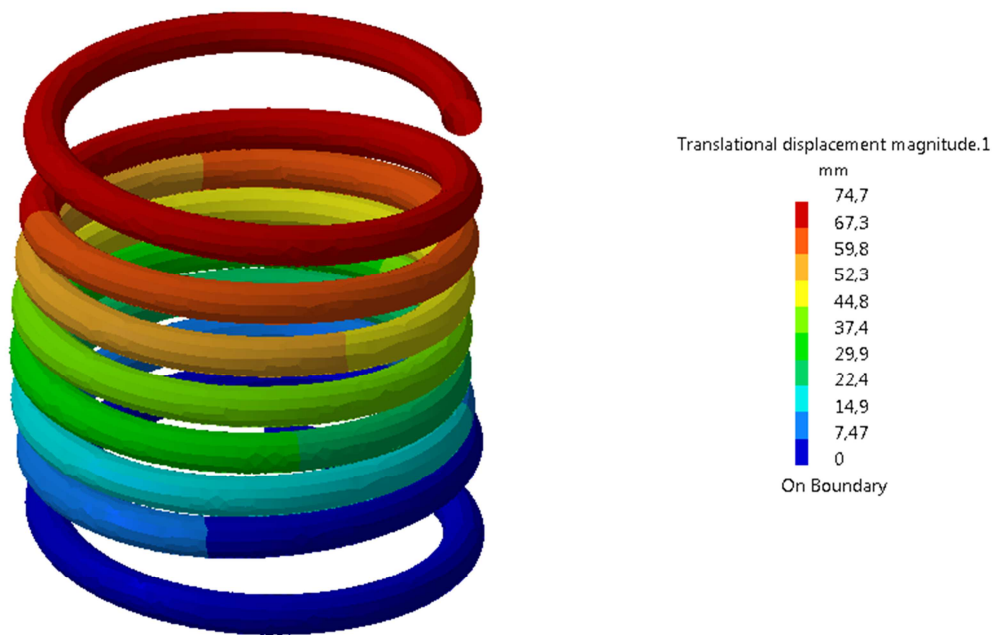
*Figure 4-25: 9 layer layup*
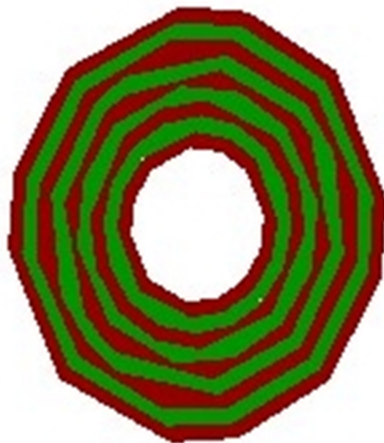


Although this method considers similar thickness and plies orientation, its results are far more imprecise than the complete method. This example shows the importance of the ply position and its orientation in the orthotropic laminate layup, especially in cases where the laminate is under the bending and twisting loadings.

As in the complete method, simulation is similar to the real composite part and there is a possibility to test and optimize the layup model with variable parameters. In other words, this method will provide an opportunity for the user to change the model in the

type of layup, ply orientation, materials and mechanical constants. These data can be gathered and compared and the best simulation can be applied based on the specific demand.

The FEM complete layup simulation has an extra advantage option. By using this option each ply deformation, stress distribution, curvature and etc. can be studied separately. This study can find the plies which have a critical status of stress or strain. Accordingly the layup model can be improved or the plies orientation can be optimized to obtain a better model. This option is also considered as an advantage of the complete method.

The time consuming process of simulating a composite laminate layup is considered as the disadvantage of this method. When the layup model is more complicated, more time is needed to find a proper simulation strategy, although this depends on the layup model. For instance for the orthotropic laminate layup (described in section 4.1.5) there is no choice but the complete layup. Hence before getting involved in the simulation process, first the composite layup should be studied and an appropriate method should be selected.

# 5 Summery

In this project the application of FEM in structures made of composite material has been studied. The strategy is to find the appropriate theoretical method for obtaining the strain or curvature of the composite laminate based on applied forces and moments. The next step is to model the composite laminate in the FEM software by using different methods, and comparing them to the theoretical method in order to see the precision of each method as well as the possibility of using them in the FEM composite analysis.

First, the theoretical and FEM methods have been introduced. The first theoretical method is called CLT (classical laminate Theory). The CLT formulations for achieving the average mechanical constants of a laminate have been described. The CLT formulation considers the thickness and orientation of each ply or a lamina 'which in this project is considered as the smallest part of the laminate' and calculates the average quantity of mechanical constants ($E_1, E_2, G_{12}, \nu$) for the whole laminate. The second theoretical method is called the ABD method which uses the ABD matrix for calculating the strain and curvature of the laminate based on the forces and moments acting on the laminate. The procedure for obtaining the 6×6 ABD matrix has been described. After getting to the ABD matrix the application and effect of each sub matrix has been introduced. This method has been considered as the principle method in this project for calculating the laminate deformation and curvatures. The average method is the first FEM solution. In this method the neutral surface of the composite part is modeled in the FEM software. This FEM method uses the resultant average mechanical constants of the CLT method and uses them as an input for the FEM model. The complete method is the second FEM solution, in this way the laminate is modeled ply by ply in the FEM software. There is no simplification in modeling of the laminate and each ply is modeled with its own mechanical constants and of course its orientation. The complete method is a pure FEM solution without any theoretical pre-calculations.

Second, the following proposal methods have been used for calculating two composite samples. After calculating and modeling all methods for each sample, the obtained results have been compared to each other. This comparison shows the advantage and disadvantage of each method and also shows the proper usage case for each method. The first sample is a cylindrical tube under internal pressure. To be able to obtain the theoretical calculation, one square element on the surface of the cylinder has been considered as sample 1 (The theoretical calculation for the whole cylinder is a long and complicated process). The result of the internal pressure is stress in the X and Y directions on the square element, and the stresses result is deformation at the X and Y directions. These deformations have first been established for each method and second have been compared. The laminate layup

types for this sample are a symmetric nine layer layup and an eight layer layup of the epoxy carbon material. The second sample is a square surface element under a bending momentum. In this sample a momentum in the Y direction is acting on the surface, and the bending momentum result is curvature in the X and Y directions. Same as sample 1 the curvatures have been calculated in all methods and the established results have been compared. The laminate layup type in this sample is a nine layer layup of the epoxy carbon material. In these two samples the complete method has been applied by two different FEM software (CATIA, ANSYS). The reason for this is to be able to view the precision of each FEM software on each sample.

Third, after proving the applicability of the FEM methods and recognizing their usage cases, each method has been applied in a practical project. In the first example an internal body of the medical helicopter has been introduced and one part of it has been selected as an example. The average method has been selected for modeling this example in the FEM software. The CLT formulations for obtaining the average amounts of mechanical constants have been calculated. The load cases, mesh and boundary conditions for this part has been described. The resultant deformation of the part has been introduced, and the advantage and disadvantage of the average method has been described. The second example is a spring made of the composite material under vertical force. The complete method has been used for simulation and calculation of a spring in the FEM software. The procedure of complete layup modeling of the spring has been described; load, mesh and the boundary conditions have been introduced. After calculating the spring deformations in the FEM software, they have been compared with the practical results. To illustrate the other facilities of the full method, the optimization of the spring has been described with different layup angles. In the advantage and disadvantage description of the full method, for proving the necessity of using the complete method for the spring, it has been simulated with a combined method (average and complete method has been combined), and the results have been compared.

The comparison of the results obtained for sample 1 using all the different methods illustrates that the precision of the average method is acceptable for simulating the composite layup. The first practical example (helicopter internal body) which has been modeled by using the average method is also proof of this claim. Although a comparison of sample 2 results have also been presented, however, in cases where bending and twisting are a major part of loading or where the ply position are important, the average results do not seem to be accurate enough and the complete method needs to be applied. This assertion has been proven by the second practical example (spring) which has been simulated by the complete method. Hence the strategy of simulating the composite layup in the FEM software depends on the type of layup and type of loading.

# 6  References

1. H.Altenbach, J.Altenbach, W.Kissing. Mechanics of Composite Structural Elements:Springer, 2004.
2. Autur K.Kaw. Mechanics of composite materials, 2nd edition: Taylor & Francis Group, 2006. P. 79-99.
3. R&G Faserverbundwerkstoffe GmbH. Handbook Composite Materials. 2003.

4. Vincent Calard .Formulas and Equations for the Classical Laminate Theory, 2011.

5. 2.A.T.Nettles. Basic Mechanics of Laminated Composite Plates: NASA Reference Publication 1351, 1994.
6. Russell C.Hibbeler. Engineering Mechanics: Statics (German version): Pearson, 2005.
7. A.B.H. Kueh , S. Pellegrino. ABD Matrix of Single-Ply Triaxial Weave Fabric Composites. University of Cambridge, Cambridge UK, 2007.
8. H.Tafaghodi, M.Grafinger. The precision of FEM simulation results compared with theoretical composite layup calculation, Composite Part B: Engineering, 2016.

**Web Reference:**

9. Toray carbon fibers America, INC., T300 composite properties,  website link: http://www.toraycfa.com/standardmodulus.html
10. ELAMX 2,2 . Author: Andreas Hauffe, Technical University of Dresden. Website                                                                          link: http://tudresden.de/die_tu_dresden/fakultaeten/fakultaet_maschinenwesen/ilr/aero/download/laminatetheory/index_html/document_view?set_language=en andreas.hauffe@tu-dresden.de
11. Wolfram Math World, Radius of curvature,  website link: http://mathworld.wolfram.com/RadiusofCurvature.html
12. ANSYS, Engineering data source, Composite Materials, website link: http://www.ansys.com/Products/Simulation+Technology/Structural+Analysis/ANSYS+Composite+PrePost
13. ORIBI Manufacturing, UNI directional VS Woven, Website link: http://oribimanufacturing.com/uni-directional-vs-woven/

**Software:**

1. ANSYS wokbench16, Static structure, Composite PrePost modules
2. CATIA V5, Part design, Surface design, Composite design modules
3. ElamX2,2

# Hosein Tafaghodi Helali

**E-MAIL:** hosein.tafaghodi@tuwien.ac.at
**Telefon:** +43 (0) 6606086742
**Geburtsdatum:** 31.August 1982
**Geburtsort:** Teheran
**Staatsangehörigkeit:** Iran

## Ausbildung

2012-2016    **TU Wien, 1060 Wien**
**Doktorats Studium Maschinenbau**
Institut für Konstruktionswissenschaften und Technische Logistik

Schwerpunkt: Finite Element Methode und Verbundmaterial
Doktorarbeit zum Thema: "Methodology of modeling Composite components with FEM software and investigation of the influence of modeling method in the quality of results"

2006-2009    **Islamic Azad University, Teheran, Iran**
**Masterstudium Luft-und Raumfahrttechnik**

Masterarbeit zum Thema: "Convective effect of pressure and stress distribution for contact of tilted wedge with a half space using FEM",

2001-2005    **Islamic Azad University, Teheran, Iran**
**Bachelorstudium Maschinenbau**

Bachelorarbeit zum Thema: "Design of rings under different load conditions and comparing the theoretical results with ANSYS"

## Forschungserfahrungen

**TU Wien, Getreidemarkt 9**
**Projektassistent**

2015    Analyse eines Hubschrauberhauptgetriebes
2014-2015    Modellierung und Analyse einer Spiralfeder aus Verbundwerkstoff mit FEM
2013-2014    Analyse und Optimierung eines Innenraumkörpers aus verbundmaterial in einem Rettungshelikopter
2012-2013    Deformationsanalyse eines Hubschrauberhauptgetriebes
2012    Analyse und Optimierung verschiedener Getriebemodelle für Krane

## Zusatzausbildungen

**CADFEM (Österreich)**
2014    ANSYS Strukturmechanik

**CADFEM (Deutschland)**
2013    ANSYS Verbundmodul

**Siemens (Österreich)**
2013    Grundlagen Siemens NX 8.5 CAD

## Publikation

"The precision of FEM simulation results compared with theoretical composite layup calculation", Published on Composite part B: Engineering, online April 09, 2016

"Pressure and Stress Distribution for Contact of Wedge with a Half space Using FEM", Published on Mechanical Engineering (science and researches University) magazine, 2009

## Forschungsinteressen

Finite Elemente Methode, Spannungs- und Dehnungsanalyse, Mechanik von Verbundmaterial, Analyse der mechanischen Strukturen

## Sprachkenntnisse

Deutsch:         Mittelstufe (Sprachenzentrum der Universität Wien, B2   Niveau)
Englisch:         verhandlungssicher (IBT TOEFL: 80)
Persisch (Farsi):  Muttersprache

## EDV-Kenntnisse

CATIA, ANSYS, ANSYS workbench, SIEMENS NX, MATHCAD, MS Office

## Interessen und Hobbies

Zeichnung, Film, Musik, Bergsteigen, Schwimmen, Fußball spielen, Tischfußball spielen

## Referenzen

**Dr. Manfred Grafinger**, Ao.Univ. Prof. Dipl.-Ing. Dr.techn.
    Technische Universität Wien
    Email: manfred.grafinger@tuwien.ac.at

**Dr. Michael Weigand**, Univ. Prof. Dipl.-Ing. Dr.-Ing.
    Technische Universität Wien
    Email: Michael.weigand@tuwien.ac.at